

12-2019

Global Acetylation Dynamics in the Heat Shock Response of *Saccharomyces cerevisiae*

Rebecca E. Hardman
University of Arkansas, Fayetteville

Follow this and additional works at: <https://scholarworks.uark.edu/etd>



Part of the [Amino Acids, Peptides, and Proteins Commons](#), and the [Molecular Biology Commons](#)

Citation

Hardman, R. E. (2019). Global Acetylation Dynamics in the Heat Shock Response of *Saccharomyces cerevisiae*. *Theses and Dissertations* Retrieved from <https://scholarworks.uark.edu/etd/3489>

This Dissertation is brought to you for free and open access by ScholarWorks@UARK. It has been accepted for inclusion in Theses and Dissertations by an authorized administrator of ScholarWorks@UARK. For more information, please contact ccmiddle@uark.edu.

Global Acetylation Dynamics in the Heat Shock Response of *Saccharomyces cerevisiae*

A dissertation submitted in partial fulfillment
of the requirements for the degree of
Doctor of Philosophy in Cell and Molecular Biology

by

Rebecca E. Hardman
Drury University
Bachelor of Arts in Biology, 2012

December 2019
University of Arkansas

This dissertation is approved for recommendation to the Graduate Council.

Jeffrey A. Lewis, Ph.D.
Dissertation Director

Paul D. Adams, Ph.D.
Committee Member

Yuchun Du, Ph.D.
Committee Member

Daniel J. Lessner, Ph.D.
Committee Member

Abstract

All organisms face a constant barrage of environmental stresses. Single-cell organisms such as *Saccharomyces cerevisiae*, or common Baker's yeast, must rely solely on cellular responses in order to survive. This response must occur in a rapid and highly coordinated manner to quickly inhibit all unnecessary processes and shuttle all available resources to those necessary for survival. One method that cells utilize for rapid protein regulation is the use of post-translational modifications. Enzymes within the cell add or remove a variety of chemical modifications, thus altering the local chemical environment of a protein. This creates a conformational change in the protein that can increase, decrease, or completely change the activity of the protein, as well as target them for relocation or degradation. Examples of common post-translational modifications include phosphorylation, ubiquitination, and the focus of this dissertation, acetylation.

That protein acetylation occurs has been known for decades, but it is only recently that advances in technology such as high-resolution mass spectrometry and immunoprecipitation have led to the recognition of thousands of acetylated proteins across all domains of life. The roles and regulation of this modification, however, are still widely unknown. One approach to better understand possible roles for acetylation is to look at its dynamics in response to environmental stress. In this dissertation, I examine global changes in protein acetylation in the response of *Saccharomyces cerevisiae* to a mild heat shock and the potential mechanisms regulating these changes.

Following an introductory literature review, this dissertation will cover the results of a large time-scale profiling of acetylome dynamics in response to heat shock. Proteins identified in this experiment are enriched for many cellular processes, suggesting that acetylation may play a much wider regulatory role than previously believed. These proteins are also enriched for interactions with many lysine acetyltransferases and deacetylases, suggesting that the regulation of this modification is complex. The next chapter will then discuss possible

mechanisms regulating this response. This includes the investigation into concentrations of metabolites known to affect acetylation and deacetylation, lysine acetyltransferase and deacetylase complex remodeling, and localization changes for those complexes within the cell.

©2019 by Rebecca E. Hardman
All Rights Reserved

Acknowledgments

To Mom, Dad, Wendy and Alan and Karen Kavanaugh, thank you for your unwavering support that has kept me going to the very end. It is because of my parents' support that I grew to love science at a young age and motivated me to pursue my education to the fullest.

To my amazing friends, and especially Amanda Scholes and Joshua Rohrich, you lent me an ear when I needed to talk and reminding me that I am not alone. I wouldn't have gotten through this process without you by my side.

To my partner, Joey, thank you for helping me find my inner strength and for providing me with a loving home. You loved me even when I had trouble loving myself, and that is the most valuable gift I could ever receive.

And finally, to my advisor Dr. Jeffrey Lewis and Dr. Tara Stuecker, thank you for taking a chance and never giving up on me. No matter what life threw at me you always gave me the support, and sometimes the push, that I needed to keep going. Had I been in any other lab I don't think I would have made it to this point. While I may have had many doubts throughout the past six and a half years, choosing your lab has never been one of them, and I could not have asked for better mentors.

Table of Contents

Chapter 1 Introduction.....	1
1.1 Cellular stress response.....	1
1.2 Enzymes involved in protein acetylation.....	2
1.3 History of acetylation.....	7
1.4 Metabolism.....	8
1.4.1 Acetyl CoA.....	8
1.4.2 NAD ⁺ /NADH.....	9
1.4.3 Butyrate.....	10
1.4.4 Metabolic changes in response to stress.....	10
1.5 Lysine acetylation and the cellular response to heat shock.....	11
1.5.1 Transcription.....	12
1.5.2 Translation.....	14
1.5.3 Cell wall and membrane effects.....	14
1.5.4 Chaperones.....	15
1.6 Dissertation outline.....	18
1.7 References.....	19
Chapter 2 Identifying the dynamics of protein acetylation in response to heat shock.....	31
2.1 Abstract.....	32
2.2 Introduction.....	33
2.3 Materials and Methods.....	35
2.3.1 Strains.....	35
2.3.2 Acquired thermotolerance assays.....	35
2.3.2 Western blot analysis of whole cell lysate.....	36
2.3.3 2-D electrophoretic analysis of acetyl-enriched peptides.....	37
2.3.4 Collection for global acetylation analysis.....	37

2.3.5 Cell lysis and TMT10 labelling.....	38
2.3.6 High pH fractionation.....	39
2.3.7 Acetyl-lysine Enrichment.....	39
2.3.8 LC-MS/MS Data Analysis.....	39
2.3.9 Statistical analysis, clustering, and enrichment, and motif analysis	41
2.4 Results and Discussion	43
2.4.1 Acetylation is required for full acquisition of thermotolerance.	43
2.4.2 The acetylome exhibits clear remodeling in response to heat shock.	43
2.4.2 The acetylome is highly dynamic in response to heat stress.	46
2.4.3 Process and component enrichments	52
2.4.4 Enrichments for known KAT and KDAC interactions	54
2.5 Conclusion.....	54
2.6 Acknowledgements	57
2.7 References	57
2.8 Appendix	61
Chapter 3 Mechanisms regulating protein acetylation in response to heat shock in <i>S. cerevisiae</i>	65
3.1 Abstract.....	66
3.2 Introduction.....	67
3.3 Materials and Methods	71
3.3.1 Strains.....	71
3.3.2 Metabolite extraction	71
3.3.3 Mass spectrometry for acetyl-CoA, CoA, and nicotinamide	72
3.3.4 NAD:NADH assay	74
3.3.5 TAP purification.....	75
3.3.6 Fluorescence microscopy.....	76
3.4 Results and Discussion	77

3.4.1 Metabolite changes occur early in the response to heat stress.....	77
3.4.2 KAT and KDAC complexes show little component changes	79
3.4.3 Hda1 translocates from the nucleus to the cytoplasm	86
3.5 Conclusion.....	86
3.6 Acknowledgements	89
3.7 References	89
3.8 Appendix	92
Chapter 4 Conclusions and Future Directions.....	99
4.1 Conclusions.....	99
4.1.1 The yeast acetylome is highly dynamic in response to heat stress	99
4.1.2 Multiple KATs and KDACs are enriched for physical interactions with proteins experiencing significant acetylation changes.....	100
4.1.3 Acetylation dynamics are not likely due to metabolite concentration changes	101
4.2 Future Directions	101
4.2.1 Effect of acetylation changes on protein activity and function	101
4.2.2 Determine KATs and KDACs involved in the acetyl dynamics of the heat shock response	103
4.2.3 Conservation of changing acetyllysine residues	104
4.3 Future of acetylproteomics	104
4.4 References	105
Supplemental Chapter 1 Accurate and Sensitive Quantitation of the Dynamic Heat Shock Proteome using Tandem Mass Tags.....	107
Appendix	150
A.1 IBC Protocol Approval.....	150

List of Figures

Figure 1.1 Schematic of regulation by reversible lysine acetylation	4
Figure 2.1 Schematic for TMT-10 acetyl proteomics.	42
Figure 2.4 Western blot analysis shows differences in acetylation between stressed (37°C) and unstressed (25°C) cells	45
Figure 2.5 Two-dimensional gel electrophoresis (2-DE) of acetylated proteins identifies numerous changes in the acetylome during heat shock	45
Figure 2.6 The majority of significant acetylation events occur at 90 minutes of heat shock.....	47
Figure 2.7 Average acetyl fold changes compared to corresponding protein fold changes.....	48
Figure 2.8 Number of significantly changing acetyl peptides per protein	50
Figure 2.9 36 proteins experience both increasing and decreasing acetyl residues	51
Figure 2.10 Clusters and enrichments for time course acetyl proteomics.	53
Figure 2.11 Significantly changing KAT and KDAC concentrations	56
Figure 2.A.1 Modification motifs for increasing clusters.....	63
Figure 2.A.2 Modification motifs for decreasing clusters.....	64
Figure 3.1 Schematic of regulation by reversible lysine acetylation	68
Figure 3.2 Concentrations of acetyl-CoA, CoA, and nicotinamide in response to heat shock	78
Figure 3.3 NAD:NADH ratio and NAD ⁺ fold change in response to heat shock.....	80
Figure 3.4 Co-Immunoprecipitation of Esa1-TAP.	82
Figure 3.5 Co-Immunoprecipitation of Hpa3-TAP.....	83
Figure 3.6 Co-Immunoprecipitation of Taf1-TAP.	84
Figure 3.7 Hda1 relocalizes to the cytoplasm after 45 minutes of heat shock at 37°C.....	88
Figure 3.8 Hda1 resides in the nucleus in unstressed conditions at 25°C	89
Figure 3.A.1 Tap co-immunoprecipitations of KAT and KDAC enzymes and interacting proteins	92
Figure 3.A.2 Localization of KATs and KDACs during heat shock.....	94

List of Tables

Table 1.1 Functional enrichments for targets of acetylation.....	3
Table 1.2 Yeast KATs	5
Table 1.3 Yeast KDACs	5
Table 1.4 Yeast Hsp70 proteins	17
Table 2.1 Inhibitors added for acquisition experiment.....	36
Table 2.2 Secondary Stress Gradient	36
Table 2.3 Cellular process enrichments by number of changing acetyl peptides	50
Table 2.4 Hypergeometric p-values for KATs and increasing acetylation clusters	55
Table 2.5 Hypergeometric p-values for KDACs and decreasing acetylation clusters.....	55
Table 3.1 Yeast KATs	70
Table 3.2 Yeast KDACs	70
Table 3.3 MS/MS precursor and product ions in duplicate	73
Table 3.6 Fold change in Rpl12A and Snc2 interacting with Esa1 compared to control.....	82
Table 3.7 Fold change of Tdh3 interacting with Taf1 compared to control.....	84
Table 3.8 Known KAT and KDAC localization	87

Chapter 1 Introduction

At the cellular level, life exists in an almost continuous battle against the environment to maintain homeostasis. While gradual changes can be managed through appropriate gene expression responses geared at up-regulating stress defenses, rapid environmental changes necessitate a much more immediate response. For this purpose, cells maintain a “standing army” of stress defense proteins. Keeping certain proteins in a constitutively active state can be energetically wasteful, however, and may interfere with other cellular processes. Cells resolve this conflict by tightly regulating these proteins so that under stress these proteins can be rapidly activated to protect the cell. One mechanism for protein rapid activation is through the use of rapid and reversible chemical modifications collectively termed post-translational modifications (PTMs) (Rhee et al. 2005, Dai and Gu 2010, Wani et al. 2015, Hofer and Wenz 2014). Common PTMs include phosphorylation, methylation, ubiquitination, and the subject of this dissertation, reversible N ϵ -lysine acetylation.

1.1 Cellular stress response

In the laboratory setting, we often try to maintain optimal culture conditions including nutrient availability, temperature, oxygenation, etc. For cells in their natural environment, however, expecting stable conditions is far from realistic. Cells are frequently battling a variety of stresses including temperature shifts, oxidation, osmotic stress, nutrient limitations, and competition with other organisms secreting toxins in an effort to gain a foothold. To combat these stresses, cells have evolved highly conserved stress defense proteins. These proteins focus on minimizing damage in key areas such as DNA damage and protein misfolding, halting cell growth to conserve energy, and streamlining metabolism to optimize energy production for stress defense proteins (Gasch et al. 2000b, Kültz 2005).

Many studies have shown that a large number of key stress-defense protein classes are regulated by acetylation including transcription factors [reviewed in (Bannister and Miska 2000)],

heat-shock proteins, and superoxide dismutase. Acetylation also plays an important role in the assembly and function of stress granules, ribonucleoprotein assemblies that sequester mRNAs to inhibit their translation (Ohn and Anderson 2010) and in the activity of many metabolic proteins (Zhao et al. 2010, Choudhary et al. 2014), which are tightly regulated in response to stress. In yeast, a study by Henriksen et al. (2012) identified over 4000 acetyllysine sites showing strong enrichments for many processes that are involved in the environmental stress response (ESR), a set of ~900 genes that experience significant induction (iESR) or repression (rESR) in response to a wide variety of environmental stresses in *S. cerevisiae* (Table 1.1) (Gasch et al. 2000b). Here, we describe the current literature regarding the role of non-histone protein acetylation in the cellular stress response including, metabolism, transcriptional regulation, and more specifically in response to heat shock. For a more general review of acetylation, especially as it pertains to mammals, please see Narita et al. (2019).

1.2 Enzymes involved in protein acetylation

There are three classes of proteins involved in lysine acetylation: the “writers,” lysine acetyltransferases (KATs); the “erasers,” lysine deacetylases (KDACs); and the “readers,” which assist in substrate recruitment and complex formation, and often contain bromodomains which are responsible to recognizing acetylated lysines (Smith and Zhou 2016, Fujisawa and Filippakopoulos 2017). Protein acetylation occurs when a KAT transfers an acetyl group from acetyl-CoA to the ϵ -amino groups of a free lysine residue (Fig. 1.1). This neutralizes the strong positive charge of the amine, affecting the polar environment in that region of the protein. Lysine residues are often found in regions of proteins interacting with other proteins or substrates and removing that charge weakens these interactions. Currently, there are 12 proteins known to have lysine acetyltransferase activity in *S. cerevisiae* (Table 1.2) and 17 in humans (Yates et al. 2017). Most fall into three main families: GNAT (Gcn5-related N-acetyltransferase), MYST (named after members MOZ, Ybf2/Sas3, Sas2, and Tip 60) and p300/CBP (named for its

Table 1.1 Functional enrichments for targets of acetylation

Enriched categories for acetylated proteins ^a	p-value	Enriched for ESR? ^b	Enriched categories for acetylated proteins ^a	p-value	Enriched for ESR? ^b
Translation	1 x 10 ⁻³⁵	rESR	Phosphorus metabolism	9 x 10 ⁻¹²	rESR
Amino acid metabolism	1 x 10 ⁻³¹		Glycolysis	8 x 10 ⁻¹¹	
Gene expression	3 x 10 ⁻²⁶	rESR	Protein folding	5 x 10 ⁻⁶	
RNA metabolism	3 x 10 ⁻²⁴	rESR	Protein acetylation	6 x 10 ⁻⁶	rESR
Ribosome biogenesis	2 x 10 ⁻²¹	rESR	Response to stress	5 x 10 ⁻⁵	iESR
Chromatin organization	4 x 10 ⁻¹⁸		Carbohydrate metabolism	3 x 10 ⁻³	iESR
Oxidation-reduction	9 x 10 ⁻¹⁸	iESR	Response to heat	7 x 10 ⁻³	iESR

a GO functional enrichments for acetylated proteins identified in Henriksen et al. 2012 using the Princeton GO-Term finder (Boyle et al. 2004b).

b Assessment of whether the target genes in each functional category were enriched for the reduced (rESR) or induced (iESR) environmental stress response as defined in (Gasch et al. 2000b).

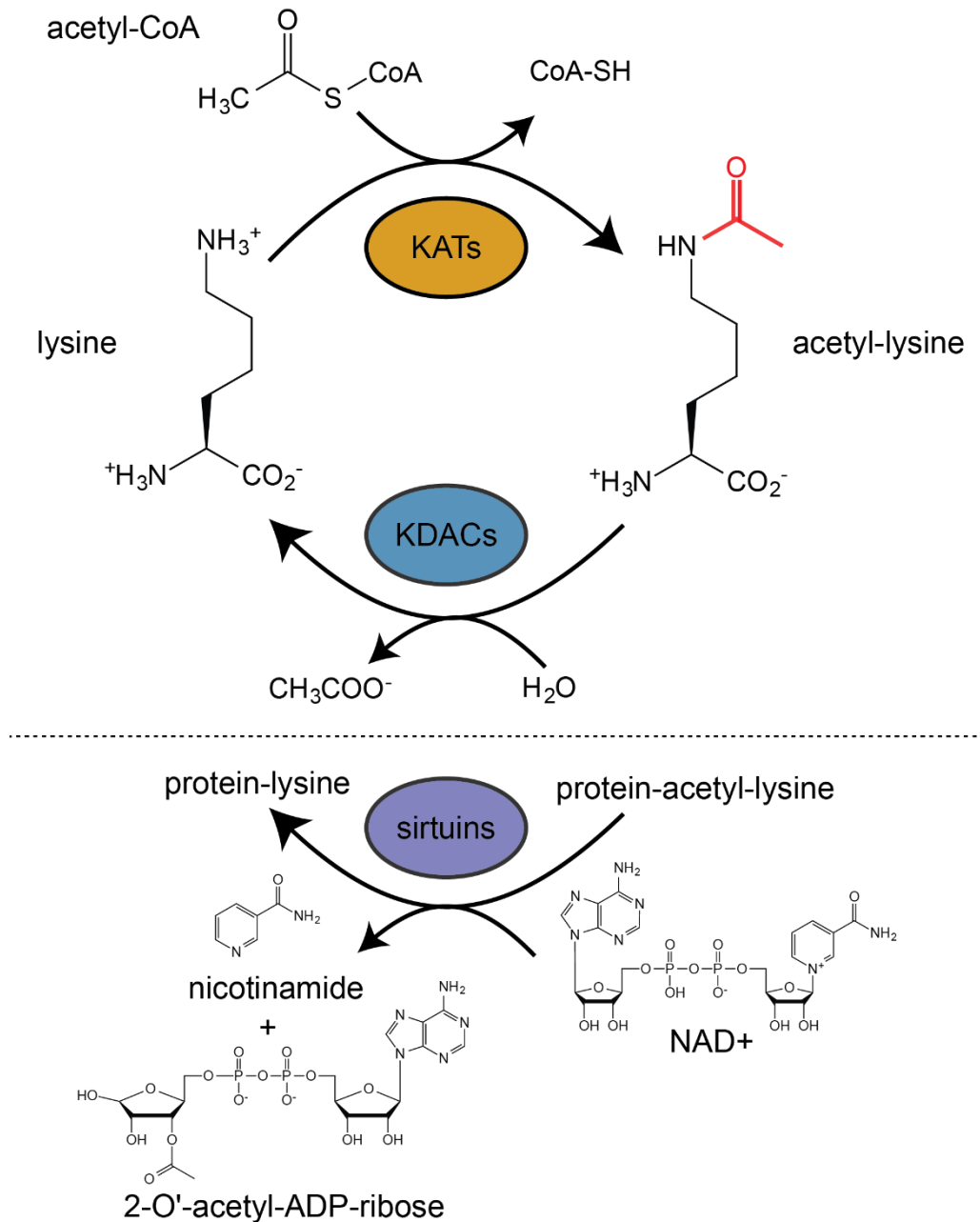


Figure 1.1 Schematic of regulation by reversible lysine acetylation. Lysine acetylation is a highly conserved post-translational modification, where acetyltransferases (KATs) transfer the acetyl group from acetyl-CoA. Class I, II, and IV zinc-dependent lysine deacetylases (KDACs) remove the acetyl group via hydrolysis. Class III deacetylases (i.e. sirtuins), use NAD⁺ as a substrate, producing nicotinamide and 2-O'-acetyl-ADP-ribose, a novel metabolite only known to be produced by sirtuins.

Table 1.2 Yeast KATs

Enzymatic subunit	Complexes	Family	Genetic Interactions	Physical Interactions
Eco1p			128	28
Elp3p	Elongator	GNAT	514	25
Esa1p	NuA4, piccolo NuA4,	MYST	768	205
Gcn5p	SAGA, SLIK, ADA	GNAT	422	283
Hat1p	Hat1p-Hat2p	GNAT	131	44
Hpa2p		GNAT	94	11
Hpa3p		GNAT	39	9
Rtt109p	Rtt109-Vps75		559	18
Sas2p	SAS	MYST	128	28
Sas3p	NuA3	MYST	174	21
Spt10p		GNAT	116	306
Taf1p	TFIID		859	112

Table 1.3 Yeast KDACs

Enzymatic subunit	Complexes	Class	Genetic Interactions	Physical Interactions
Hda1p	Hda1-2-3	II	708	26
Hos1p		I	87	9
Hos2p	Set3 and Rpd3(L)	I	376	18
Hos3p		II	69	23
Hst1p	Sum1p/Rfm1p/Hst1p	III	136	20
Hst2p		III	45	7
Hst3p		III	286	13
Hst4p		III	94	6
Rpd3p	Rpd3(L), Rpd3(S), SNT2C	I	966	81
Set3p	Set3C	III	394	25
Sir2p	SIR2-3-4, RENT	III	316	75

members)(Bazan 2008, Wang et al. 2008, Tang et al. 2008, Hansen et al. 2019) and are components of many different complexes to aid in substrate specificity. There are also many proteins that have putative KAT activity (The UniProt Consortium 2017).

The acetyl group can then be removed by KDACs (Fig. 1.1), of which there are four classes. Classes I, II, and IV are considered the “classical” KDACs, in that they require a Zn^{2+} cofactor, and are inhibited by butyrate and trichostatin A (Boffa et al. 1978, Sealy and Chalkley 1978, Candido, Reeves and Davie 1978, Sekhavat, Sun and Davie 2007). Class III, most commonly known as the “sirtuins,” require NAD^+ as a cofactor, and are inhibited by nicotinamide [Reviewed in (Menzies et al. 2016)]. An example of this class, Sir2p in yeast has been heavily studied as it has been linked to life-span extension (Kaeberlein, McVey and Guarente 1999, Lin, Defossez and Guarente 2000, Lin et al. 2004). There are currently 11 known KDACs in yeast (Table 1.3) and 18 in humans (Yates et al. 2017). Class I KDACs have strong deacetylase activity and primarily localize to the nucleus. Class II KDACs, on the other hand, have weak deacetylase activity and are able to move between the nucleus and cytoplasm (Haberland, Montgomery and Olson 2009, Dokmanovic, Clarke and Marks 2007). Little is known of the enzymatic activity and functions of the one member of the Class IV KDACs, HDAC11, found only in mammals. The cellular localization, enzymatic activity, and substrate specificity vary dramatically among the Class III KDACs.

Sirtuins have been heavily studied for the critical roles they play in metabolism via mitochondrial protein acetylation (Carrico et al. 2018). In *S. cerevisiae*, mitochondrial Acetyl-CoA levels are ~20-30 fold higher than cytosolic and nuclear levels (Weinert et al. 2014). Due to these high levels of acetyl-CoA paired with the relatively high pH of the mitochondrial matrix, non-enzymatic lysine acetylation is widespread (Weinert et al. 2015). This phenomenon is also seen in mammals, where the majority of acetylated residues are deacetylated by SIRT3 (Weinert et al. 2015, Lombard et al. 2007, Rardin et al. 2013, Baeza, Smallegan and Denu

2016). Whether the removal of these acetylation events is regulatory or simply correcting environmental artifacts is still under investigation.

1.3 History of acetylation

Although the discoveries of protein phosphorylation in the 1950s (Burnett and Kennedy 1954, Fischer and Krebs 1955, Fischer et al. 1959) and lysine acetylation in 1963 (Phillips 1963, Allfrey, Faulkner and Mirsky 1964) occurred within a decade of each other, further investigation into phosphorylation was aggressively pursued while the scope of acetylation as a global regulatory phenomenon was not appreciated until recently. This is largely due to the fact that acetylation was first thought to solely regulate histone protein function, and the technology at the time was not sensitive enough to detect such a small modification. In the thirty years following its discovery, only three non-histone proteins were found to be acetylated: alpha-tubulin, the tumor suppressor p53, and HIV-1 Tat protein (L'Hernault and Rosenbaum 1985, Gu and Roeder 1997, Ott et al. 1999). The surprising discovery in the early 2000s that acetylation regulates the activity of the central metabolic enzyme acetyl-CoA synthetase in bacteria and mammals (Starai et al. 2002, Starai et al. 2003) suggested that acetylation may have a much broader regulatory scope. Global proteomic studies subsequently revealed a large number of acetylated proteins across all domains of life (Henriksen et al. 2012, Weinert et al. 2011, Kim et al. 2006, Liu et al. 2017).

As of 2019, there are over forty-two thousand acetyllysine sites annotated in the Uniprot database (The UniProt Consortium 2017), and the majority of which occur on non-nuclear proteins representing most cellular processes. Many of these sites are also conserved from bacteria to humans (Nakayasu et al. 2017, Hwang et al. 2016, Hansen et al. 2019), suggesting conserved function. In humans, aberrant acetylation has been linked to diverse aspects of human health ranging from cancer to aging, and in the pathogenesis of viruses and bacteria [recently reviewed in (Auburger, Gispert and Jendrach 2014, Hadden and Advani 2018, Li et al.

2018, Parodi-Rullán, Chapa-Dubocq and Javadov 2018, Zhou et al. 2017, Zheng et al. 2017, Conrad and Ott 2016, Lin et al. 2018, Poulouse and Raju 2015, Drazic et al. 2016, Ren et al. 2017)]. However, despite the importance of properly regulated acetylation for organismal fitness, the function of acetylation for these proteins and processes is widely unknown. The most well-conserved acetylation sites are enriched for proteins involved in metabolism, transcription, translation, and the focus of this dissertation, cellular stress responses.

1.4 Metabolism

One process that is strongly enriched for protein acetylation is metabolism. Recent studies have found that many highly conserved metabolic enzymes are acetylated (Henriksen et al. 2012, Weinert et al. 2011, Choudhary et al. 2009, Zhao et al. 2010, Guarente 2011), including the majority of intermediate metabolic enzymes. The pathways in which this has been well characterized include gluconeogenesis, glycolysis, glycogen metabolism, fatty acid metabolism, and the urea cycle and nitrogen metabolism (Guan and Xiong 2011). Not only are many metabolic enzymes regulated by lysine acetylation, but the enzymes involved in the process of reversible lysine acetylation are regulated by metabolites.

1.4.1 Acetyl CoA

All KATs use acetyl-CoA as the acetyl donor during protein acetylation reactions and most have a high affinity for both acetyl-CoA and CoA (Albaugh, Arnold and Denu 2011a). This causes CoA to act as a competitive inhibitor, which is reversed when acetyl-CoA levels are high during nutrient-rich conditions (Galdieri et al. 2014) and means that the acetyl CoA/CoA ratio could have significant regulatory consequences (Albaugh, Kolonko and Denu 2010, Albaugh et al. 2011b, Berndsen et al. 2007, Tanner et al. 2000). The exception to this is Rtt109, which has a relatively low binding affinity for CoA and is likely constitutively active (Albaugh et al. 2010). Because acetyl-CoA is a key central metabolite, this directly links protein acetylation to the

metabolic state of the cell. When cells are in media containing glucose under aerobic conditions, they process the glucose mainly via glycolysis, producing pyruvate. Pyruvate can then either enter the mitochondria where it is converted to acetyl-CoA by the pyruvate dehydrogenase complex (PDC) (Weinert et al. 2014, Gombert et al. 2001, Heyland, Fu and Blank 2009) or more likely be further processed to acetate which is then converted to acetyl-CoA by the acetyl-CoA synthetases Acs1p in the mitochondria or by Acs1p and Acs2p in the cytosol and nucleus (De Virgilio et al. 1992, Kumar et al. 2002, Huh et al. 2003, Takahashi et al. 2006). The Acs proteins are then regulated through feedback inhibition by acetyl-CoA. (Schwer et al. 2006, Hallows, Lee and Denu 2006, Newman, He and Verdin 2012, Starai et al. 2004)

In the mitochondria, acetyl-CoA can also be produced via fatty acid β -oxidation, ketone body metabolism, or amino acid metabolism. In the cytosol and nucleus, citrate from the mitochondria can be broken down by ATP-citrate lyase to yield acetyl-CoA and oxaloacetate. While Acetyl CoA can freely move in and out of the nucleus through the nuclear pore complexes (Talcott and Moore 1999, Wentz and Rout 2010), it cannot leave the mitochondria (Takahashi et al. 2006). This keeps the nuclear, cytosolic, and mitochondrial pools of acetyl-CoA separate. During stress, pools of acetyl-CoA can also be regulated by the translocation of Acs2 into the nucleus where it helps retain acetate lost by histone deacetylation (Bulusu et al. 2017, Li et al. 2017).

1.4.2 NAD⁺/NADH

Like KATs, KDACs are also heavily regulated by metabolites. Controlling the levels and localization of NAD⁺ in the cell can have dramatic effects on the activity of sirtuins, which rely on NAD⁺ as a cofactor. This has been well studied in energy-deficient cells, which experience an increase in NAD⁺ followed by an increase in sirtuin activity (Lin et al. 2000). NAD⁺ and NADH cannot diffuse through membranes, so the localization of precursors, such as nicotinamide, regulates NAD⁺/NADH dynamics, and thus sirtuin activity. Mitochondria produces

NAD⁺ separately from the cytoplasm and nucleus and retains this NAD⁺ pool. This allows the mitochondrial NAD⁺ to remain constant despite the levels in the cytoplasm. This is important for maintaining the activity of sirtuins to combat the high levels of non-enzymatic acetylation. Sirtuins are noncompetitively inhibited by nicotinamide, a product of their deacetylase activity (Avalos, Bever and Wolberger 2005). Whether NADH also acts as an inhibitor is debated (Madsen et al. 2016, Lin et al. 2004).

1.4.3 Butyrate

Another metabolite, butyrate, is important in the regulation of class I, II, and IV KDACS. Butyrate is a short-chain fatty acid generated by carbohydrate fermentation in bacteria that serves as a precursor for acetyl-CoA via β -oxidation (Vital et al. 2014). Due to the anti-neoplastic nature of butyrate treatment, it is of major interest for the treatment of many types of cancers. While this is of little consequence to microbes unless they share an environment with bacteria producing this compound, butyrate is vital to healthy gastrointestinal health in humans and other mammals. Existing in mM levels in the colon, butyrate serves as a main source of energy for colonocytes, but in cancer cells, it is not metabolized due to the fact that cancer cells prioritize metabolism via glycolysis (Encarnaç o et al. 2015). It then accumulates in the nucleus and acts as a KDAC inhibitor, inhibiting their growth and proliferation.

1.4.4 Metabolic changes in response to stress

In response to stress, metabolism is retooled in different ways for the cell to survive. During the initial stress, processes involved in growth are inhibited to shuttle resources to survival mechanisms such as energy production. Yeast, for example, prefer glucose as their main source of energy, so genes involved in glucose import and metabolism are induced during the environmental stress response. Following an increase in glucose via import and activation and glycogen degradation, it is then shuttled to pathways involved in trehalose production, ATP

synthesis, and NADPH regeneration (Shenton and Grant 2003). In hyperosmotic stress, glycolysis is also shifted to increase glycerol production and retention (Petelenz-Kurdziel et al. 2013).

The nonreducing storage carbohydrate trehalose plays a vital role in stress response, and metabolism shifts to the production of trehalose in response to heat. One heat stress is detected, the cell begins shuttling glucose towards trehalose production where it serves as a protein stabilizer, preventing aggregation (Hottiger et al. 1994, Singer and Lindquist 1998a, Singer and Lindquist 1998b). Deletion of trehalose synthases decreases thermotolerance, whereas increasing levels by deactivating degradation enzymes extend thermotolerance. (De Virgilio et al. 1994). Trehalose also served as an antidehydration agent, minimizing the effects of desiccation (Crowe 2007). Finally, the full transcriptional response to heat would not be possible without trehalose, as it acts as a stabilizing agent for the key transcription factor Hsf1p (Bulman and Nelson 2005, Conlin and Nelson 2007).

Heat stress heavily affects the membrane by causing “hyperfluidity,” and thus lipid metabolism adjusts to absorb and utilize damaged lipids and maintain membrane integrity by adjusting lipid composition (Panaretou and Piper 1992, Balogh et al. 2013). Following beta-oxidation in the peroxisome, acetyl groups can then be transferred to the mitochondria for energy production via the TCA cycle (Hetteema and Tabak 2000). Though genes involved in β -oxidation are not induced by the ESR, genes involved in metabolite import and export to the peroxisome where β -oxidation occurs are (Gasch et al. 2000b). To mitigate increased membrane fluidity, cells utilize sterols such as cholesterol in mammals and ergosterol in fungi (Swan and Watson 1998, Cress et al. 1982)

1.5 Lysine acetylation and the cellular response to heat shock

One of the most common stresses that cells face is an increase in temperature, and the heat stress response is one of the most studied cellular responses and is highly conserved. The

response consists of many components including cell cycle arrest, the previously discussed metabolic shifts, global changes in transcription and translation, and cell wall and membrane effects. This culminates in the rapid upregulation of protein chaperones that mediate protein cytotoxicity, prevent cell death, and prepare the cell for future stresses. This response in yeast has been well-reviewed (Verghese et al. 2012b).

1.5.1 Transcription

The first to be discovered and iconic role of protein acetylation is in the regulation of transcription through DNA/histone interactions. Positively charged lysines on histones bind tightly to the negatively charged backbone of DNA, decreasing its ability to be transcribed. During gene activation, acetyltransferases acetylate these lysine residues, thus weakening their interaction with DNA and allowing transcription factors to bind and transcription to occur. This is not, however, the only way that acetylation regulates transcription.

Lysine acetylation has been implicated in the regulation of a wide variety of transcription factors in a highly conserved manner including Hsf1 (Purwana et al. 2017), Irf1 (Downey et al. 2013), FOXO (Daitoku, Sakamaki and Fukamizu 2011), NF- κ B (Chen and Greene 2003), p53 (Gu and Roeder 1997) and the general transcription factors TFIIE- β and TFIIF (Imhof et al. 1997). Since its discovery as the second non-histone proteins to be acetylated in 1997, tumor protein p53 has been of special interest, as it plays key roles in cell cycle regulation and apoptosis, and aberrant p53 function is involved in many types of cancers. The expression profile of the various p53 isoforms can even be used to predict cancer progression, response to therapy, and prognosis (Surget, Khoury and Bourdon 2014). Acetylation of p53 is vital for its function, as it leads to stabilization and activation and inhibits repression of p53-mediated transcription activation by blocking ubiquitination and methylation sites (Meek and Anderson 2009, Li et al. 2002).

1.5.1.1 Hsf1

In yeast, the transcriptional response to heat is mediated by the general stress transcription factors Msn2/4 and, to a greater extent, heat shock factor 1 (Hsf1). Hsf1 is a highly conserved transcription factor that plays a key role in stress defense as well as a central role in homeostasis (Gallo, Prentice and Kingston 1993, Jedlicka, Mortin and Wu 1997). Upon exposure to stress, Hsf1 quickly induces the expression of over 165 genes containing a five base pair heat shock element in their promoter (Sorger and Pelham 1987a), including chaperones and chaperonins such as Hsp90 and Hsp70 (Vihervaara et al. 2013, Hahn et al. 2004). Hsf1 also activates polyubiquitin genes, the products of which can then target proteins for degradation.

In yeast, Hsf1p is bound to DNA, even in the absence of stress, suggesting that it is mostly regulated posttranslationally. (Sorger, Lewis and Pelham 1987). Extensive phosphorylation has been observed when converting to the active form, and target gene expression correlates with the level of phosphorylation (Sorger and Pelham 1988). It is then dephosphorylated for transient expression (Liu and Thiele 1996). The sites that are phosphorylated are stress-specific (Liu and Thiele 1996), and other phosphosites contribute to decreasing Hsf1p activity, (Hashikawa and Sakurai 2004, Høj and Jakobsen 1994).

Upon initiation of the heat stress response, Hsf1 is deacetylated, trimerizes, and localizes to target genes for activation. Upon acetylation around 30 minutes of heat shock, however, the trimer releases the DNA, attenuating the response (Westerheide et al. 2009b). Attenuation is also carried out through feedback inhibition in which Hsp70 and Hsp90 bind to Hsf1 (Voellmy and Boellmann 2007). In fact, the deletion of the Hsp70s *SSA1* and *SSA2* activates Hsf1 even under non-stressed conditions (Matsumoto et al. 2005).

1.5.2 Translation

One way in which acetylation regulates translation via transcription is through the transcription of ribosomal proteins (RP). A key step in the expression of RP transcription is the association of the transcription factor Lfh1 with RP promoters. Under stress, there is a rapid reduction in Lfh1 association at RP promoters, rapidly decreasing their transcription (Wade, Hall and Struhl 2004). The activity of Lfh1 is in turn regulated by acetylation by Gcn5 and deacetylation by Hst1 and Sir2. In response to stress, Lfh1 is rapidly deacetylated, limiting its ability to activate RP, which slowly rebounds over time (Downey et al. 2013).

Acetylation mediated control of translation is also found through acetylation of the eukaryotic translation initiation factor 5A (eIF5A). Following acetylation, eIF5A accumulates in the nucleus, thus inhibiting its ability to initiate translation (Ishfaq et al. 2012). Acetylation has also been detected on eIF1 α , but whether or not this acetylation has any functional consequence is unknown (Kim et al. 2006). Several proteomic studies have shown strong enrichments for acetylation on ribosomal proteins themselves (Weinert et al. 2011, Henriksen et al. 2012, Liu et al. 2018), but possible roles it plays is also unknown.

1.5.3 Cell wall and membrane effects

One of the biggest targets of heat stress is the cell membrane. Increases in temperature lead to increases in membrane fluidity which can affect the structure of membrane-bound proteins and result in changes in ion transport (Cyert 2003). Yeast cells maintain high internal turgor pressure, and any weakness in membrane and cell wall integrity can lead to lysis. Alterations in lipid composition also affect the temperature at which the heat shock response is initiated (Carratù et al. 1996). While the exact mechanism through which cells detect temperature changes is unknown, it is very likely that many of the key sensors are located in the membrane and are parts of the cell wall integrity pathway (Levin 2005). There is increasing evidence that specific classes of lipids play a role in heat sensing including sphingolipids,

ceramides (Dickson and Lester 2002) and phosphoinositides (Levin 2011) which rapidly accumulate in response to heat. One membrane sensing pathway that is known to be involved in the heat shock response is the protein kinase C-activated MAP kinase pathway, in which the cell detects cell wall weakness via membrane stretch and this as well as Ca²⁺ influx activates the GTPase Rho1p, triggering a kinase cascade leading to transcription activation (Levin 2005, Kamada et al. 1995). Cells with mutations in this pathway grow normally at lower temperatures but lyse at 37°C (Torres et al. 1991), demonstrating the importance of this cascade in the heat shock response.

1.5.4 Chaperones

In haploid budding yeast, there is estimated to be between 100-150 million proteins packed into a 40µm³ cell (Milo 2013). This does not allow a lot of room for the proper folding of nascent proteins while also identifying damaged proteins that need to be refolded or removed for degradation. The cell thus maintains a battery of chaperones, whose job it is to help with folding and remodeling proteins throughout the cell to maintain homeostasis (Ellis 1987). This highly conserved family of proteins has been heavily studied, and improper chaperone function has been linked to disease causation as well as possible therapeutic targets (Ebrahimi-Fakhari, Saidi and Wahlster 2013, Roodveldt, Outeiro and Braun 2017, Macario and Conway de Macario 2000). Due to the physiological consequences of protein misfolding during heat stress, chaperones are one of the largest groups of genes that are transcriptionally activated in the heat shock response by Hsf1p, which is why many of them have the as “HSPs” for “heat shock protein.” Many of these chaperones are targets of acetylation.

1.5.4.1 Hsp90p

The chaperone Hsp90p, represented by the yeast paralogs Hsp82p and Hsc82p, is a highly conserved, essential protein that plays a wide variety of roles in the cell. Transcriptionally

regulated by Hsf1p, levels of Hsp90p quickly rise within the cell in response to heat shock to assist with the refolding of proteins, especially those involved in signal transduction that are especially labile due to frequent conformation changes (Nathan, Vos and Lindquist 1997). Hsp90p regulation occurs across multiple fronts including an array of various complex partners (reviewed in (Mollapour and Neckers 2012), as well as post-translational modification including phosphorylation, acetylation, S-nitrosylation, oxidation, and ubiquitination. The effect of these modifications varies depending on the organism and the residue involved. The main effects of acetylation include altering interactions with other complex partners and modifying interaction with ATP and ATPase activity (Kovacs et al. 2005, Scroggins et al. 2007). For example, in humans when Hsp90 is acetylated it can no longer interact with p23, inhibiting its chaperone function. HDAC6 can remove this acetylation, restoring functionality (Kovacs et al. 2005). In yeast, deletion of the KDACs Hda1p and Rpd3p inhibits the ability of the Hsp90s to bind and activate calcineurin, which plays an important role in cellular stress responses (Robbins, Leach and Cowen 2012, Cyert 2003).

1.5.4.2 Hsp70p

In yeast, the Hsp70 family consists of 10 proteins (Table 1.4) and 4 Hsp70 nucleotide exchange factors. All of these play a role in the unfolded protein response, but only the paralogs Ssa3 and Ssa4 are specifically induced by the stress response. The four Ssa proteins are highly redundant, and constitutive expression of just one is all that is necessary for viability. While the deletion of either SSA1 or its paralog SSA2 has no known phenotypic consequence, the deletion of both leads to slow growth and sensitivity at 37°C, suggesting that even though SSA3/4 have high sequence similarity to SSA1/2, they are not completely redundant (Werner-Washburne, Stone and Craig 1987). The Ssa proteins in yeast are acetylated, and a recent study found that deacetylation of Ssa1 residues K86, K185, K354, and K562 occurs rapidly in

response to heat shock. Mutation of these residues leads to substantial changes in chaperone and client

Table 1.4 Yeast Hsp70 proteins

Protein	Location	Function(s) ^a
Ssa1	Cytosol	Protein folding, nuclear transport, prion propagation
Ssa2	Cytosol	Protein folding, vacuolar import, involved in ubiquitin-dependent degradation, prion propagation, tRNA import
Ssa3	Cytosol	Protein folding in response to stress, protein-membrane targeting and translocation
Ssa4	Cytosol	Protein folding, highly induced upon stress, protein-membrane targeting, and translocation
Ssb1	Cytosol	Ribosome associated, folding of nascent proteins
Ssb2	Cytosol	Ribosome associated, folding of nascent proteins
Ssc1	Mitochondria	Inner mitochondrial membrane translocation and protein folding
Ssc3	Mitochondria	Protein translocation in mitochondrial nucleoids
Ssq1	Mitochondria	Assembly of iron-sulfur clusters
Kar3	Endoplasmic reticulum	Microtubule motor, required for nuclear fusion during mating

a. from the *Saccharomyces* Genome Database (SGD)(Cherry et al. 2012)

interactions without affecting chaperone functionality (Xu et al. 2019). In higher eukaryotes, the Ssa homolog Hsp70 is immediately acetylated on K77 in response to stress and binds to the co-chaperone Hop to focus on refolding denatured proteins. Later on, Hsp70 is deacetylated and binds to the ubiquitin ligase protein CHIP to assist in protein degradation (Seo et al. 2016). Acetylated Hsp70 also prevents apoptosis by binding to apoptotic protease-activating factor 1 (Apaf1) and apoptosis-inducing factor (AIF), modulators of apoptotic pathways, and this plays a role in oncogenesis (Park et al. 2017).

1.5.4.3 Hsp104p

Hsp104 is unique in that its main role in the cell is as a protein disaggregase (Parsell et al. 1994). When proteins misfold they often clump together, making it impossible for other chaperones to refold them. Hsp104, however, is able to disentangle these proteins and feed them to the Hsp70/40 complex for proper refolding (Glover and Lindquist 1998). Under various stresses and in normal cellular functioning, oxidized proteins become carbonylated and form aggregates (Requena et al. 2001). During division, these clumps remain in the mother cell, likely contributing to senescence (Aguilaniu et al. 2003). This segregation requires Hsp104 and Sir2 (Erjavec et al. 2007). Hsp104 also plays a vital role in prion propagation and thus has been a focus of study for prion disease (Romanova and Chernoff 2009, Chernoff et al. 1995). Hsp104 has been found to be heavily acetylated, but the possible role(s) of this acetylation remains unknown (Henriksen et al. 2012).

1.6 Dissertation outline

While our understanding of proteins acetylation and the many roles it plays in the cell has grown dramatically over the past few decades, we still know very little about how global acetylation is changing in response to environmental perturbation. Most studies that have looked at global acetylation, referred to as the acetylome, have only looked in static, often

unstressed, conditions, and while this provides insight into which proteins are acetylated, it provides no information as to possible ways in which acetylation is regulating protein function. Other studies have homed in on a protein of interest, but with the thousands of acetylation targets, determining whether acetylation influences these individually would take decades.

To take a more global approach to determine possible roles of acetylation in the cell, we performed a large time-scale analysis of the acetylome in response to heat shock in the model organism, *Saccharomyces cerevisiae*. Chapter 2 describes the results of this experiment, including analysis of cellular functions enriched for acetylation changes, the timing of these changes, and the possible KATs and KDACs regulating this response. Chapter 3 further investigates the possible mechanisms regulating these changes including metabolite levels, KAT and KDAC localization, and KAT and KDAC complex components. Supplementary chapter 1 further discusses the mass spectrometry analysis that we developed to analyze the time scale proteomics data.

1.7 References

- Aguilaniu, H., L. Gustafsson, M. Rigoulet & T. Nyström (2003) Asymmetric inheritance of oxidatively damaged proteins during cytokinesis. *Science*, 299, 1751-3.
- Albaugh, B. N., K. M. Arnold & J. M. Denu (2011a) KAT(ching) Metabolism by the Tail: Insight into the links between lysine acetyltransferases and metabolism. *Chembiochem*, 12, 290-8.
- Albaugh, B. N., K. M. Arnold, S. Lee & J. M. Denu (2011b) Autoacetylation of the histone acetyltransferase Rtt109. *J Biol Chem*, 286, 24694-701.
- Albaugh, B. N., E. M. Kolonko & J. M. Denu (2010) Kinetic mechanism of the Rtt109-Vps75 histone acetyltransferase-chaperone complex. *Biochemistry*, 49, 6375-85.
- Allfrey, V. G., R. Faulkner & A. E. Mirsky (1964) Acetylation and methylation of histones and their possible role in the regulation of RNA synthesis. *Proc Natl Acad Sci U S A*, 51, 786-94.
- Auburger, G., S. Gispert & M. Jendrach (2014) Mitochondrial acetylation and genetic models of Parkinson's disease. *Prog Mol Biol Transl Sci*, 127, 155-82.

- Avalos, J. L., K. M. Bever & C. Wolberger (2005) Mechanism of sirtuin inhibition by nicotinamide: altering the NAD(+) cosubstrate specificity of a Sir2 enzyme. *Mol Cell*, 17, 855-68.
- Baeza, J., M. J. Smallegan & J. M. Denu (2016) Mechanisms and Dynamics of Protein Acetylation in Mitochondria. *Trends Biochem Sci*, 41, 231-44.
- Balogh, G., M. Péter, A. Glatz, I. Gombos, Z. Török, I. Horváth, J. L. Harwood & L. Vígh (2013) Key role of lipids in heat stress management. *FEBS Lett*, 587, 1970-80.
- Bannister, A. J. & E. A. Miska (2000) Regulation of gene expression by transcription factor acetylation. *Cell Mol Life Sci*, 57, 1184-92.
- Bazan, J. F. 2008. An old HAT in human p300/CBP and yeast Rtt109. In *Cell Cycle*, 1884-6. United States.
- Berndsen, C. E., B. N. Albaugh, S. Tan & J. M. Denu (2007) Catalytic mechanism of a MYST family histone acetyltransferase. *Biochemistry*, 46, 623-9.
- Boffa, L. C., G. Vidali, R. S. Mann & V. G. Allfrey (1978) Suppression of histone deacetylation in vivo and in vitro by sodium butyrate. *J Biol Chem*, 253, 3364-6.
- Bulman, A. L. & H. C. Nelson (2005) Role of trehalose and heat in the structure of the C-terminal activation domain of the heat shock transcription factor. *Proteins*, 58, 826-35.
- Bulusu, V., S. Tumanov, E. Michalopoulou, N. J. van den Broek, G. MacKay, C. Nixon, S. Dhayade, Z. T. Schug, J. Vande Voorde, K. Blyth, E. Gottlieb, A. Vazquez & J. J. Kamphorst (2017) Acetate Recapturing by Nuclear Acetyl-CoA Synthetase 2 Prevents Loss of Histone Acetylation during Oxygen and Serum Limitation. *Cell Rep*, 18, 647-658.
- Burnett, G. & E. P. Kennedy (1954) The enzymatic phosphorylation of proteins. *J Biol Chem*, 211, 969-80.
- Candido, E. P., R. Reeves & J. R. Davie (1978) Sodium butyrate inhibits histone deacetylation in cultured cells. *Cell*, 14, 105-13.
- Carratù, L., S. Franceschelli, C. L. Pardini, G. S. Kobayashi, I. Horvath, L. Vigh & B. Maresca (1996) Membrane lipid perturbation modifies the set point of the temperature of heat shock response in yeast. *Proc Natl Acad Sci U S A*, 93, 3870-5.
- Carrico, C., J. G. Meyer, W. He, B. W. Gibson & E. Verdin (2018) The Mitochondrial Acylome Emerges: Proteomics, Regulation by Sirtuins, Metabolic and Disease Implications. *Cell Metab*, 27, 497-512.
- Chen, L. F. & W. C. Greene (2003) Regulation of distinct biological activities of the NF-kappaB transcription factor complex by acetylation. *J Mol Med (Berl)*, 81, 549-57.
- Chernoff, Y. O., S. L. Lindquist, B. Ono, S. G. Inge-Vechtomov & S. W. Liebman (1995) Role of the chaperone protein Hsp104 in propagation of the yeast prion-like factor [psi+]. *Science*, 268, 880-4.

- Choudhary, C., C. Kumar, F. Gnad, M. L. Nielsen, M. Rehman, T. C. Walther, J. V. Olsen & M. Mann (2009) Lysine acetylation targets protein complexes and co-regulates major cellular functions. *Science*, 325, 834-40.
- Choudhary, C., B. T. Weinert, Y. Nishida, E. Verdin & M. Mann (2014) The growing landscape of lysine acetylation links metabolism and cell signalling. *Nat Rev Mol Cell Biol*, 15, 536-50.
- Conlin, L. K. & H. C. Nelson (2007) The natural osmolyte trehalose is a positive regulator of the heat-induced activity of yeast heat shock transcription factor. *Mol Cell Biol*, 27, 1505-15.
- Conrad, R. J. & M. Ott (2016) Therapeutics Targeting Protein Acetylation Perturb Latency of Human Viruses. *ACS Chem Biol*, 11, 669-80.
- Cress, A. E., P. S. Culver, T. E. Moon & E. W. Gerner (1982) Correlation between amounts of cellular membrane components and sensitivity to hyperthermia in a variety of mammalian cell lines in culture. *Cancer Res*, 42, 1716-21.
- Crowe, J. H. (2007) Trehalose as a "chemical chaperone": fact and fantasy. *Adv Exp Med Biol*, 594, 143-58.
- Cyert, M. S. (2003) Calcineurin signaling in *Saccharomyces cerevisiae*: how yeast go crazy in response to stress. *Biochem Biophys Res Commun*, 311, 1143-50.
- Dai, C. & W. Gu (2010) p53 post-translational modification: deregulated in tumorigenesis. *Trends Mol Med*, 16, 528-36.
- Daitoku, H., J. Sakamaki & A. Fukamizu (2011) Regulation of FoxO transcription factors by acetylation and protein-protein interactions. *Biochim Biophys Acta*, 1813, 1954-60.
- De Virgilio, C., N. Burckert, G. Barth, J. M. Neuhaus, T. Boller & A. Wiemken (1992) Cloning and disruption of a gene required for growth on acetate but not on ethanol: the acetyl-coenzyme A synthetase gene of *Saccharomyces cerevisiae*. *Yeast*, 8, 1043-51.
- De Virgilio, C., T. Hottiger, J. Dominguez, T. Boller & A. Wiemken (1994) The role of trehalose synthesis for the acquisition of thermotolerance in yeast. I. Genetic evidence that trehalose is a thermoprotectant. *Eur J Biochem*, 219, 179-86.
- Dickson, R. C. & R. L. Lester (2002) Sphingolipid functions in *Saccharomyces cerevisiae*. *Biochim Biophys Acta*, 1583, 13-25.
- Dokmanovic, M., C. Clarke & P. A. Marks (2007) Histone deacetylase inhibitors: overview and perspectives. *Mol Cancer Res*, 5, 981-9.
- Downey, M., B. Knight, A. A. Vashisht, C. A. Seller, J. A. Wohlschlegel, D. Shore & D. P. Toczyski (2013) Gcn5 and sirtuins regulate acetylation of the ribosomal protein transcription factor Lfh1. *Curr Biol*, 23, 1638-48.
- Drazic, A., L. M. Myklebust, R. Ree & T. Arnesen (2016) The world of protein acetylation. *Biochim Biophys Acta*, 1864, 1372-401.

- Ebrahimi-Fakhari, D., L. J. Saidi & L. Wahlster (2013) Molecular chaperones and protein folding as therapeutic targets in Parkinson's disease and other synucleinopathies. *Acta Neuropathol Commun*, 1, 79.
- Ellis, J. (1987) Proteins as molecular chaperones. *Nature*, 328, 378-9.
- Encarnação, J. C., A. M. Abrantes, A. S. Pires & M. F. Botelho (2015) Revisit dietary fiber on colorectal cancer: butyrate and its role on prevention and treatment. *Cancer Metastasis Rev*, 34, 465-78.
- Erjavec, N., L. Larsson, J. Grantham & T. Nyström (2007) Accelerated aging and failure to segregate damaged proteins in Sir2 mutants can be suppressed by overproducing the protein aggregation-remodeling factor Hsp104p. *Genes Dev*, 21, 2410-21.
- Fischer, E. H., D. J. Graves, E. R. Crittenden & E. G. Krebs (1959) Structure of the site phosphorylated in the phosphorylase b to a reaction. *J Biol Chem*, 234, 1698-704.
- Fischer, E. H. & E. G. Krebs (1955) Conversion of phosphorylase B to phosphorylase B in muscle extracts. *J Biol Chem*, 216, 121-32.
- Fujisawa, T. & P. Filippakopoulos (2017) Functions of bromodomain-containing proteins and their roles in homeostasis and cancer. *Nat Rev Mol Cell Biol*, 18, 246-262.
- Galdieri, L., T. Zhang, D. Rogerson, R. Lleshi & A. Vancura. 2014. Protein Acetylation and Acetyl Coenzyme A Metabolism in Budding Yeast. In *Eukaryot Cell*, 1472-83.
- Gallo, G. J., H. Prentice & R. E. Kingston (1993) Heat shock factor is required for growth at normal temperatures in the fission yeast *Schizosaccharomyces pombe*. *Mol Cell Biol*, 13, 749-61.
- Gasch, A. P., P. T. Spellman, C. M. Kao, O. Carmel-Harel, M. B. Eisen, G. Storz, D. Botstein & P. O. Brown. 2000. Genomic Expression Programs in the Response of Yeast Cells to Environmental Changes. In *Mol Biol Cell*, 4241-57.
- Glover, J. R. & S. Lindquist (1998) Hsp104, Hsp70, and Hsp40: a novel chaperone system that rescues previously aggregated proteins. *Cell*, 94, 73-82.
- Gombert, A. K., M. Moreira dos Santos, B. Christensen & J. Nielsen (2001) Network identification and flux quantification in the central metabolism of *Saccharomyces cerevisiae* under different conditions of glucose repression. *J Bacteriol*, 183, 1441-51.
- Gu, W. & R. G. Roeder (1997) Activation of p53 sequence-specific DNA binding by acetylation of the p53 C-terminal domain. *Cell*, 90, 595-606.
- Guan, K. L. & Y. Xiong (2011) Regulation of intermediary metabolism by protein acetylation. *Trends Biochem Sci*, 36, 108-16.
- Guarente, L. (2011) The logic linking protein acetylation and metabolism. *Cell Metab*, 14, 151-3.

- Haberland, M., R. L. Montgomery & E. N. Olson (2009) The many roles of histone deacetylases in development and physiology: implications for disease and therapy. *Nat Rev Genet*, 10, 32-42.
- Hadden, M. J. & A. Advani (2018) Histone Deacetylase Inhibitors and Diabetic Kidney Disease. *Int J Mol Sci*, 19.
- Hahn, J. S., Z. Hu, D. J. Thiele & V. R. Iyer (2004) Genome-wide analysis of the biology of stress responses through heat shock transcription factor. *Mol Cell Biol*, 24, 5249-56.
- Hallows, W. C., S. Lee & J. M. Denu (2006) Sirtuins deacetylate and activate mammalian acetyl-CoA synthetases. *Proc Natl Acad Sci U S A*, 103, 10230-5.
- Hansen, B. K., R. Gupta, L. Baldus, D. Lyon, T. Narita, M. Lammers, C. Choudhary & B. T. Weinert (2019) Analysis of human acetylation stoichiometry defines mechanistic constraints on protein regulation. *Nat Commun*, 10, 1055.
- Hashikawa, N. & H. Sakurai (2004) Phosphorylation of the yeast heat shock transcription factor is implicated in gene-specific activation dependent on the architecture of the heat shock element. *Mol Cell Biol*, 24, 3648-59.
- Henriksen, P., S. A. Wagner, B. T. Weinert, S. Sharma, G. Bacinskaja, M. Rehman, A. H. Juffer, T. C. Walther, M. Lisby & C. Choudhary (2012) Proteome-wide analysis of lysine acetylation suggests its broad regulatory scope in *Saccharomyces cerevisiae*. *Mol Cell Proteomics*, 11, 1510-22.
- Hettema, E. H. & H. F. Tabak (2000) Transport of fatty acids and metabolites across the peroxisomal membrane. *Biochim Biophys Acta*, 1486, 18-27.
- Heyland, J., J. Fu & L. M. Blank (2009) Correlation between TCA cycle flux and glucose uptake rate during respiro-fermentative growth of *Saccharomyces cerevisiae*. *Microbiology*, 155, 3827-37.
- Hofer, A. & T. Wenz (2014) Post-translational modification of mitochondria as a novel mode of regulation. *Exp Gerontol*, 56, 202-20.
- Hottiger, T., C. De Virgilio, M. N. Hall, T. Boller & A. Wiemken (1994) The role of trehalose synthesis for the acquisition of thermotolerance in yeast. II. Physiological concentrations of trehalose increase the thermal stability of proteins in vitro. *Eur J Biochem*, 219, 187-93.
- Huh, W.-K., J. V. Falvo, L. C. Gerke, A. S. Carroll, R. W. Howson, J. S. Weissman & E. K. O'Shea (2003) Global analysis of protein localization in budding yeast. *Nature*, 425, 686.
- Hwang, A. W., H. Trzeciakiewicz, D. Friedmann, C. X. Yuan, R. Marmorstein, V. M. Lee & T. J. Cohen (2016) Conserved Lysine Acetylation within the Microtubule-Binding Domain Regulates MAP2/Tau Family Members. *PLoS One*, 11, e0168913.
- Høj, A. & B. K. Jakobsen (1994) A short element required for turning off heat shock transcription factor: evidence that phosphorylation enhances deactivation. *EMBO J*, 13, 2617-24.

- Imhof, A., X. J. Yang, V. V. Ogryzko, Y. Nakatani, A. P. Wolffe & H. Ge (1997) Acetylation of general transcription factors by histone acetyltransferases. *Curr Biol*, 7, 689-92.
- Ishfaq, M., K. Maeta, S. Maeda, T. Natsume, A. Ito & M. Yoshida (2012) Acetylation regulates subcellular localization of eukaryotic translation initiation factor 5A (eIF5A). *FEBS Lett*, 586, 3236-41.
- Jedlicka, P., M. A. Mortin & C. Wu (1997) Multiple functions of *Drosophila* heat shock transcription factor in vivo. *EMBO J*, 16, 2452-62.
- Kaeberlein, M., M. McVey & L. Guarente (1999) The SIR2/3/4 complex and SIR2 alone promote longevity in *Saccharomyces cerevisiae* by two different mechanisms. *Genes Dev*, 13, 2570-80.
- Kamada, Y., U. S. Jung, J. Piotrowski & D. E. Levin (1995) The protein kinase C-activated MAP kinase pathway of *Saccharomyces cerevisiae* mediates a novel aspect of the heat shock response. *Genes Dev*, 9, 1559-71.
- Kim, S. C., R. Sprung, Y. Chen, Y. Xu, H. Ball, J. Pei, T. Cheng, Y. Kho, H. Xiao, L. Xiao, N. V. Grishin, M. White, X. J. Yang & Y. Zhao (2006) Substrate and functional diversity of lysine acetylation revealed by a proteomics survey. *Mol Cell*, 23, 607-18.
- Kovacs, J. J., P. J. Murphy, S. Gaillard, X. Zhao, J. T. Wu, C. V. Nicchitta, M. Yoshida, D. O. Toft, W. B. Pratt & T. P. Yao (2005) HDAC6 regulates Hsp90 acetylation and chaperone-dependent activation of glucocorticoid receptor. *Mol Cell*, 18, 601-7.
- Kumar, A., S. Agarwal, J. A. Heyman, S. Matson, M. Heidtman, S. Piccirillo, L. Umansky, A. Drawid, R. Jansen, Y. Liu, K. H. Cheung, P. Miller, M. Gerstein, G. S. Roeder & M. Snyder (2002) Subcellular localization of the yeast proteome. *Genes Dev*, 16, 707-19.
- Kültz, D. (2005) Molecular and evolutionary basis of the cellular stress response. *Annu Rev Physiol*, 67, 225-57.
- L'Hernault, S. W. & J. L. Rosenbaum (1985) *Chlamydomonas* alpha-tubulin is posttranslationally modified by acetylation on the epsilon-amino group of a lysine. *Biochemistry*, 24, 473-8.
- Levin, D. E. (2005) Cell wall integrity signaling in *Saccharomyces cerevisiae*. *Microbiol Mol Biol Rev*, 69, 262-91.
- (2011) Regulation of cell wall biogenesis in *Saccharomyces cerevisiae*: the cell wall integrity signaling pathway. *Genetics*, 189, 1145-75.
- Li, M., J. Luo, C. L. Brooks & W. Gu (2002) Acetylation of p53 inhibits its ubiquitination by Mdm2. *J Biol Chem*, 277, 50607-11.
- Li, T., C. Zhang, S. Hassan, X. Liu, F. Song, K. Chen, W. Zhang & J. Yang (2018) Histone deacetylase 6 in cancer. *J Hematol Oncol*, 11, 111.
- Li, X., W. Yu, X. Qian, Y. Xia, Y. Zheng, J. H. Lee, W. Li, J. Lyu, G. Rao, X. Zhang, C. N. Qian, S. G. Rozen, T. Jiang & Z. Lu (2017) Nucleus-translocated ACS2 promotes the gene transcription for lysosomal biogenesis and autophagy. *Mol Cell*, 66, 684-697 e9.

- Lin, P. C., H. Y. Hsieh, P. C. Chu & C. S. Chen (2018) Therapeutic Opportunities of Targeting Histone Deacetylase Isoforms to Eradicate Cancer Stem Cells. *Int J Mol Sci*, 19.
- Lin, S. J., P. Defossez & L. Guarente (2000) Requirement of NAD and SIR2 for Life-Span Extension by Calorie Restriction in *Saccharomyces cerevisiae*.
- Lin, S. J., E. Ford, M. Haigis, G. Liszt & L. Guarente. 2004. Calorie restriction extends yeast life span by lowering the level of NADH. In *Genes Dev*, 12-6.
- Liu, J., Q. Wang, X. Jiang, H. Yang, D. Zhao, J. Han, Y. Luo & H. Xiang (2017) Systematic Analysis of Lysine Acetylation in the Halophilic Archaeon *Haloferax mediterranei*. *J Proteome Res*, 16, 3229-3241.
- Liu, X. D. & D. J. Thiele (1996) Oxidative stress induced heat shock factor phosphorylation and HSF-dependent activation of yeast metallothionein gene transcription. *Genes Dev*, 10, 592-603.
- Liu, Y. T., Y. Pan, F. Lai, X. F. Yin, R. Ge, Q. Y. He & X. Sun (2018) Comprehensive analysis of the lysine acetylome and its potential regulatory roles in the virulence of *Streptococcus pneumoniae*. *J Proteomics*, 176, 46-55.
- Lombard, D. B., F. W. Alt, H. L. Cheng, J. Bunkenborg, R. S. Streeper, R. Mostoslavsky, J. Kim, G. Yancopoulos, D. Valenzuela, A. Murphy, Y. Yang, Y. Chen, M. D. Hirschey, R. T. Bronson, M. Haigis, L. P. Guarente, R. V. Farese, S. Weissman, E. Verdin & B. Schwer (2007) Mammalian Sir2 homolog SIRT3 regulates global mitochondrial lysine acetylation. *Mol Cell Biol*, 27, 8807-14.
- Macario, A. J. & E. Conway de Macario (2000) Stress and molecular chaperones in disease. *Int J Clin Lab Res*, 30, 49-66.
- Madsen, A. S., C. Andersen, M. Daoud, K. A. Anderson, J. S. Laursen, S. Chakladar, F. K. Huynh, A. R. Colaco, D. S. Backos, P. Fristrup, M. D. Hirschey & C. A. Olsen (2016) Investigating the Sensitivity of NAD⁺-dependent Sirtuin Deacylation Activities to NADH. *J Biol Chem*, 291, 7128-41.
- Matsumoto, R., K. Akama, R. Rakwal & H. Iwahashi (2005) The stress response against denatured proteins in the deletion of cytosolic chaperones SSA1/2 is different from heat-shock response in *Saccharomyces cerevisiae*. *BMC Genomics*, 6, 141.
- Meek, D. W. & C. W. Anderson (2009) Posttranslational Modification of p53: Cooperative Integrators of Function. *Cold Spring Harb Perspect Biol*, 1.
- Menzies, K. J., H. Zhang, E. Katsyuba & J. Auwerx (2016) Protein acetylation in metabolism - metabolites and cofactors. *Nat Rev Endocrinol*, 12, 43-60.
- Milo, R. (2013) What is the total number of protein molecules per cell volume? A call to rethink some published values. *Bioessays*, 35, 1050-5.
- Mollapour, M. & L. Neckers (2012) Post-translational modifications of Hsp90 and their contributions to chaperone regulation. *Biochim Biophys Acta*, 1823, 648-55.

- Nakayasu, E. S., M. C. Burnet, H. E. Walukiewicz, C. S. Wilkins, A. K. Shukla, S. Brooks, M. J. Plutz, B. D. Lee, B. Schilling, A. J. Wolfe, S. Muller, J. R. Kirby, C. V. Rao, J. R. Cort & S. H. Payne (2017) Ancient Regulatory Role of Lysine Acetylation in Central Metabolism. *MBio*, 8.
- Narita, T., B. T. Weinert & C. Choudhary (2018) Functions and mechanisms of non-histone protein acetylation. *Nat Rev Mol Cell Biol*.
- Nathan, D. F., M. H. Vos & S. Lindquist (1997) In vivo functions of the *Saccharomyces cerevisiae* Hsp90 chaperone. *Proc Natl Acad Sci U S A*, 94, 12949-56.
- Newman, J. C., W. He & E. Verdin (2012) Mitochondrial protein acylation and intermediary metabolism: regulation by sirtuins and implications for metabolic disease. *J Biol Chem*, 287, 42436-43.
- Ohn, T. & P. Anderson (2010) The role of posttranslational modifications in the assembly of stress granules. *Wiley Interdiscip Rev RNA*, 1, 486-93.
- Ott, M., M. Schnölzer, J. Garnica, W. Fischle, S. Emiliani, H. R. Rackwitz & E. Verdin (1999) Acetylation of the HIV-1 Tat protein by p300 is important for its transcriptional activity. *Curr Biol*, 9, 1489-92.
- Panaretou, B. & P. W. Piper (1992) The plasma membrane of yeast acquires a novel heat-shock protein (hsp30) and displays a decline in proton-pumping ATPase levels in response to both heat shock and the entry to stationary phase. *Eur J Biochem*, 206, 635-40.
- Park, Y. H., J. H. Seo, J. H. Park, H. S. Lee & K. W. Kim (2017) Hsp70 acetylation prevents caspase-dependent/independent apoptosis and autophagic cell death in cancer cells. *Int J Oncol*, 51, 573-578.
- Parodi-Rullán, R. M., X. R. Chapa-Dubocq & S. Javadov (2018) Acetylation of Mitochondrial Proteins in the Heart: The Role of SIRT3. *Front Physiol*, 9, 1094.
- Parsell, D. A., A. S. Kowal, M. A. Singer & S. Lindquist (1994) Protein disaggregation mediated by heat-shock protein Hsp104. *Nature*, 372, 475-8.
- Petelenz-Kurdziel, E., C. Kuehn, B. Nordlander, D. Klein, K. K. Hong, T. Jacobson, P. Dahl, J. Schaber, J. Nielsen, S. Hohmann & E. Klipp (2013) Quantitative analysis of glycerol accumulation, glycolysis and growth under hyper osmotic stress. *PLoS Comput Biol*, 9, e1003084.
- Phillips, D. M. (1963) The presence of acetyl groups of histones. *Biochem J*, 87, 258-63.
- Poulose, N. & R. Raju (2015) Sirtuin regulation in aging and injury. *Biochimica et Biophysica Acta (BBA) - Molecular Basis of Disease*, 1852, 2442-2455.
- Purwana, I., J. J. Liu, B. Portha & J. Buteau (2017) HSF1 acetylation decreases its transcriptional activity and enhances glucolipotoxicity-induced apoptosis in rat and human beta cells. *Diabetologia*, 60, 1432-1441.

- Rardin, M. J., J. C. Newman, J. M. Held, M. P. Cusack, D. J. Sorensen, B. Li, B. Schilling, S. D. Mooney, C. R. Kahn, E. Verdin & B. W. Gibson. 2013. Label-free quantitative proteomics of the lysine acetylome in mitochondria identifies substrates of SIRT3 in metabolic pathways. In *Proc Natl Acad Sci U S A*, 6601-6.
- Ren, J., Y. Sang, J. Lu & Y. F. Yao (2017) Protein Acetylation and Its Role in Bacterial Virulence. *Trends Microbiol*, 25, 768-779.
- Requena, J. R., C. C. Chao, R. L. Levine & E. R. Stadtman (2001) Glutamic and aminoadipic semialdehydes are the main carbonyl products of metal-catalyzed oxidation of proteins. *Proc Natl Acad Sci U S A*, 98, 69-74.
- Rhee, S. G., K. S. Yang, S. W. Kang, H. A. Woo & T. S. Chang (2005) Controlled elimination of intracellular H₂O₂: regulation of peroxiredoxin, catalase, and glutathione peroxidase via post-translational modification. *Antioxid Redox Signal*, 7, 619-26.
- Robbins, N., M. D. Leach & L. E. Cowen (2012) Lysine deacetylases Hda1 and Rpd3 regulate Hsp90 function thereby governing fungal drug resistance. *Cell Rep*, 2, 878-88.
- Romanova, N. V. & Y. O. Chernoff (2009) Hsp104 and prion propagation. *Protein Pept Lett*, 16, 598-605.
- Roodveldt, C., T. F. Outeiro & J. E. A. Braun (2017) Editorial: Molecular Chaperones and Neurodegeneration. *Front Neurosci*, 11, 565.
- Schwer, B., J. Bunkenborg, R. O. Verdin, J. S. Andersen & E. Verdin (2006) Reversible lysine acetylation controls the activity of the mitochondrial enzyme acetyl-CoA synthetase 2. *Proc Natl Acad Sci U S A*, 103, 10224-9.
- Scroggins, B. T., K. Robzyk, D. Wang, M. G. Marcu, S. Tsutsumi, K. Beebe, R. J. Cotter, S. Felts, D. Toft, L. Karnitz, N. Rosen & L. Neckers (2007) An acetylation site in the middle domain of Hsp90 regulates chaperone function. *Mol Cell*, 25, 151-9.
- Sealy, L. & R. Chalkley (1978) The effect of sodium butyrate on histone modification. *Cell*, 14, 115-21.
- Sekhavat, A., J. M. Sun & J. R. Davie (2007) Competitive inhibition of histone deacetylase activity by trichostatin A and butyrate. *Biochem Cell Biol*, 85, 751-8.
- Seo, J. H., J. H. Park, E. J. Lee, T. T. Vo, H. Choi, J. Y. Kim, J. K. Jang, H. J. Wee, H. S. Lee, S. H. Jang, Z. Y. Park, J. Jeong, K. J. Lee, S. H. Seok, J. Y. Park, B. J. Lee, M. N. Lee, G. T. Oh & K. W. Kim (2016) ARD1-mediated Hsp70 acetylation balances stress-induced protein refolding and degradation. *Nat Commun*, 7, 12882.
- Shenton, D. & C. M. Grant. 2003. Protein S-thiolation targets glycolysis and protein synthesis in response to oxidative stress in the yeast *Saccharomyces cerevisiae*. In *Biochem J*, 513-9.
- Singer, M. A. & S. Lindquist (1998a) Multiple effects of trehalose on protein folding in vitro and in vivo. *Mol Cell*, 1, 639-48.

- (1998b) Thermotolerance in *Saccharomyces cerevisiae*: the Yin and Yang of trehalose. *Trends Biotechnol*, 16, 460-8.
- Smith, S. G. & M.-M. Zhou. 2016. The Bromodomain as an Acetyl-Lysine Reader Domain. In *Chromatin Signaling and Diseases*, eds. O. Binda & M. E. Fernandez-Zapico, 97-111. London, United Kingdom: Academic Press.
- Sorger, P. K., M. J. Lewis & H. R. Pelham (1987) Heat shock factor is regulated differently in yeast and HeLa cells. *Nature*, 329, 81-4.
- Sorger, P. K. & H. R. Pelham (1987) Purification and characterization of a heat-shock element binding protein from yeast. *EMBO J*, 6, 3035-41.
- (1988) Yeast heat shock factor is an essential DNA-binding protein that exhibits temperature-dependent phosphorylation. *Cell*, 54, 855-64.
- Starai, V. J., I. Celic, R. N. Cole, J. D. Boeke & J. C. Escalante-Semerena (2002) Sir2-dependent activation of acetyl-CoA synthetase by deacetylation of active lysine. *Science*, 298, 2390-2.
- Starai, V. J., H. Takahashi, J. D. Boeke & J. C. Escalante-Semerena (2003) Short-chain fatty acid activation by acyl-coenzyme A synthetases requires SIR2 protein function in *Salmonella enterica* and *Saccharomyces cerevisiae*. *Genetics*, 163, 545-55.
- (2004) A link between transcription and intermediary metabolism: a role for Sir2 in the control of acetyl-coenzyme A synthetase. *Curr Opin Microbiol*, 7, 115-9.
- Surget, S., M. P. Khoury & J. C. Bourdon (2014) Uncovering the role of p53 splice variants in human malignancy: a clinical perspective. *Onco Targets Ther*, 7, 57-68.
- Swan, T. M. & K. Watson (1998) Stress tolerance in a yeast sterol auxotroph: role of ergosterol, heat shock proteins and trehalose. *FEMS Microbiol Lett*, 169, 191-7.
- Takahashi, H., J. H. U. S. o. M. High Throughput Biology Center, 339 Broadway Research Building, 733 North Broadway, Baltimore, Maryland 21205, J. M. McCaffery, J. H. U. Department of Biology and Integrated Imaging Center, Baltimore, Maryland 21218, R. A. Irizarry, J. H. U. S. o. P. H. Department of Biostatistics, Baltimore, Maryland 21205, J. D. Boeke, jboeke@jhmi.edu & J. H. U. S. o. M. High Throughput Biology Center, 339 Broadway Research Building, 733 North Broadway, Baltimore, Maryland 21205 (2006) Nucleocytosolic Acetyl-Coenzyme A Synthetase Is Required for Histone Acetylation and Global Transcription. *Molecular Cell*, 23, 207-217.
- Talcott, B. & M. S. Moore (1999) Getting across the nuclear pore complex. *Trends Cell Biol*, 9, 312-8.
- Tang, Y., M. A. Holbert, H. Wurtele, K. Meeth, W. Rocha, M. Gharib, E. Jiang, P. Thibault, A. Verreault, P. A. Cole & R. Marmorstein (2008) Fungal Rtt109 histone acetyltransferase is an unexpected structural homolog of metazoan p300/CBP. *Nat Struct Mol Biol*, 15, 738-45.

- Tanner, K. G., M. R. Langer, Y. Kim & J. M. Denu (2000) Kinetic mechanism of the histone acetyltransferase GCN5 from yeast. *J Biol Chem*, 275, 22048-55.
- The UniProt Consortium (2017) UniProt: the universal protein knowledgebase. *Nucleic Acids Res*, 45, D158-D169.
- Torres, L., H. Martín, M. I. García-Saez, J. Arroyo, M. Molina, M. Sánchez & C. Nombela (1991) A protein kinase gene complements the lytic phenotype of *Saccharomyces cerevisiae* *lyt2* mutants. *Mol Microbiol*, 5, 2845-54.
- Verghese, J., J. Abrams, Y. Wang & K. A. Morano (2012) Biology of the heat shock response and protein chaperones: budding yeast (*Saccharomyces cerevisiae*) as a model system. *Microbiol Mol Biol Rev*, 76, 115-58.
- Vihervaara, A., C. Sergelius, J. Vasara, M. A. Blom, A. N. Elsing, P. Roos-Mattjus & L. Sistonen (2013) Transcriptional response to stress in the dynamic chromatin environment of cycling and mitotic cells. *Proc Natl Acad Sci U S A*, 110, E3388-97.
- Vital, M., A. C. Howe, J. M. Tiedje & M. A. Moran (2014) Revealing the Bacterial Butyrate Synthesis Pathways by Analyzing (Meta)genomic Data.
- Voellmy, R. & F. Boellmann (2007) Chaperone regulation of the heat shock protein response. *Adv Exp Med Biol*, 594, 89-99.
- Wade, J. T., D. B. Hall & K. Struhl (2004) The transcription factor Ifh1 is a key regulator of yeast ribosomal protein genes. *Nature*, 432, 1054-8.
- Wang, L., Y. Tang, P. A. Cole & R. Marmorstein (2008) Structure and chemistry of the p300/CBP and Rtt109 histone acetyltransferases: implications for histone acetyltransferase evolution and function. *Curr Opin Struct Biol*, 18, 741-7.
- Wani, W. Y., M. Boyer-Guittaut, M. Dodson, J. Chatham, V. Darley-Usmar & J. Zhang (2015) Regulation of autophagy by protein post-translational modification. *Lab Invest*, 95, 14-25.
- Weinert, B. T., V. Iesmantavicius, T. Moustafa, C. Scholz, S. A. Wagner, C. Magnes, R. Zechner & C. Choudhary (2014) Acetylation dynamics and stoichiometry in *Saccharomyces cerevisiae*. *Mol Syst Biol*, 10, 716.
- Weinert, B. T., T. Moustafa, V. Iesmantavicius, R. Zechner & C. Choudhary (2015) Analysis of acetylation stoichiometry suggests that SIRT3 repairs nonenzymatic acetylation lesions. *EMBO J*, 34, 2620-32.
- Weinert, B. T., S. A. Wagner, H. Horn, P. Henriksen, W. R. Liu, J. V. Olsen, L. J. Jensen & C. Choudhary (2011) Proteome-wide mapping of the *Drosophila* acetylome demonstrates a high degree of conservation of lysine acetylation. *Sci Signal*, 4, ra48.
- Wente, S. R. & M. P. Rout (2010) The nuclear pore complex and nuclear transport. *Cold Spring Harb Perspect Biol*, 2, a000562.

- Werner-Washburne, M., D. E. Stone & E. A. Craig (1987) Complex interactions among members of an essential subfamily of hsp70 genes in *Saccharomyces cerevisiae*. *Mol Cell Biol*, 7, 2568-77.
- Westerheide, S. D., J. Anckar, S. M. Stevens, L. Sistonen & R. I. Morimoto (2009) Stress-inducible regulation of heat shock factor 1 by the deacetylase SIRT1. *Science*, 323, 1063-6.
- Xu, L., Nitika, N. Hasin, D. D. Cuskelly, D. Wolfgeher, S. Doyle, P. Moynagh, S. Perrett, G. W. Jones & A. W. Truman (2019) Rapid deacetylation of yeast Hsp70 mediates the cellular response to heat stress. *Sci Rep*, 9, 16260.
- Yates, B., B. Braschi, K. A. Gray, R. L. Seal, S. Tweedie & E. A. Bruford (2017) Genenames.org: the HGNC and VGNC resources in 2017. *Nucleic Acids Res*, 45, D619-D625.
- Zhao, S., W. Xu, W. Jiang, W. Yu, Y. Lin, T. Zhang, J. Yao, L. Zhou, Y. Zeng, H. Li, Y. Li, J. Shi, W. An, S. M. Hancock, F. He, L. Qin, J. Chin, P. Yang, X. Chen, Q. Lei, Y. Xiong & K. L. Guan (2010) Regulation of cellular metabolism by protein lysine acetylation. *Science*, 327, 1000-4.
- Zheng, K., Y. Jiang, Z. He, K. Kitazato & Y. Wang (2017) Cellular defense or viral assist: the dilemma of HDAC6. *J Gen Virol*, 98, 322-337.
- Zhou, Y., C. He, L. Wang & B. Ge (2017) Post-translational regulation of antiviral innate signaling. *Eur J Immunol*, 47, 1414-1426.

Chapter 2 Identifying the dynamics of protein acetylation in response to heat shock

Rebecca E. Hardman^{1,2}, Aaron J. Storey³, Stephanie D. Byrum³, Samuel G. Mackintosh³, Rick D. Edmondson⁴, Wayne P. Wahls³, Alan J. Tackett³, and Jeffrey A. Lewis²

1 Interdisciplinary Graduate Program in Cell and Molecular Biology, University of Arkansas, Fayetteville, Arkansas, United States of America

2 Department of Biological Sciences, University of Arkansas, Fayetteville, Arkansas, United States of America

3 Department of Biochemistry and Molecular Biology, University of Arkansas for Medical Sciences, Little Rock, Arkansas 72205, United States of America

4 College of Medicine, University of Arkansas for Medical Sciences, Little Rock, Arkansas 72205, United States of America

Author Contributions: AJS, SDB, and SGM performed all mass spectrometry protocols and data analysis. JAL performed Limma statistical analysis. All remaining work was conceived and planned by JAL and REH and performed by REH.

2.1 Abstract

Cells have evolved a wide variety of mechanisms to alter protein activity in response to environmental changes. One such mechanism is covalent post-translational protein modification. We have known that cells to modify proteins in this fashion for decades, but recent technological advancements have dramatically increased the number of known modifications as well as the widespread nature of these modifications throughout the proteome. While previously considered isolated to the nucleus, recent studies have shown that acetylation is much more prevalent than previously thought. While the number of known acetylation sites has significantly increased, the possible role(s) of these modifications remains largely unknown. To better understand possible functions of this modification in the cell, we examined all acetylated proteins in the cell, referred to here on as the acetylome, of the yeast *Saccharomyces cerevisiae* across a four-hour heat shock and identified over 1400 acetylated peptides representing almost 600 proteins. Of those, 387 residues representing 207 unique proteins show a significant change in acetylation compared to unstressed cells. These proteins are enriched for many cellular processes, suggesting that acetylation may play a much wider regulatory role than previously believed.

2.2 Introduction

While they may be called the “basic units of life,” the multitude of processes occurring within the cell are anything but basic. Throughout the course of evolution, cells have become finely tuned to meet the daily demands for everything from the simplest bacteria to complex multicellular organisms such as animals and plants. To do this, cells have evolved a variety of regulatory mechanisms to finely control the expression of thousands of genes and the activity of their products to optimize the response to the constant onslaught of environmental changes. Previous studies in yeast have identified a core set of genes that are either induced or repressed in response to a variety of environmental stresses termed the environmental stress response (Gasch et al. 2000b). Processes that are upregulated in response to stress include carbohydrate metabolism, redox reactions, protein folding, and fatty acid metabolism, and repressed processes center around translation including RNA metabolism and ribosome assembly. These changes, however, are not required to survive the initial stress, but rather serve as a preemptive measure against impending, more severe stresses (Giaever et al. 2002, Berry and Gasch 2008). This suggests that other, rapid-acting mechanisms must be responsible for the ability to survive the initial stress.

One such mechanism is the use of post-translational modifications, or PTMs. These are covalent modifications on various amino acids that can dramatically change protein activity through altered stability, binding affinity, structural confirmation, and targeting for degradation. While the transcriptional response to a rapid environmental change can take in the order of minutes (Vihervaara et al. 2017, Gasch et al. 2000b), post-translational modifications can occur within seconds to re-tune protein function to better survive a wide variety of conditions such as starvation, temperature fluctuation, oxidation, and so on. Currently, there are hundreds of known PTMs, the most well studied of which being phosphorylation, glycosylation, methylation, ubiquitination, and the topic of this dissertation, acetylation (Khoury, Baliban and Floudas 2011).

Protein acetylation is a reversible modification in which an acetyl group is transferred to the ϵ -amine of a lysine side chain by lysine acetyltransferases, or KATs. This consequently negates the positive charge in that region of the protein, modifying how the protein is able to interact with its environment. This can be reversed, however, by a member of the lysine deacetylases, or KDACs. This is done in one of two ways: class I and II KDACs hydrolyze the acetyl group releasing acetate while class III KDACs, known as the sirtuins, use NAD⁺ to remove the acetyl group, producing nicotinamide and O'-acetyl-ADP-ribose (Menzies et al. 2016).

Though first discovered in the early 1960s (Allfrey et al. 1964, Phillips 1963), we have only recently begun to realize the true breadth of protein acetylation in the cell. With recent advancements in mass spectrometry and immunoaffinity enrichment, thousands of new acetylation targets have been discovered across all domains of life (Liu et al. 2017, Castaño-Cerezo et al. 2014, Chen et al. 2018b, Weinert et al. 2011, Lundby et al. 2012, Henriksen et al. 2012, Hartl et al. 2017). While it was previously believed that protein acetylation was predominantly confined to the nucleus and mitochondria, most newly identified targets are found throughout the cell, implicating a large variety of cellular processes including metabolism, translation, and the cellular stress response. The majority of these global studies, however, have been done in steady-state conditions, which gives little insight into whether or not the modification is regulatory, structural, or simply an artifact.

To better understand the possible role(s) acetylation is playing in the cell, we wanted to look at acetylation dynamics in cells responding to changing environmental conditions. Based on previous work by Henriksen et al (2012), we chose to look at acetyl dynamics in cells experiencing a mild heat shock at 37°C over four hours, as proteins involved in the response to heat were enriched for acetylation. Analysis of this data has revealed that the acetylome is highly dynamic in response to heat. Here we report over 300 lysine residues experiencing a significant change in acetylation during heat shock, representing over 200 proteins involved in a

variety of cellular processes. Surprisingly, the peak acetylation response was seen around 90 minutes, which is much later than that seen with other PTMs (Kanshin et al. 2015a), suggesting that this response is not largely involved in initial survival, but could possibly be in preparation for worsening conditions, as seen with the transcriptional stress response (Berry and Gasch 2008, Giaever et al. 2002). We were also able to identify possible lysine acetyltransferases (KATs) and lysine deacetylases (KDACs) by comparing proteins experiencing changes in acetylation to known interaction partners of enzymatic subunits from these complexes.

2.3 Materials and Methods

2.3.1 Strains

All experiments in this chapter were carried out using the lab strain BY4741 (MATa *his3Δ1 leu2Δ0 met15Δ0 ura3Δ0*) and were performed in YPD (1% yeast extract, 2% peptone, 2% dextrose).

2.3.2 Acquired thermotolerance assays.

Cells were grown to saturation and then subcultured into a 50 mL YPD culture and grown for at least 8 generations to mid-log phase at 25°C, 270 rpm and 6, 5 mL aliquots were transferred to glass tubes. The protein synthesis inhibitor cycloheximide (Fisher, R663222) and KDAC inhibitors Trichostatin A (Fisher, 14-061) and nicotinamide (Fisher, AC12827) were added as indicated in table 2.1 and all samples were placed back at 25°C for 20 minutes to allow inhibitors to take effect. Samples were collected by centrifugation at 1500 x g for 3 min and suspended in either mock (25°C) or stress (37°C) media containing the same concentrations of inhibitors. Cells were incubated at their respective temperatures for 1 hour with 270 rpm shaking.

Following the primary stress, the OD₆₀₀ (Unico) of each sample was taken and cells were collected by centrifugation at 1500 x g for 3 minutes and suspended to a final OD₆₀₀ of 0.6 in

YPD containing no additional inhibitors. 50 µl of each sample was transferred to one row of a 96-well PCR plate which was subsequently sealed with a breathable membrane. Cells were then stressed in a gradient of 42°C to 48°C (Table 2.2) in a thermocycler (Bio-Rad DNA Engine) for 1 hour for the secondary stress. Cells were mixed, and samples from 42°C (100% viability) and 45°C were diluted 1:10 and then serially diluted 1:5 in fresh YPD. 100 µl of dilutions determined to provide the optimal final colony-forming unit (CFU) count were plated onto YPD and spread using sterile glass beads. All plates were incubated at 30°C until colonies were visible and CFU/mL was calculated to determine viability.

Table 2.1 Inhibitors added for acquisition experiment

Inhibitor	Sample					
	YPD 25	YPD 37	CHX 25	CHX 37	CTN 25	CTN 37
Cycloheximide	--	--	10µg/mL	10µg/mL	10µg/mL	10µg/mL
Trichostatin A	--	--	--	--	10µM	10µM
Nicotinamide	--	--	--	--	5mM	5mM

Table 2.2 Secondary Stress Gradient

Row	1	2	3	4	5	6	7	8	9	10	11	12
Temperature (°C)	42.0	42.2	42.5	43.0	43.7	44.6	45.6	46.5	47.1	47.6	47.9	48.0

2.3.2 Western blot analysis of whole-cell lysate

Cells were grown to saturation and then subcultured into 2, 250 mL YPD cultures grown for at least 8 generations to mid-log phase at 25°C, 270 rpm in an oscillating water bath and an unstressed sample was collected. 50 mL of the remaining sample was collected by centrifugation and suspended in prewarmed 37°C media and incubated an additional hour at 37°C. Cells were spheroplasted in 500 µl of 1M sorbitol, 50 mM Tris pH 7.5 by vortexing with glass beads for 1 hour. Spheroplasts were transferred to lysis buffer (20mM Tris pH 7.5, 1 mM EDTA, 150 mM NaCl, 1% Triton X-100, 50 mM sodium butyrate, 100 µM Trichostatin A, 50 mM Nicotinamide, protease inhibitor cocktail (Sigma, P8849)) where they lysed due to osmotic

pressure change. Equal amounts of lysate from both unstressed and stressed cells were resolved by SDS-PAGE, followed by Western blot analysis using an anti-acetyl lysine-specific primary antibody (Cell Signaling Technology, 9681S) and fluorescently labeled secondary antibodies (Licor, 926-32212). Fluorescent detection was performed on a LiCor Odyssey imaging system.

2.3.3 2-D electrophoretic analysis of acetyl-enriched peptides

Following subculture into 500 mL YPD in a 2 L flask from saturation, cells were grown to mid-log phase at 25°C, 270 rpm and 250 mL of unstressed sample were collected. The remaining sample was resuspended in 250 mL prewarmed 37°C YPD and incubated an additional hour at 37°C. Cells were lysed by bead beating in 50 mM MOPS, 10 mM sodium phosphate, 50 mM NaCl, 50 mM sodium butyrate, 100 µM Trichostatin A, 50 mM nicotinamide, and protease inhibitor cocktail (Sigma, P8849). Acetylated proteins were immunoprecipitated using anti-acetyl lysine resin (ImmuneChem, ICP0388). Equal amounts of cell lysate from both samples were resolved via 2-DE, using a 3-10 pH range for isoelectric focusing and a gradient of 8-16% SDS-PAGE for the second dimension. Proteins were visualized via silver staining (Chevallet, Luche and Rabilloud 2006).

2.3.4 Collection for global acetylation analysis

2, 1 L YPD cultures were started from a 2 mL saturated YPD culture, grown to an OD600 between 0.7 and 0.8 with a minimum of 8 doublings at 25°C and 125 rpm shaking, and pooled. 500mL of culture was then aliquoted into 2, 4 L flasks to which 500mL 55°C YPD was added, immediately bringing the final temperature to 37°C. To a third 4L flask, 250 mL of culture was aliquoted and 250 mL 25°C YPD and 500 mL 55°C YPD was added to prevent the later time points from entering diauxic shift. All three flasks were placed at 37°C, 125 rpm for 5, 10, 15, 30, 45, 60, 90, 120, and 240 minutes. 120 mL from the remaining culture was collected for

an unstressed sample via vacuum filtration and scraping into liquid nitrogen and stored at -80°C. Three time points were collected per heat-treated flask to ensure appropriate aeration was maintained. At each time point, 120 mL was collected via vacuum filtration and scraping into liquid nitrogen and stored at -80°C.

2.3.5 Cell lysis and TMT10 labeling

Sample processing was performed similarly to that found in Hebert et al. 2018. Samples were thawed at room temperature and collected by centrifugation at 4696xg for 2 minutes. The remaining media was removed, and cells were suspended in 1mL water, transferred to a 1.5mL microcentrifuge tube, and centrifuged at 10,000xg to remove water. Samples were suspended in 150µl 6M guanidine hydrochloride (GnHCl), 100 mM Tris pH 8 and lysed by boiling for 5 minutes, followed by a 5-minute rest at room temperature, and a second boil for 5 minutes. Samples were precipitated with 90% MeOH. Pellet was resuspended in 1mL 8M urea in 100mM Tris pH 8.0, diluted to 2M urea with 100mM Tris pH 8.0 and protein concentration was quantified by Bradford Assay. All lysate was digested with a 1:50 ratio of trypsin overnight at 25°C to prevent carbamylation due to the presence of urea with gentle mixing with 2.5mM TCEP and 10mM chloroacetamide for reduction and alkylation. Digestion was quenched with 0.6% TFA to a pH less than 2 and peptides were desalted and lyophilized. A detailed protocol for peptide desalting can be found on the protocols.io repository under DOI dx.doi.org/10.17504/protocols.io.3hegj3e. Peptides were resuspended in 200mM TEAB to a final concentration of ~8µg, quantitated with Pierce Colorimetric Peptide Assay, and diluted to 5µg/µl in 200mM TEAB. 100µl representing 500µg of each sample was mixed with one of ten TMT isobaric labels (ThermoFisher) reconstituted in 50µl acetonitrile. Samples were incubated at RT for 1 hour. Labeling was quenched with 8µl 5% hydroxylamine for 15 minutes and samples were combined, desalted, and lyophilized. A detailed protocol for cell lysis and TMT labeling can be found at dx.doi.org/10.17504/protocols.io.3g9gjz6.

2.3.6 High pH fractionation

Peptides were dissolved in 110 μ l, 10mM ammonium bicarbonate, pH 10.0, 2 μ l was removed for unenriched analysis, and the remaining sample was fractionated using an Agilent 300 Extend C18 column (770995-902) in a gradient of 0-100% acetonitrile in 10mM ammonium bicarbonate, pH 10.0 on a Shimadzu LC-20AP system. The first 10 min (flow-through) were collected as fraction 1 and the remaining fractions were collected for 2.5 minutes for a total of 10 fractions, and then back to fraction 1 for an additional 2.5 minutes each. All fractions were frozen in liquid N₂ and lyophilized.

2.3.7 Acetyl-lysine Enrichment

Each fraction was dissolved in 1.4mL IAP buffer (50mM MOPS pH 7.2, 10mM Na₂HPO₄, 50mM NaCl), transferred to a tube containing 40 μ l of washed PTMScan Acetyl-Lysine Motif [Ac-K] IAP Beads (Cell Signaling Technology, 13362S), and incubated for 2hrs at 4°C with rotation. After washing 3x with 1mL IAP buffer and 3x with ultrapure water at 4°C, peptides were eluted with 0.15% TFA (one elution with 55 μ l for 10 min at RT and one elution with 50 μ l for 10 min at RT) as per manufacturer protocol. Both eluents were combined in a 1.5mL microcentrifuge tube and frozen at -80°C until shipment for mass spectrometry.

2.3.8 LC-MS/MS Data Analysis

The following was performed at the proteomics core facility at the University of Arkansas for Medical Sciences. Whole peptides were fractionated on a 100 mm x 1.0 mm Acquity BEH C18 column (Waters) using an UltiMate 3000 UHPLC system (ThermoFisher Scientific) with a 40-min gradient from 99:1 to 60:40 buffer A:B ratio under basic pH conditions (buffer A = 0.05% acetonitrile, 10 mM NH₄OH; buffer B = 100% acetonitrile, 10 mM NH₄OH). The individual fractions were then consolidated into 24 super-fractions using the checkerboard strategy described in Yang et al. 2012.

Super fractions were loaded on a 150 mm x 0.075 mm column packed with Waters C18 CSH resin. Peptides were eluted using a 45-min gradient from 96:4 to 75:25 buffer A:B ratio into an Orbitrap Fusion Lumos mass spectrometer (Thermo Fischer Scientific). MS acquisition consisted of a full scan at 120,000 resolution, maximum injection time of 50 ms, and AGC target of 7.5×10^5 . Selection filters consisted of monoisotopic peak determination, charge state 2-7, intensity threshold of 2.0×10^4 , and mass range of 400-1200 m/z. Dynamic exclusion length was set to 15 seconds. Data-dependent cycle time was set for 2.5 seconds. Selected precursors were fragmented using CID 35% with an AGC target of 5.0×10^3 and a maximum injection time of 50 ms. MS² scans were followed by synchronous precursor selection of the 10 most abundant fragment ions, which were fragmented with HCD 65% and scanned in the Orbitrap at 50,000 resolution, AGC target of 5.0×10^4 and maximum injection time of 86 ms.

Proteins were identified by database search using MaxQuant50 (Max Planck Institute) using the Uniprot *S. cerevisiae* database from October 2014,51 with a parent ion tolerance of 3 ppm and a fragment ion tolerance of 0.5 Da. Carbamidomethylation of cysteine residues and TMT-labelling (+229.16) of peptide N-termini were used as fixed modifications. Acetylation of lysine residues and protein N-termini, oxidation of methionine, and TMT-labelling of peptide N-termini were selected as variable modifications. Mascot searches were performed using the same parameters as above, but with peptide N-terminal fixed modification of TMT 10-plex, and variable modifications of TMT + diglycine (+343.2) and TMT 10-plex on lysine residues, and phosphorylation (+79.97) of serine and threonine. Mascot search results were imported into Scaffold software (v4)52 and filtered for protein and peptide false discovery rates of 1%. Data normalization and analyses were performed using R. Reporter ion intensities were log₂ transformed, mean-centered for each spectrum, then median-centered for each channel. Peptide and protein quantitative values were obtained by taking the average of the quantitative values for all spectra mapping to the peptide or protein. All raw mass spectrometry data and MaxQuant search results have been deposited to the ProteomeXchange Consortium via the

PRIDE53 partner repository with the dataset identifier PXD014552 and 10.6019/PXD014552.

Figure 2.1 provides a graphical depiction of the TMT-10 workflow.

2.3.9 Statistical analysis, clustering, and enrichment, and motif analysis

Proteins and acetyl peptide marks with significant abundance differences in response to heat at each time point relative to the unstressed control were identified by performing an empirical Bayes moderated *t*-test using the BioConductor package Limma v 3.36.2 and Benjamini-Hochberg FDR correction (Ritchie et al. 2015). An FDR cutoff of 0.05 was used.

Peptide clustering was performed with Cluster 3.0 (<http://bonsai.hgc.jp/~mdehoon/software/cluster/software.htm>) using hierarchical clustering and Euclidian distance as the metric with centroid linkage (Eisen et al. 1998). Timepoints were weighted using a cutoff value of 0.4 and an exponent value of 1. The heat map was generated using Java TreeView v. 1.1.6r4 (Saldanha and Department of Genetics 2019). Clusters were manually chosen with a minimum correlation of 0.9.

Cellular process enrichments of gene ontology (GO) categories were performed using GO-TermFinder (Boyle et al. 2004b) with Bonferroni-corrected *P*-values < 0.01 taken as significant. KAT and KDAC enrichments were determined by performing Fisher's exact test (<https://systems.crupp.ucla.edu/hypergeometric/>) where the population size (*N*) is the number of genes in the yeast genome, 7166, the number of successes in the population (*M*) is the number of genes in the cluster, the sample size (*s*) is the total number of known KAT/KDAC interactions retrieved from the *Saccharomyces* Genome Database (SGD, Cherry et al. 2012), and the number of successes (*k*) is the number of genes found in both *M* and *s*.

Motif analysis was performed using the motif-x algorithm with a *p*-value threshold of 0.05 in the modification motifs (MoMo) tool found in the MEME suite (Cheng et al. 2019).

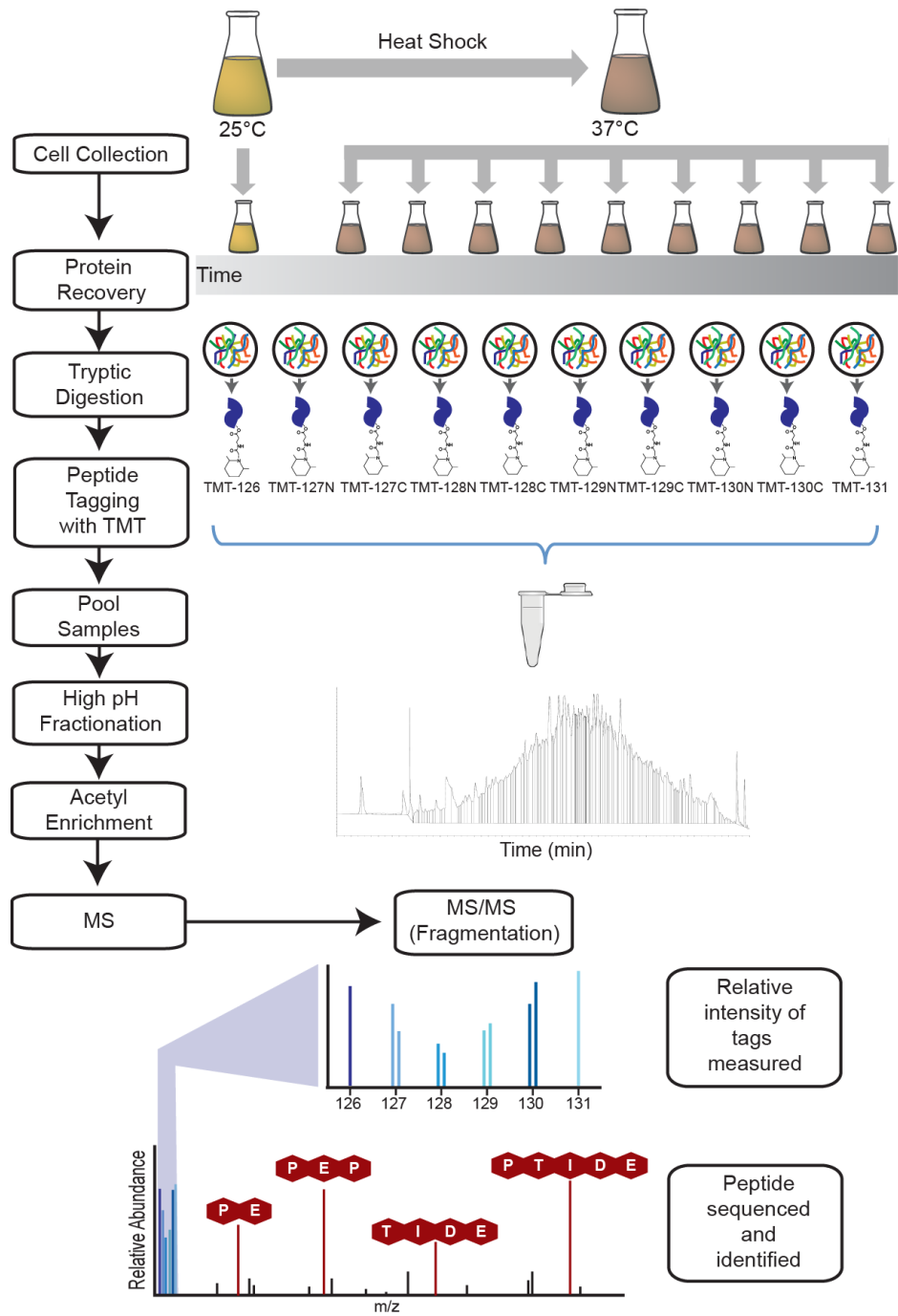


Figure 2.1 Schematic for TMT-10 acetyl proteomics.

2.4 Results and Discussion

2.4.1 Acetylation is required for the full acquisition of thermotolerance.

To determine the extent to which protein acetylation plays any role in the yeast response to heat shock, we began by looking at the effect of lysine deacetylase (KDAC) inhibitors on the phenotype of thermotolerance acquisition. Thermotolerance acquisition is the phenomenon in which cells treated with mild heat stress are able to survive much higher subsequent temperatures (Fig. 2.2). So that the effects we were seeing were not solely due to disruption of protein synthesis via histone deacetylation inhibition, we included the protein synthesis inhibitor cycloheximide in both control and KDAC inhibited samples. If inhibition of protein synthesis does not decrease acquisition, this suggests that there are other mechanisms at play, such as post-translational modification like acetylation.

In protein synthesis inhibited samples alone, we see only a very mild, non-statistically significant decrease in the cells' ability to acquire thermotolerance (Fig. 2.3). With the addition of the lysine deacetylase inhibitors Trichostatin A and nicotinamide, however, we see a significant decrease in thermotolerance acquisition. This suggests that while protein acetylation is not essential for thermotolerance, seen in the fact that the cells still showed some acquisition, it does play a role to some extent other than through transcriptional regulation.

2.4.2 The acetylome exhibits clear remodeling in response to heat shock.

To determine if there were any visible changes in the yeast acetylome in response to heat stress, we performed western blot analysis on whole cell lysate from cells grown in unstressed conditions at 25°C and under a mild heat shock of 37°C for 60 minutes using an anti-acetyllysine primary antibody (Fig. 2.4). While not the most sensitive, this clearly shows that there are species acetylated in one condition, but not the other.

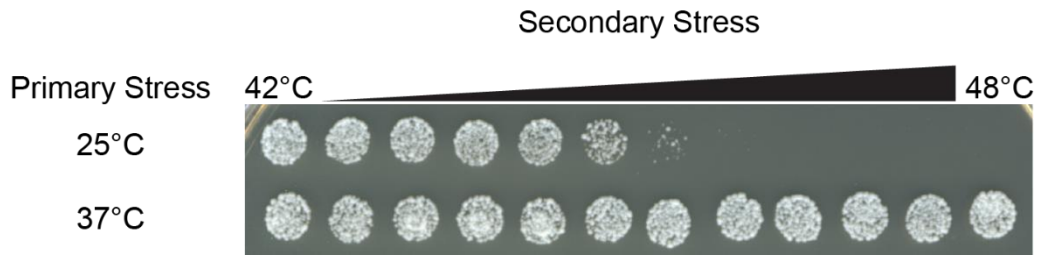


Figure 2.2 Mild primary stress protects against severe secondary stress. Cells were exposed to either 25°C or a mild primary stress of 37°C for one hour. After normalizing to an OD600 of 0.6, each sample was transferred to one row of a 96-well PCR plate and subjected to a range of more severe secondary stresses from 42°C to 48°C, diluted and plated on YPD, and incubated at 30°C until colonies were visible. Cells exposed to a mild primary stress can survive much higher subsequent temperatures than without the primary stress. This phenomenon is called thermotolerance acquisition.

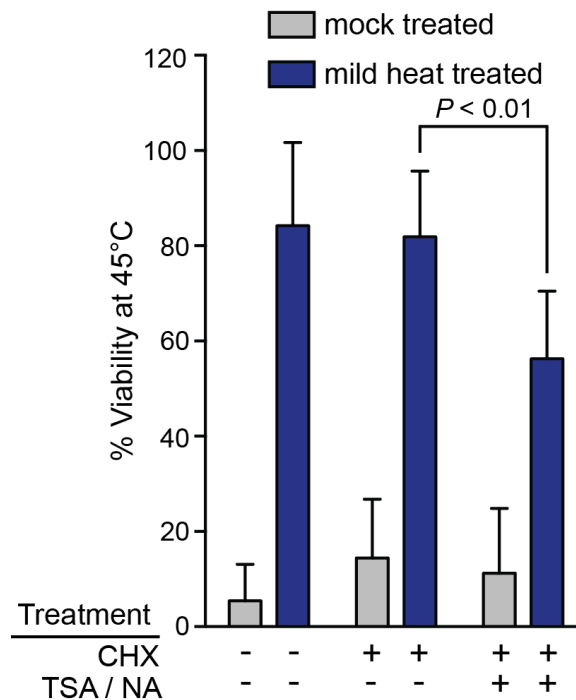


Figure 2.3 Protein acetylation deregulation decreases thermotolerance acquisition.

Cells were exposed to either 25°C or a mild primary stress of 37°C followed by a more severe stress of 45°C with and without protein inhibition with cycloheximide (CHX) and the KDAC inhibitors trichostatin a (TSA) and nicotinamide (NA). Percent viability was calculated by the CFU count of cells stressed at 45°C compared to cells exhibiting 100% viability at 42°C. While cells experience protein synthesis inhibition showed a non-significant decrease in thermotolerance acquisition, cells in which lysine deacetylation was inhibited showed a dramatic decrease. This suggests that properly regulated lysine deacetylation plays an important role in thermotolerance acquisition.

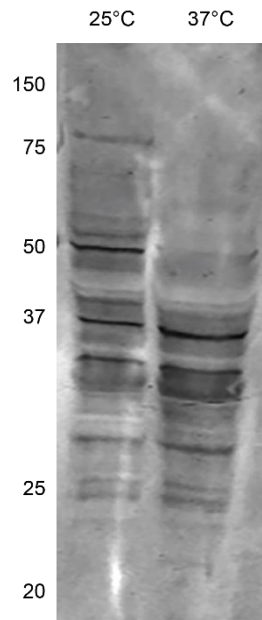


Figure 2.4 Western blot analysis shows differences in acetylation between stressed (37°C) and unstressed (25°C) cells. Equal amounts of lysate from both unstressed and stressed cells were resolved by SDS-PAGE, followed by Western blot analysis using an anti-acetyl lysine-specific primary antibody and fluorescently labeled secondary antibodies. The acetylome clearly shows remodeling in response to heat stress.

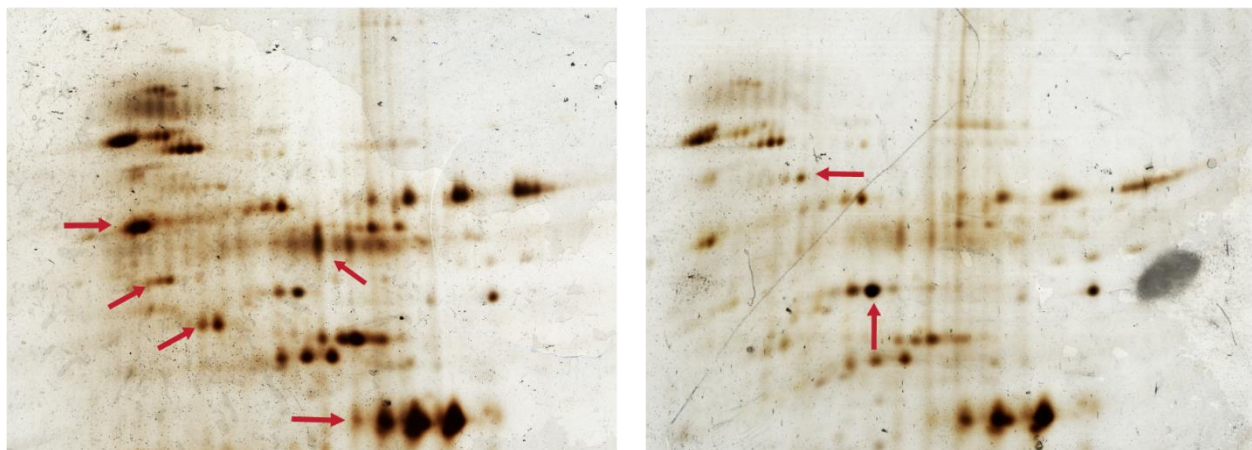


Figure 2.5 Two-dimensional gel electrophoresis (2-DE) of acetylated proteins identifies numerous changes in the acetylome during heat shock. Acetylated proteins from stressed (37°C) and unstressed (25°C) cells were immunoprecipitated using anti-acetyl lysine resin and equal amounts of cell lysate from both samples were resolved via 2-DE. Samples were visualized via silver staining. Again, we see clear remodeling of the acetylome in response to heat stress.

To increase visibility and sensitivity, 2-dimensional gel electrophoresis was performed on samples collected as before, but this time acetylated lysines were enriched using an anti-acetyllysine resin (ImmuneChem). Again, there are clear differences between the two samples suggesting that there are at least some proteins that are experiencing acetylation changes in response to heat stress (Fig. 2.5). This provided the necessary confidence to proceed with more in-depth experimentation.

2.4.2 The acetylome is highly dynamic in response to heat stress.

To further investigate previous experiments suggesting global changes in protein acetylation occur in response to heat shock, we performed a time-scale analysis of acetylated protein species over the course of a 4-hour heat shock. While this temperature is elevated enough to illicit the heat shock response, it is not severe enough to decrease viability, allowing us to monitor the acetylation dynamics occurring in this response. Samples were collected at 5, 10, 15, 30, 45, 60, 90, 120, and 240 minutes following initiation of a 37°C heat shock, digested, labeled using isobaric tandem mass tags (TMT) for multiplexing, enriched using an anti-acetyllysine resin, and analyzed on an Orbitrap mass spectrometer. Enrichment paired with the extreme sensitivity of the Orbitrap allowed us to detect acetylation sites across hundreds of proteins throughout the time course (Fig. 2.1) (Storey et al. 2019).

In triplicate, we identified 1473 acetylated peptides representing 596 proteins. Of those, 387 residues representing 207 unique proteins showed a significant fold change (Benjamini-Hochberg corrected p-value <0.05) in acetylation in at least one time point compared to the pre-stress sample. Surprisingly, the majority and the largest fold change of this response occurred at the 90 min time point with 74% of changing residues showing a significant fold change at this time point (Fig. 2.6 and Fig 2.7). Post-translational modifications are often regarded as a means

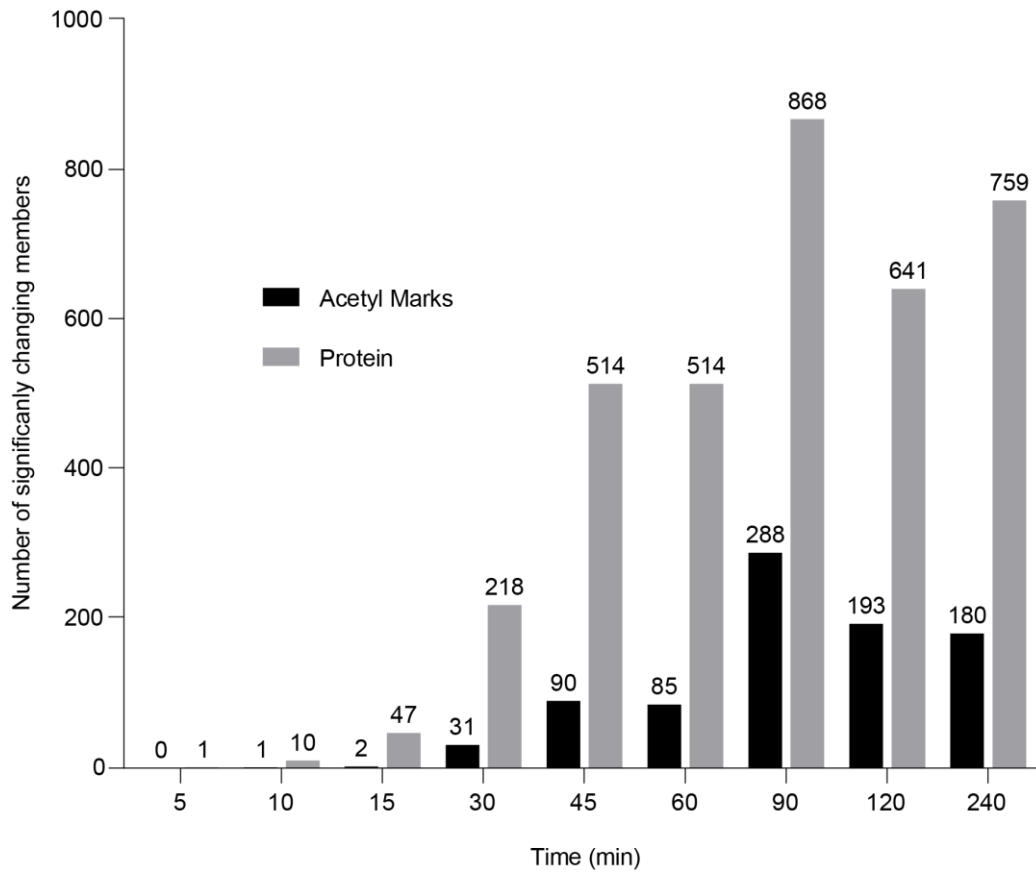


Figure 2.6 The majority of significant acetylation events occur at 90 minutes of heat shock. The number of significant differentially acetylated peptides and differentially expressed proteins at each time point.

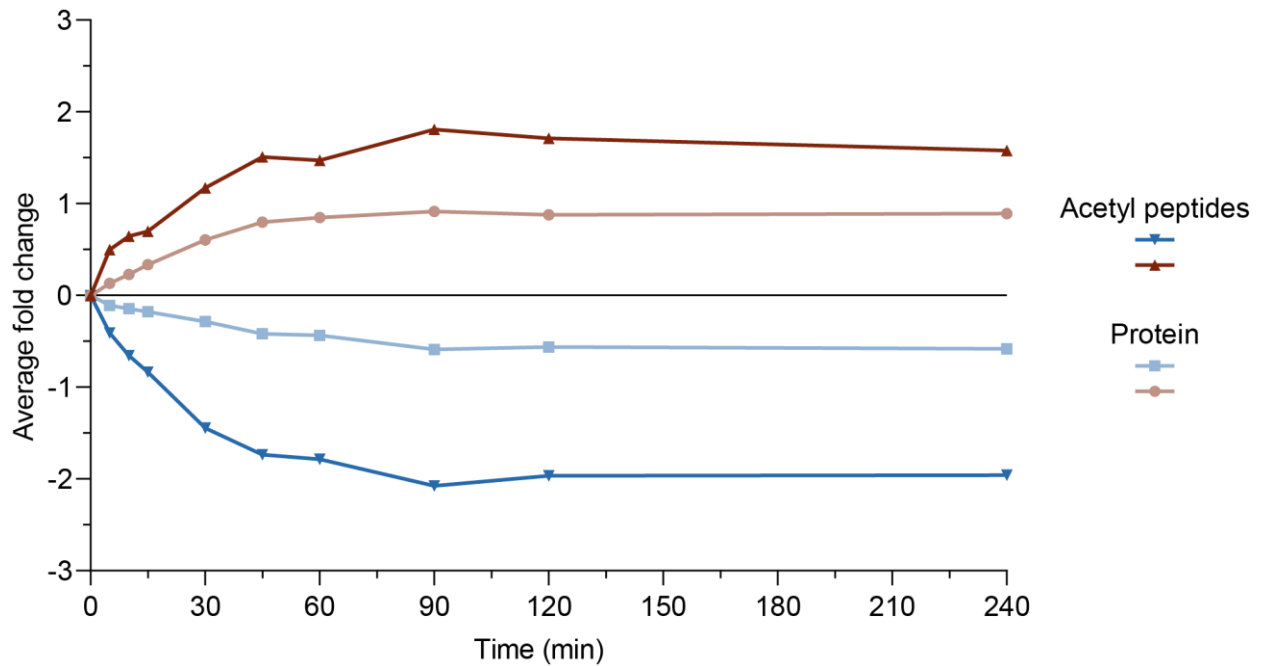


Figure 2.7 Average acetyl fold changes compared to corresponding protein fold changes.

The average fold change at each time point of all acetyl peptides and proteins experiencing a significant change in at least three time points (FDR < 0.05). The maximum average fold change in both increasing and decreasing acetyl marks is at 90 minutes, whereas protein level changes appear constant after 60 minutes.

of rapid protein regulation occurring before the cell has had enough time to perform the necessary translational response, which appears to be the case for other PTMs such as phosphorylation which levels off around 20 minutes in response to heat (Kanshin et al. 2015a). This does not appear to be the case for the majority of acetylation changes in the response to heat stress.

Also of interest, over a third of proteins with significantly changing acetyl marks (34%) had more than one significantly changing residue (Fig. 2.8), the most affected of which is the translation elongation factor Tef1p with 10 significantly changing acetyl marks. Proteins with fewer than 4 changing marks were enriched for processes such as translation, metabolism, and gene expression. Proteins with greater than 4 changing marks, however, were enriched for protein folding and refolding, and the cellular response to heat (Table 2.3). This strengthens our suspicions that acetylation is a key regulatory mechanism during the response to heat. We also identified 36 non-histone proteins with both increasing and decreasing acetyl marks during the heat shock (Fig. 2.9). These proteins show process enrichments for a variety of cellular processes including protein folding ($p = 4.21 \times 10^{-7}$) and refolding ($p = 1.33 \times 10^{-9}$), small molecule biosynthesis ($p = 8.26 \times 10^{-6}$), carbohydrate metabolism (2.1×10^{-4}), and translation ($p = 1.89 \times 10^{-13}$), 14 belonging to the ribosome. The fact that we see increasing and decreasing acetylation on the same protein suggests that this modification is being regulated and is not just occurring due to aberrant KAT and KDAC function or simply chemical acetylation, a common criticism of acetylation studies.

Another trend suggesting that this response is being regulated and not happening by chance is the fact that some proteins that show significant changes in protein acetylation are not experiencing changes in concentration. If no regulation were occurring, one would expect that proteins showing greater concentration increases would show greater acetylation changes and the opposite for proteins decreasing in concentration. As concentration increases, proteins are more likely to interact with acetyltransferases and deacetylations which could lead to spurious

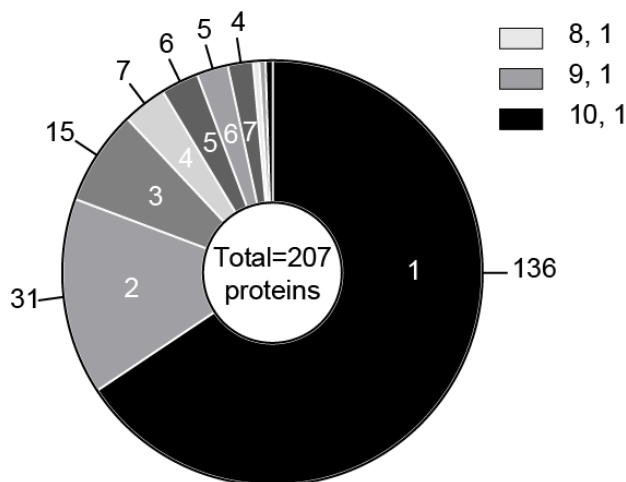


Figure 2.8 Number of significantly changing acetyl peptides per protein.

Table 2.3 Cellular process enrichments by number of changing acetyl peptides

1 acetyl mark	p-value	4+ acetyl marks	p-value
cytoplasmic translation	1.05E-	'de novo' protein folding	2.15E-
metabolic process	9.83E-	protein refolding	2.37E-
nitrogen metabolic process	1.08E-	protein folding	2.12E-
biosynthetic process	4.82E-	ADP metabolic process	1.99E-
ribosome biogenesis	8.04E-	cellular response to heat	2.93E-
gene expression	5.13E-	glycolytic process	3.13E-
protein metabolic process	6.84E-	ATP biosynthetic process	6.95E-
rRNA processing	1.21E-	oxidoreduction coenzyme	1.36E-
ribosome assembly	1.63E-	gluconeogenesis	2.39E-
RNA processing	9.8E-04	cytoplasmic translation	7.05E-

2-3 acetyl marks	p-value
cytoplasmic translation	2.39E-
biosynthetic process	4.23E-
peptide metabolic process	2.47E-
nitrogen metabolic process	5.45E-
metabolic process	1.69E-
gene expression	4.44E-
cellular protein metabolic	5.18E-
nicotinamide metabolic	6.42E-

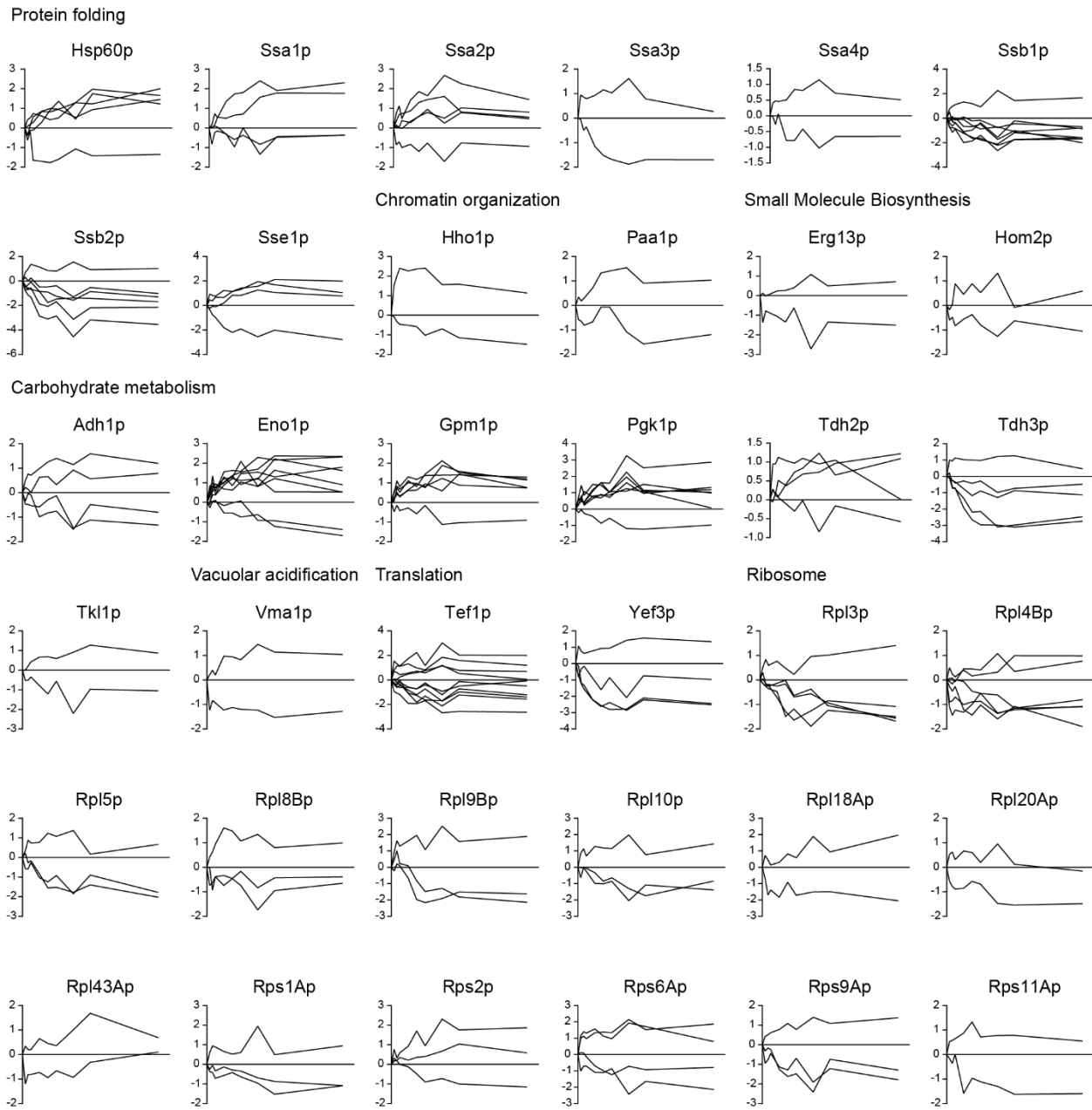


Figure 2.9 36 proteins experience both increasing and decreasing acetyl residues. Each line represents the fold change of one residue over the 240-minute time course.

acetylation and deacetylation events. While there is a strong enrichment for proteins experiencing significant abundance changes to also be experiencing significant acetylation changes (hypergeometric p-value = 2.52×10^{-6}), we identified 64 non-histone proteins that show significant changes in acetylation in at least one time point while showing no significant changes in protein abundance throughout the heat shock, including 12 of the 36 proteins that show concurrent increases and decreases on different residues. These proteins were highly enriched for those involved in translation ($p = 1.17 \times 10^{-19}$), peptide biosynthesis ($p = 6.83 \times 10^{-10}$), gene expression ($p = 7.47 \times 10^{-10}$), and nitrogen compound metabolic processes ($p = 1.41 \times 10^{-9}$).

2.4.3 Process and component enrichments

Following clustering of the dynamics of the 387 significantly changing residues, we identified 8 clusters for analysis for GO process enrichments (Princeton GO Term Finder) to determine if there are processes potentially being regulated by these acetylation changes. Among the peptides showing increasing acetylation during heat shock, we found strong enrichment ($p < 0.001$) for protein folding and refolding, response to heat, nucleotide metabolic processes, small molecule metabolism, carbohydrate metabolism. For peptides showing a significant decrease in acetylation, strong enrichments were found for translation, nitrogen metabolism, gene expression, ribosome biogenesis and assembly and peptide metabolism (Fig. 2.10). The processes enriched for increasing and decreasing acetylation highly overlap with processes known to be induced and repressed in response to stress respectively (Gasch 2003), suggesting that acetylation generally acts to activate the cellular stress response. All clusters show enrichments for localization in the ribosome and cytosol in general, strongly debunking the long-held belief that significant acetylation events predominantly occur in the nucleus (Table 2.A.1).

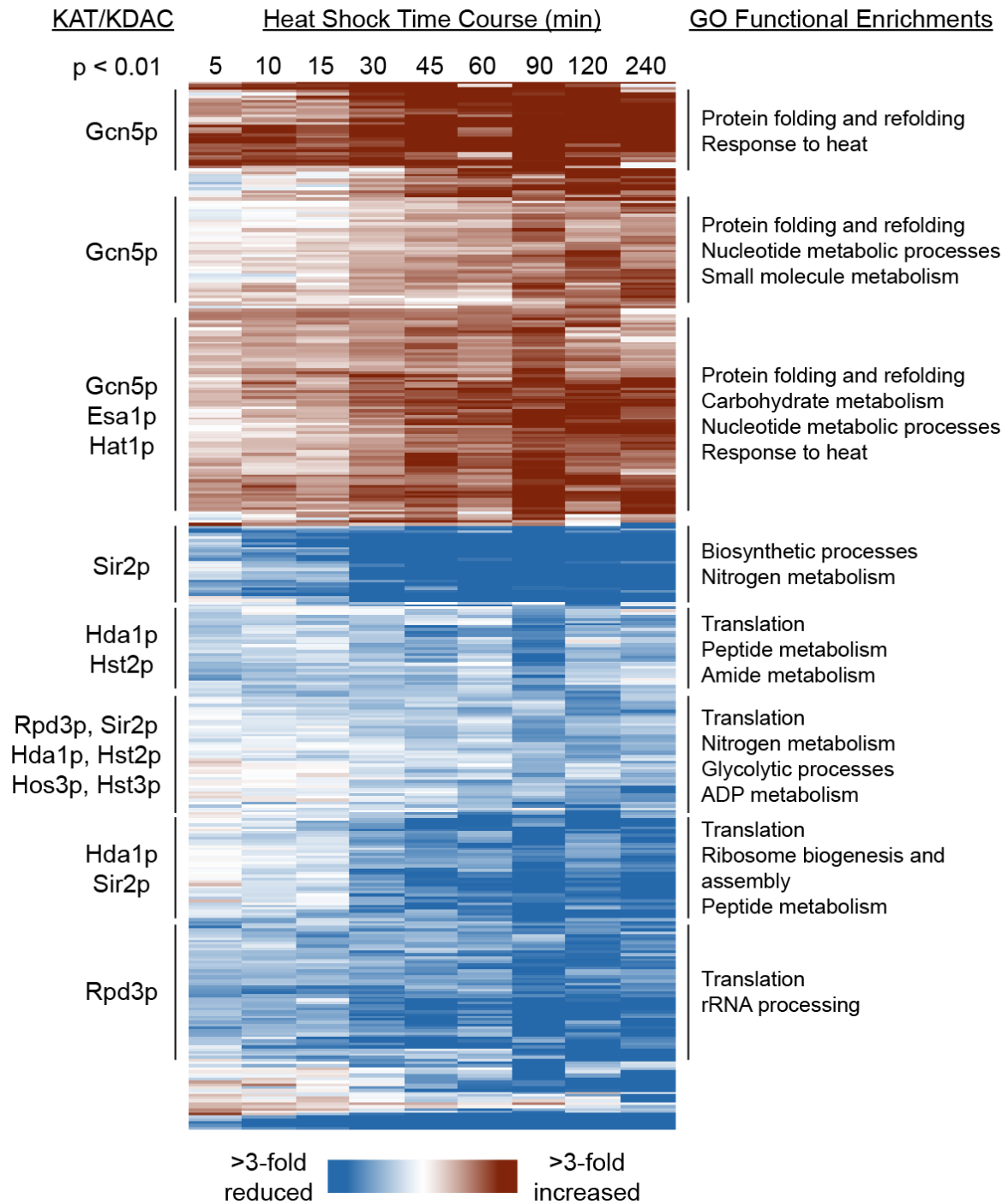


Figure 2.10 Clusters and enrichments for time course acetyl proteomics. Acetyl peptides significantly changing in at least one time point were clustered using Cluster 3.0 and visualized with TreeView. Eight clusters were manually chosen with a correlation of at least 0.9 and functional enrichments were analyzed using the Princeton GO term finder. KAT and KDAC enrichments were performed by pulling known physical interactions for each enzymatic subunit from the *Saccharomyces* Genome Database (SGD) and comparing those interactions to proteins experiencing changes in acetylation using a hypergeometric distribution test.

2.4.4 Enrichments for known KAT and KDAC interactions

For these same clusters, we also wanted to determine if there were any enrichments for known physical interactions with KAT and KDAC enzymatic subunits to suggest which enzymes are regulating these changes. All the clusters showing increasing acetylation showed enrichments for interactions with Gcn5, with Esa1 and Hat1 enriched to a lesser degree in one of the three clusters. The decreasing acetylation clusters, however, showed significant enrichments for a wide variety of KDACs including, Sir2, Rpd3, Hda1, Hst2, Hst3, and Hos3 (Fig. 2.10 and Tables 2.4 and 2.5). We also looked at enrichments for the KATs and KDACs that could possibly be reversing these changes in other conditions and found that the decreasing acetyl marks were highly enriched for physical interactions with the KAT Spt10 ($p = 1.18 \times 10^{-6}$). When analyzed for possible modification motifs using the MeMe suite tool MoMo, but none were found that passed the significance threshold (Figures 2.A.1 and 2.A.2).

We also looked at changing concentration levels of KATs and KDACs to determine if any are induced or repressed in response to heat, and while we were only able to identify 3 KATs (Elp3, Hat1, and Hpa3) and 5 KDACs (Hos3, Hst1, Rpd3, Hda1, and Sir2) in triplicate, we identified two KATs and one KDAC experiencing a significant concentration change during the time course (Fig. 2.11). Notably, these concentration changes are occurring later in the response, similar to when we see the majority of acetylation changes. While Sir2 and Hat1 were enriched in the previous data set, Hpa3 was not. It is very possible that this KAT plays a larger role in the stress response than it does under the non-stressed conditions from which the majority of the physical interaction data used in the enrichment calculation was obtained.

2.5 Conclusion

In this chapter, we show that the acetylome is highly dynamic in response to heat stress, involving proteins that serve a variety of functions in the cell and in the response to heat stress. The many clusters of varied dynamics and variety of KATs and KDACs implicated in the data

Table 2.4 Hypergeometric p-values for KATs and increasing acetylation clusters

KAT	Cluster		
	1	2	3
Eco1p	--	--	--
Elp3p	--	--	0.17547
Esa1p	0.12959	0.23259	0.00459
Gcn5p	0.00015	2.40162E-05	1.61560E-10
Hat1p	0.12689	0.17923	0.00033
Hpa2p	--	--	0.06702
Hpa3p	--	--	0.58089
Rtt109p	0.05390	--	0.12964
Sas2p	--	0.11799	0.19437
Sas3p	--	--	--
Spt10p	0.24136	--	0.21214
Taf1p	0.29324	--	0.08131

Table 2.5 Hypergeometric p-values for KDACs and decreasing acetylation clusters

KDAC	Cluster				
	4	5	6	7	8
Hda1p	0.10023	0.00380	0.01016	0.00728	0.15357
Hos1p	--	--	--	--	--
Hos2p	--	--	0.09620	--	--
Hos3p	--	0.07437	0.00702	--	--
Hst1p	--	--	--	--	--
Hst2p	0.02513	--	0.00057	0.03086	0.03939
Hst3p	0.04619	--	0.00206	0.05657	0.07194
Hst4p	--	--	--	--	--
Rpd3p	0.27518	0.24771	0.01107	0.05831	0.00152
Set3p	--	--	0.12466	--	--
Sir2p	0.00241	0.02373	0.00714	0.00032	0.35117

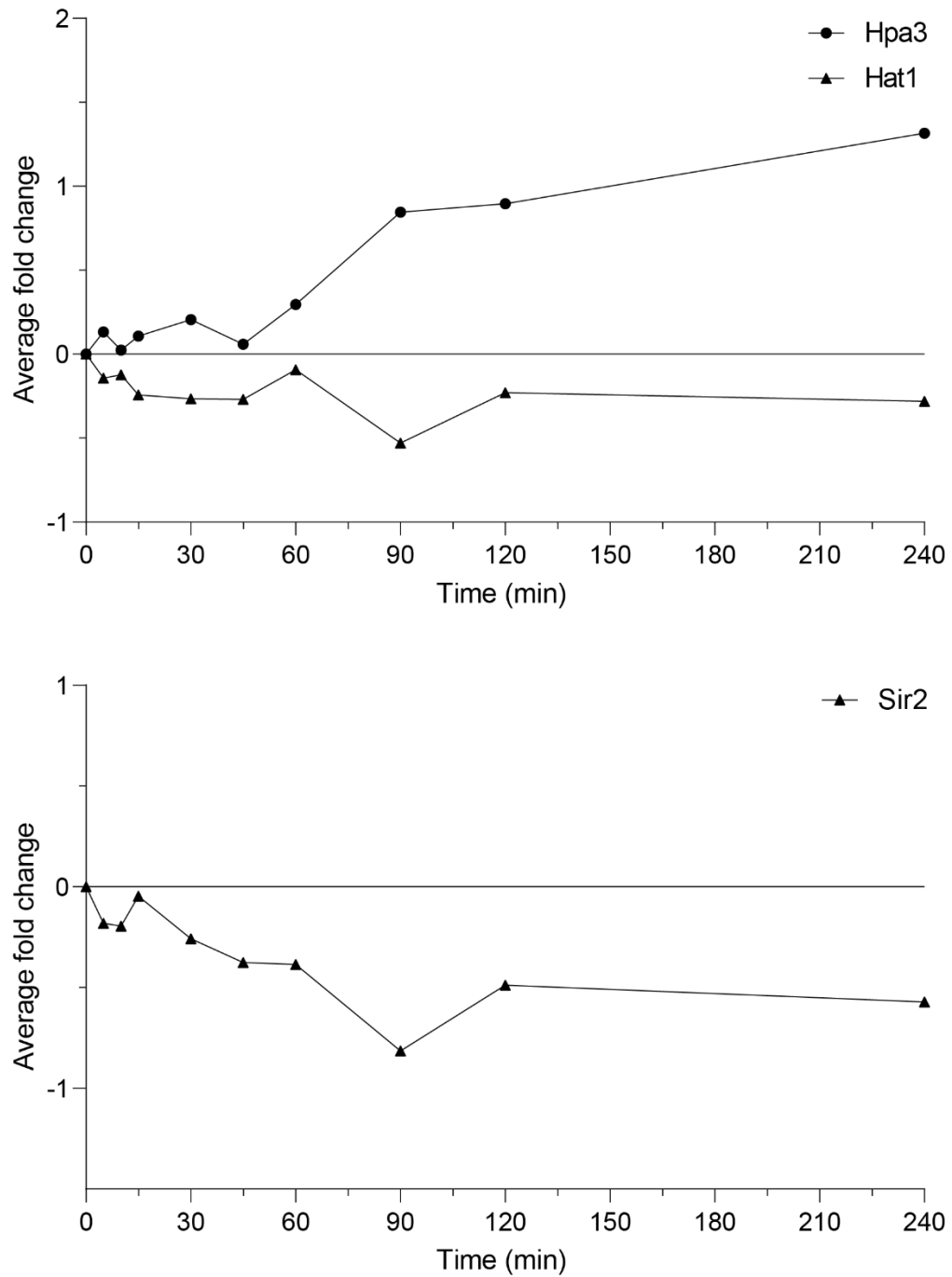


Figure 2.11 Significantly changing KAT and KDAC concentrations The KATs Hpa3 and Hat1 and KDAC Sir2 show significant changes in concentration late in the response to heat shock.

suggest that this response is being regulated in a complex manner. Further evidence of the degree to which this is regulated is the fact that we see increasing and decreasing acetylation within the same protein and in proteins that are not experiencing changing concentration levels that would affect their interaction with KATs and KDACs. It is possible, however, that changing KAT and KDAC concentrations are a method of regulating these dynamics.

This data suggests that a much larger set of proteins is being regulated by protein acetylation than previously believed. Only a small number of these proteins were known to be acetylated previous to this study, and of those even fewer were known to experience changing acetylation on those residues. These changing acetylations could have significant effects on these proteins including subcellular localization, substrate and protein interactions, and enzymatic activity. Not only does this data suggest a possible new mechanism of regulation for hundreds of proteins, but it also highlights the necessity of performing global studies in cells responding to changing environments to identify levels of protein regulation that are not apparent in standard laboratory conditions.

2.6 Acknowledgements

We would like to thank Dr. Shannon Servoss and Dr. Neda Mahmoudi for the use and assistance with the lyophilizer, Dr. Andrew Alverson and Dr. Elizabeth Ruck for equipment use and scientific advice, Mark Powell of Agilent for HPLC protocol development, Dr. Suresh Kumar and Dr. Srinivas Jayanthi with HPLC protocol development Dr. Ravi Barabote for use of the Shimadzu HPLC, and Dr. Alex Hebert for helpful conversations on TMT proteomic sample processing.

2.7 References

Allfrey, V. G., R. Faulkner & A. E. Mirsky (1964) Acetylation and methylation of histones and their possible role in the regulation of RNA synthesis. *Proc Natl Acad Sci U S A*, 51, 786-94.

- Berry, D. B. & A. P. Gasch (2008) Stress-activated genomic expression changes serve a preparative role for impending stress in yeast. *Mol Biol Cell*, 19, 4580-7.
- Boyle, E. I., S. Weng, J. Gollub, H. Jin, D. Botstein, J. M. Cherry & G. Sherlock (2004) GO:TermFinder--open source software for accessing Gene Ontology information and finding significantly enriched Gene Ontology terms associated with a list of genes. *Bioinformatics*, 20, 3710-5.
- Castaño-Cerezo, S., V. Bernal, H. Post, T. Fuhrer, S. Cappadona, N. C. Sánchez-Díaz, U. Sauer, A. J. Heck, A. F. Altelaar & M. Cánovas (2014) Protein acetylation affects acetate metabolism, motility and acid stress response in *Escherichia coli*. *Mol Syst Biol*, 10, 762.
- Chen, Z., L. Luo, R. Chen, H. Hu, Y. Pan, H. Jiang, X. Wan, H. Jin & Y. Gong (2018) Acetylome Profiling Reveals Extensive Lysine Acetylation of the Fatty Acid Metabolism Pathway in the Diatom. *Mol Cell Proteomics*, 17, 399-412.
- Cheng, A., U. o. W. Department of Genome Sciences, Seattle, WA, USA, C. E. Grant, U. o. W. Department of Genome Sciences, Seattle, WA, USA, W. S. Noble, U. o. W. Department of Genome Sciences, Seattle, WA, USA, U. o. W. Department of Computer Science and Engineering, Seattle, WA, USA, T. L. Bailey & U. o. N. Department of Pharmacology, Reno, NV, USA (2019) MoMo: discovery of statistically significant post-translational modification motifs. *Bioinformatics*, 35, 2774-2782.
- Cherry, J. M., E. L. Hong, C. Amundsen, R. Balakrishnan, G. Binkley, E. T. Chan, K. R. Christie, M. C. Costanzo, S. S. Dwight, S. R. Engel, D. G. Fisk, J. E. Hirschman, B. C. Hitz, K. Karra, C. J. Krieger, S. R. Miyasato, R. S. Nash, J. Park, M. S. Skrzypek, M. Simison, S. Weng & E. D. Wong (2012) Saccharomyces Genome Database: the genomics resource of budding yeast. *Nucleic Acids Res*, 40, D700-5.
- Chevallet, M., S. Luche & T. Rabilloud (2006) Silver staining of proteins in polyacrylamide gels. *Nat Protoc*, 1, 1852-8.
- Eisen, M. B., P. T. Spellman, P. O. Brown & D. Botstein (1998) Cluster analysis and display of genome-wide expression patterns. *Proc Natl Acad Sci U S A*, 95, 14863-14868.
- Gasch, A. P. 2003. The environmental stress response: a common yeast response to diverse environmental stresses. In *Yeast Stress Responses*, eds. S. Hohmann & W. H. Mager, 11-70. Springer, Berlin, Heidelberg.
- Gasch, A. P., P. T. Spellman, C. M. Kao, O. Carmel-Harel, M. B. Eisen, G. Storz, D. Botstein & P. O. Brown. 2000. Genomic Expression Programs in the Response of Yeast Cells to Environmental Changes. In *Mol Biol Cell*, 4241-57.
- Giaever, G., A. M. Chu, L. Ni, C. Connelly, L. Riles, S. Véronneau, S. Dow, A. Lucau-Danila, K. Anderson, B. André, A. P. Arkin, A. Astromoff, M. El-Bakkoury, R. Bangham, R. Benito, S. Brachat, S. Campanaro, M. Curtiss, K. Davis, A. Deutschbauer, K. D. Entian, P. Flaherty, F. Foury, D. J. Garfinkel, M. Gerstein, D. Gotte, U. Güldener, J. H. Hegemann, S. Hempel, Z. Herman, D. F. Jaramillo, D. E. Kelly, S. L. Kelly, P. Kötter, D. LaBonte, D. C. Lamb, N. Lan, H. Liang, H. Liao, L. Liu, C. Luo, M. Lussier, R. Mao, P. Menard, S. L. Ooi, J. L. Revuelta, C. J. Roberts, M. Rose, P. Ross-Macdonald, B. Scherens, G. Schimmack, B. Shafer, D. D. Shoemaker, S. Sookhai-Mahadeo, R. K. Storms, J. N.

- Strathern, G. Valle, M. Voet, G. Volckaert, C. Y. Wang, T. R. Ward, J. Wilhelmy, E. A. Winzeler, Y. Yang, G. Yen, E. Youngman, K. Yu, H. Bussey, J. D. Boeke, M. Snyder, P. Philippsen, R. W. Davis & M. Johnston (2002) Functional profiling of the *Saccharomyces cerevisiae* genome. *Nature*, 418, 387-91.
- Hartl, M., M. Füßl, P. J. Boersema, J. O. Jost, K. Kramer, A. Bakirbas, J. Sindlinger, M. Plöschinger, D. Leister, G. Uhrig, G. B. Moorhead, J. Cox, M. E. Salvucci, D. Schwarzer, M. Mann & I. Finkemeier (2017) Lysine acetylome profiling uncovers novel histone deacetylase substrate proteins in. *Mol Syst Biol*, 13, 949.
- Hebert, A. S., S. Prasad, M. W. Belford, D. J. Bailey, G. C. McAlister, S. E. Abbatiello, R. Huguet, E. R. Wouters, J.-J. Dunyach, D. R. Brademan, M. S. Westphall & J. J. Coon (2018) Comprehensive Single-Shot Proteomics with FAIMS on a Hybrid Orbitrap Mass Spectrometer.
- Henriksen, P., S. A. Wagner, B. T. Weinert, S. Sharma, G. Bacinskaja, M. Rehman, A. H. Juffer, T. C. Walther, M. Lisby & C. Choudhary (2012) Proteome-wide analysis of lysine acetylation suggests its broad regulatory scope in *Saccharomyces cerevisiae*. *Mol Cell Proteomics*, 11, 1510-22.
- Kanshin, E., P. Kubiniok, Y. Thattikota, D. D'Amours & P. Thibault (2015) Phosphoproteome dynamics of *Saccharomyces cerevisiae* under heat shock and cold stress. *Mol Syst Biol*, 11.
- Khoury, G. A., R. C. Baliban & C. A. Floudas (2011) Proteome-wide post-translational modification statistics: frequency analysis and curation of the swiss-prot database. *Sci Rep*, 1.
- Liu, J., Q. Wang, X. Jiang, H. Yang, D. Zhao, J. Han, Y. Luo & H. Xiang (2017) Systematic Analysis of Lysine Acetylation in the Halophilic Archaeon *Haloferax mediterranei*. *J Proteome Res*, 16, 3229-3241.
- Lundby, A., K. Lage, B. T. Weinert, D. B. Bekker-Jensen, A. Secher, T. Skovgaard, C. D. Kelstrup, A. Dmytriyev, C. Choudhary, C. Lundby & J. V. Olsen (2012) Proteomic analysis of lysine acetylation sites in rat tissues reveals organ specificity and subcellular patterns. *Cell Rep*, 2, 419-31.
- Menzies, K. J., H. Zhang, E. Katsyuba & J. Auwerx (2016) Protein acetylation in metabolism - metabolites and cofactors. *Nat Rev Endocrinol*, 12, 43-60.
- Phillips, D. M. (1963) The presence of acetyl groups of histones. *Biochem J*, 87, 258-63.
- Ritchie, M. E., B. Phipson, D. Wu, Y. Hu, C. W. Law, W. Shi & G. K. Smyth (2015) limma powers differential expression analyses for RNA-sequencing and microarray studies. *Nucleic Acids Res*, 43, e47.
- Saldanha, A. J. & S. U. S. o. M. Department of Genetics, Stanford, CA 94305, USA (2019) Java Treeview—extensible visualization of microarray data. *Bioinformatics*, 20, 3246-3248.

- Storey, A. J., R. E. Hardman, S. D. Byrum, S. G. Mackintosh, R. D. Edmondson, W. P. Wahls, A. J. Tackett, V. O. Profile & J. A. Lewis. 2019. Accurate and Sensitive Quantitation of the Dynamic Heat Shock Proteome using Tandem Mass Tags. *Biorxiv*.
- Vihervaara, A., D. B. Mahat, M. J. Guertin, T. Chu, C. G. Danko, J. T. Lis & L. Sistonen (2017) Transcriptional response to stress is pre-wired by promoter and enhancer architecture. *Nat Commun*, 8, 255.
- Weinert, B. T., S. A. Wagner, H. Horn, P. Henriksen, W. R. Liu, J. V. Olsen, L. J. Jensen & C. Choudhary (2011) Proteome-wide mapping of the *Drosophila* acetylome demonstrates a high degree of conservation of lysine acetylation. *Sci Signal*, 4, ra48.
- Yang, F., Y. Shen, D. G. Camp & R. D. Smith (2012) High-pH reversed-phase chromatography with fraction concatenation for 2D proteomic analysis. *Expert Rev Proteomics*, 9, 129-34.

2.8 Appendix

Table 2.A.1 Enrichments for cellular localization/component

Cluster 1

GO ID	TERM	CORRECTED_PVALUE
GO:0005829	cytosol	1.04E-06
GO:0032991	protein-containing complex	1.03E-05
GO:1990904	ribonucleoprotein complex	0.002237364
GO:0000015	phosphopyruvate hydratase complex	0.00572667
GO:0005844	polysome	0.007526836
GO:0022626	cytosolic ribosome	0.009345474

Cluster 2

GO:0005829	cytosol	3.01E-07
GO:0042645	mitochondrial nucleoid	0.000339
GO:0022626	cytosolic ribosome	0.00082
GO:0044444	cytoplasmic part	0.002659
GO:0043228	non-membrane-bounded organelle	0.006317
GO:1990904	ribonucleoprotein complex	0.006476

Cluster 3

GO:0005829	cytosol	2.23E-14
GO:0022626	cytosolic ribosome	3.08E-08
GO:1990904	ribonucleoprotein complex	1.10E-06
GO:0005886	plasma membrane	2.41E-05

Cluster 4

GO:1990904	ribonucleoprotein complex	2.89E-05
GO:0043228	non-membrane-bounded organelle	4.88E-05
GO:0005840	ribosome	0.000208
GO:0032991	protein-containing complex	0.000837
GO:0044445	cytosolic part	0.000945

Cluster 5

GO:0022626	cytosolic ribosome	2.08E-09
GO:0044445	cytosolic part	2.58E-09
GO:1990904	ribonucleoprotein complex	3.28E-07
GO:0022625	cytosolic large ribosomal subunit	6.80E-07
GO:0015934	large ribosomal subunit	1.13E-05

Cluster 6

GO:0044445	cytosolic part	3.88E-11
GO:0022626	cytosolic ribosome	1.47E-10
GO:0044391	ribosomal subunit	1.65E-08
GO:1990904	ribonucleoprotein complex	1.03E-07
GO:0022625	cytosolic large ribosomal subunit	2.43E-06
GO:0043228	non-membrane-bounded organelle	4.07E-05

Table 2.A.1 (Cont.)**Cluster 7**

GO ID	TERM	CORRECTED_PVALUE
GO:0005840	ribosome	1.50E-14
GO:1990904	ribonucleoprotein complex	4.45E-13
GO:0044445	cytosolic part	3.54E-11
GO:0044391	ribosomal subunit	4.94E-11
GO:0043228	non-membrane-bounded organelle	3.74E-09
GO:0022627	cytosolic small ribosomal subunit	2.38E-08
GO:0032991	protein-containing complex	5.02E-06
GO:0030684	preribosome	3.03E-05

Cluster 8

GO:0044445	cytosolic part	1.58E-14
GO:0022626	cytosolic ribosome	2.91E-14
GO:0044391	ribosomal subunit	1.08E-11
GO:1990904	ribonucleoprotein complex	7.16E-11
GO:0043228	non-membrane-bounded organelle	4.68E-10
GO:0043232	intracellular non-membrane-bounded organelle	4.68E-10
GO:0032991	protein-containing complex	8.49E-08
GO:0022627	cytosolic small ribosomal subunit	2.31E-07
GO:0030684	preribosome	1.56E-06
GO:0022625	cytosolic large ribosomal subunit	4.35E-06
GO:0015935	small ribosomal subunit	6.94E-06
GO:0032040	small-subunit processome	0.000968
GO:0005844	polysome	0.002127

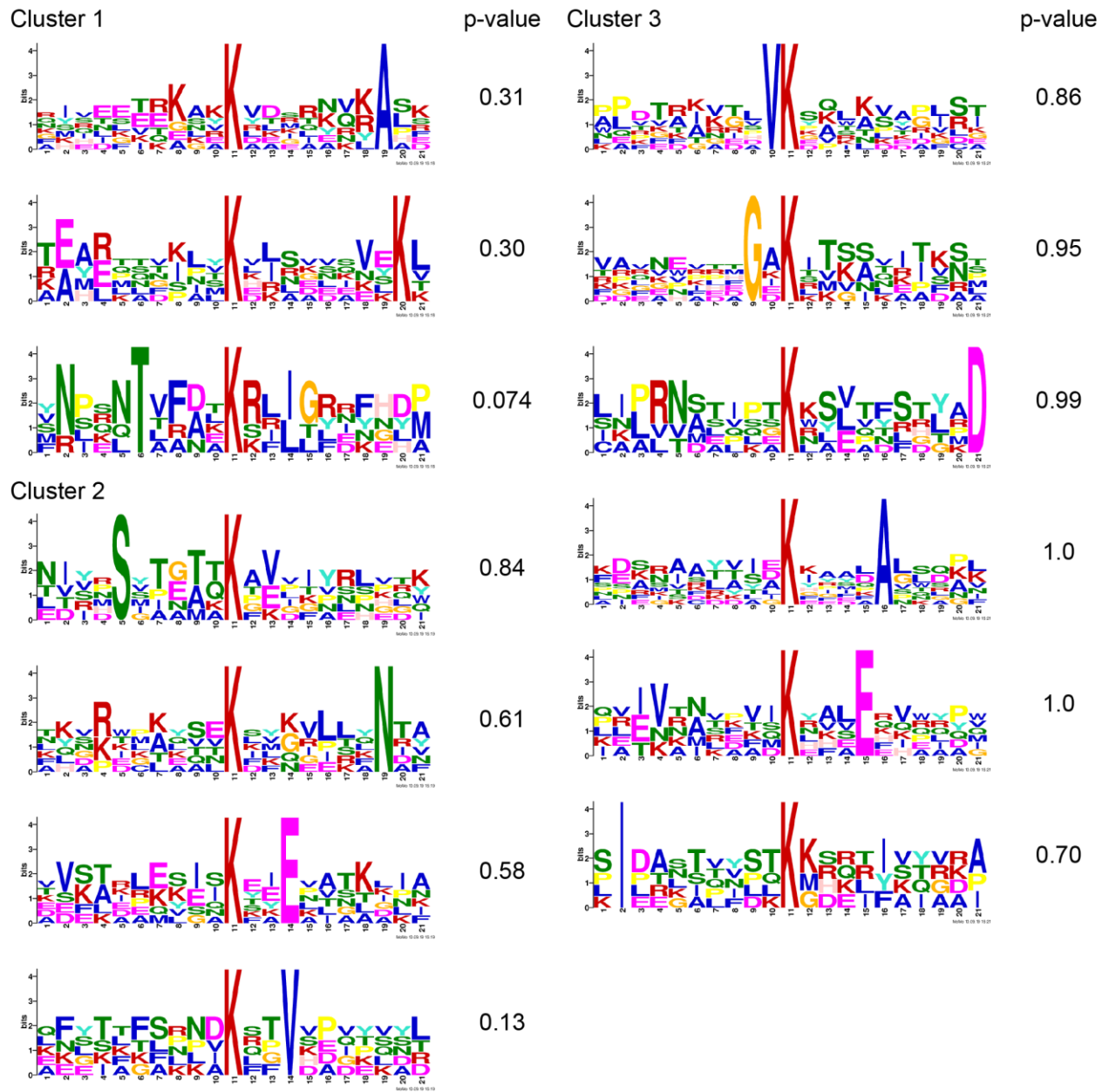


Figure 2.A.1 Modification motifs for increasing clusters. Possible modification motifs for each cluster were analyzed using the MoMo tool in the MeMe suite.

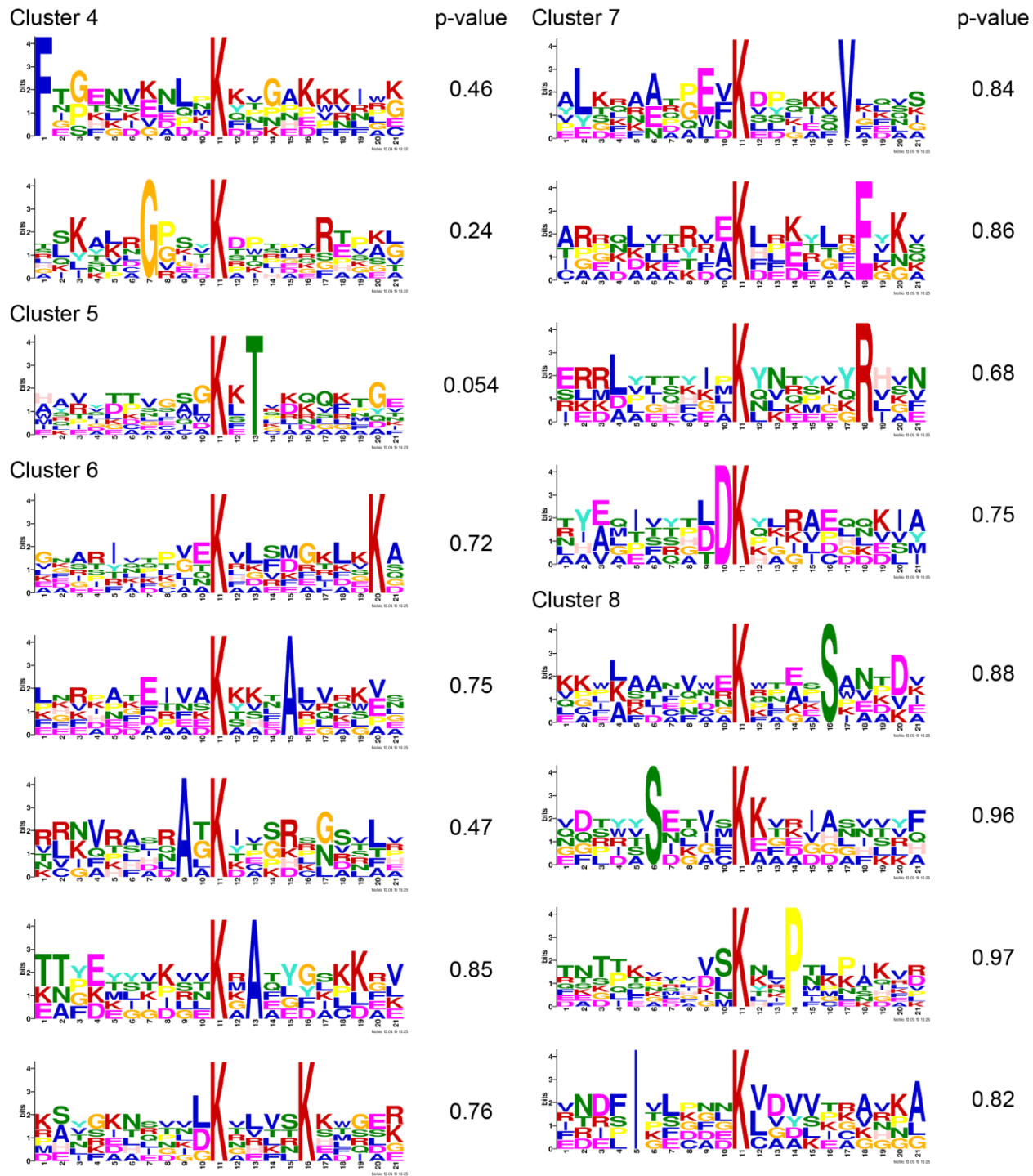


Figure 2.A.2 Modification motifs for decreasing clusters. Possible modification motifs for each cluster were analyzed using the MoMo tool in the MeMe suite.

Chapter 3 Mechanisms regulating protein acetylation in response to heat shock in *S. cerevisiae*

Rebecca E. Hardman^{1,2}, Venkata Rao Krishnamurthi³, Gregory A. Barrett-Wilt⁴, Samuel G. Mackintosh⁵, Yong Wang³, and Jeffrey A. Lewis²

1 Interdisciplinary Graduate Program in Cell and Molecular Biology, University of Arkansas, Fayetteville, Arkansas, United States of America

2 Department of Biological Sciences, University of Arkansas, Fayetteville, Arkansas, United States of America

3 Department of Physics, University of Arkansas, Fayetteville, Arkansas, United States of America

4 Biotechnology Center, University of Wisconsin, Madison, Wisconsin, United States of America

5 Department of Biochemistry and Molecular Biology, University of Arkansas for Medical Sciences, Little Rock, Arkansas 72205, United States of America

Author contributions: V.R.K. performed the fluorescence microscopy. G.A.B.W. developed and performed the metabolite mass spectrometry. S.G.M. performed mass spectrometry for protein identification. All remaining work was conceived and planned by JAL and REH and performed by REH.

3.1 Abstract

Though there are over a thousand acetylated proteins in the yeast proteome, the mechanisms by which these acetylation events are regulated remain unknown. Following a global time-course analysis of the entire set of acetylated proteins in response to heat shock, we identified multiple groups of peptides experiencing similar acetylation dynamics. To determine possible mechanisms regulating these groups, we began by looking at the concentrations of metabolites that play central roles in these reactions as substrates or inhibitors. We then used a statistical analysis to compare proteins identified in these clusters to known physical interactions with acetyltransferases and deacetylases, we identified 11 candidate enzymes that may be regulating acetylation changes during heat shock for further study. Finally, we purified these enzymes to identify possible binding partner remodeling and analyzed whether these enzymes were relocalizing, thus changing substrate pools.

3.2 Introduction

One of the mechanisms the cell has evolved to modulate protein activity is the use of covalent modifications broadly termed post-translational modifications (PTMs). While hundreds of PTMs have been identified, some of the most widespread and highly studied include phosphorylation, methylation, ubiquitination, and acetylation. Though long overlooked, recent advances in technology have led to the identification of thousands of acetylated proteins across a variety of processes spanning all domains of life, making it one of the most ubiquitous and conserved PTMs in the cell (Kouzarides 2000). Two classes of proteins are responsible for modulating this response: the KATs and KDACs.

Lysine acetylation occurs when an acetyl group is transferred from acetyl-CoA to the ϵ -amino group in the lysine side chain. This effectively neutralizes the positive charge of the residue (Fig. 3.1). This alteration in the chemical environment of the protein can have dramatic consequences on protein function due to conformational changes and altered ability to interact with other proteins and/or substrates. Due to the requirement of acetyl-CoA as the acetyl donor, concentrations of this metabolite can affect KAT activity (Albaugh et al. 2010, Albaugh et al. 2011a, Berndsen et al. 2007, Tanner et al. 2000). When acetyl-CoA concentrations are low, CoA can bind to most KATs and act as a competitive inhibitor. When levels of acetyl-CoA increase, it displaces the CoA allowing the KAT to resume normal activity (Galdieri et al. 2014). In the yeast *Saccharomyces cerevisiae*, there are 12 known proteins with confirmed KAT activity (Table 3.1) as well as many putative KATs that remain uncharacterized.

Following acetylation by a KAT, or in some cases through non-enzymatic acetylation, the acetylation moiety can be removed by a member of the KDAC family, of which there are 11 in *S. cerevisiae* (Table 3.2). In yeast, these are divided into three classes. The class I and class II KDACs are considered the “classical” KDACs, and using a zinc cofactor they use hydrolysis to remove the acetyl group as acetate and are inhibited by butyrate and trichostatin A (Fig. 3.1) (Boffa et al. 1978, Sekhavat et al. 2007). The class III KDACs are known as the “sirtuins,”

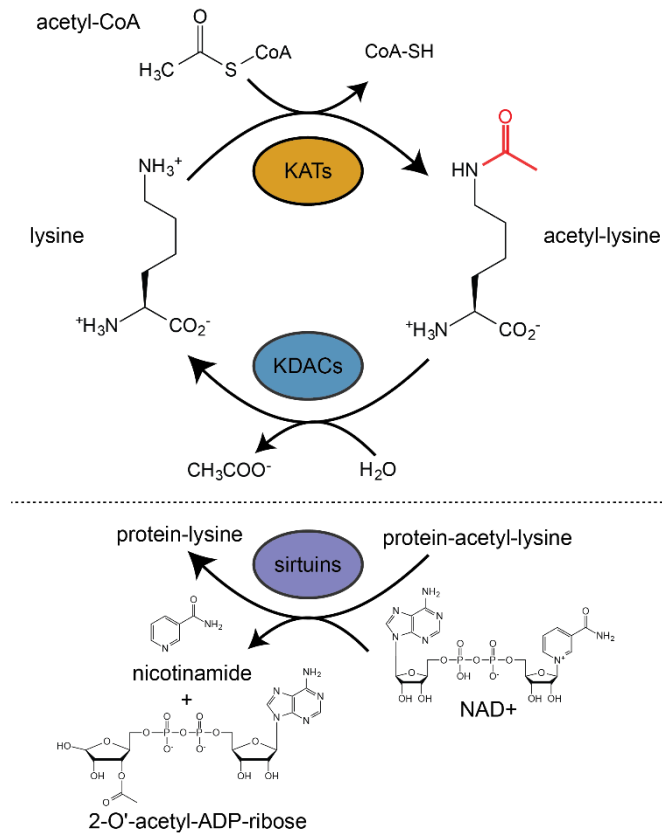


Figure 3.1 Schematic of regulation by reversible lysine acetylation. Lysine acetylation is a highly conserved post-translational modification, where acetyltransferases (KATs) transfer the acetyl group from acetyl-CoA. Class I, II, and IV zinc-dependent lysine deacetylases (KDACs) remove the acetyl group via hydrolysis. Class III deacetylases (i.e. sirtuins), use NAD⁺ as a substrate, producing nicotinamide and 2-O'-acetyl-ADP-ribose, a novel metabolite only known to be produced by sirtuins.

named after the inaugural member, Sir2. These enzymes consume NAD⁺ and remove the acetyl group producing nicotinamide and O'-acetyl-ADP-ribose (Fig 3.1). Sirtuins are then inhibited by nicotinamide through feedback inhibition (Menzies et al. 2016).

For the majority of KATs and KDACs, peak enzymatic activity requires the assistance of many protein subunits, which can form multiple different complexes (Tables 3.1 and 3.2). For example, the KAT Gcn5 has very weak acetylation capabilities alone and is unable to acetylate nucleosomes, a key step in gene expression. When bound to Ada2 and Ada3, however, this functionality is restored (Balasubramanian et al. 2002, Sun et al. 2018). The subunits found within these complexes serve various roles including substrate recognition and catalytic stability, and it is likely that this evolved to finely tune substrate recognition to prevent promiscuous acetylation events. Another method of enzyme regulation is sequestration and relocalization within the cell. The majority of the known functions of KATs and KDACs are involved in chromatin remodeling for gene expression, occurring in the nucleus, and yet we see thousands of non-nuclear proteins in global acetylation screens. It is thus likely that many of the enzymes are moving in and out of the nucleus to act upon a variety of substrates, though the mechanism(s) behind this is unknown.

In Chapter 2 I showed that over 200 proteins that experienced changes in acetylation in response to a four-hour heat shock at 37°C. These proteins represented a variety of different processes, many of which are known to be highly involved in the cellular response to stress. We identified 8 different dynamic clusters, 3 showing a general increase in acetylation and 5 showing a general decrease, and statistically identified enrichments for acetyltransferases and deacetylases interacting with these groups. This chapter will discuss further experiments performed to determine some of the possible mechanisms regulating these dynamics including lysine acetyltransferase (KAT) and deacetylase (KDAC) localization changes, KAT and KDAC complex remodeling, and metabolite dynamics in response to heat stress.

Table 3.1 Yeast KATs

Enzymatic subunit	Complexes	Family	Genetic Interactions ^a	Physical Interactions ^a
Eco1			128	28
Elp3	Elongator	GNAT	514	25
Esa1	NuA4, piccolo NuA4	MYST	768	205
Gcn5	SAGA, SLIK, ADA	GNAT	422	283
Hat1	Hat1p-Hat2p	GNAT	131	44
Hpa2		GNAT	94	11
Hpa3		GNAT	39	9
Rtt109	Rtt109-Vps75		559	18
Sas2	SAS	MYST	128	28
Sas3	NuA3	MYST	174	21
Spt10		GNAT	116	306
Taf1	TFIID		859	112

a. Genetic and physical interactions were obtained from the Saccharomyces Genome Database (SGD, Cherry et al. 2012).

Table 3.2 Yeast KDACs

Enzymatic subunit	Complexes	Class	Genetic Interactions ^a	Physical Interactions ^a
Hda1	Hda1-2-3	II	708	26
Hos1		I	87	9
Hos2	Set3 and Rpd3(L)	I	376	18
Hos3		II	69	23
Hst1	Sum1p/Rfm1p/Hst1p	III	136	20
Hst2		III	45	7
Hst3		III	286	13
Hst4		III	94	6
Rpd3	Rpd3(L), Rpd3(S), SNT2C	I	966	81
Set3	Set3C	III	394	25
Sir2	SIR2-3-4, RENT	III	316	75

a. Genetic and physical interactions were obtained from the Saccharomyces Genome Database (SGD, Cherry et al. 2012).

3.3 Materials and Methods

3.3.1 Strains

Metabolite experiments were carried out using the lab strain BY4741 (MATa *his3Δ1 leu2Δ0 met15Δ0 ura3Δ0*) and were performed in YPD (1% yeast extract, 2% peptone, 2% dextrose). TAP immunoprecipitations were performed using strains from the TAP Tagged ORF Collection by GE Dharmacon (MATa *his3Δ1 leu2Δ0 met15Δ0 ura3Δ0* ORF::TAP-HIS3) and performed in YPD. Fluorescence microscopy experiments were performed using strains from the Yeast GFP Clone Collection by Invitrogen (MATa *his3Δ1 leu2Δ0 met15Δ0 ura3Δ0* ORF::GFP-hisMX6) and were performed in SC (6.7 g/L Yeast nitrogen base with ammonium sulfate, 2% dextrose, complete amino acid mix). All TAP and GFP-tagged strains were verified by PCR.

3.3.2 Metabolite extraction

Cells were grown for at least 8 doublings in 500 mL YPD in a 2-L flask at 200 rpm, 25°C from a saturated culture to a final OD₆₀₀ (Unico) between 0.4 and 0.6. Seventy-five milliliters of culture were aliquoted into 5, 500 mL flasks, to which 75 mL of prewarmed 55°C YPD was added. Flasks were placed in a 37°C, 200 rpm incubator for stress. 1 x 10⁸ cells from the remaining unstressed culture were collected via vacuum filtration using a 47 mM filtration apparatus (VWR KT953755-0000) and 47 mm, 0.45 μM nylon membrane (Millipore HNWP04700) and scraping into liquid nitrogen. The stressed samples were collected at 5, 15, 30, 60, and 120 minutes. Approximately 30 seconds before time, OD₆₀₀ was measured to determine the volume needed to collect 1 x 10⁸ cells.

Extraction was performed based on the protocol used in Crutchfield et al. 2010. One mL -20°C extraction solvent (40% acetonitrile, 40% methanol, and 20% water) was pipetted into a 60-mM glass petri dish. Immediately following filtration, the filter was placed cell-side down into

the solvent, metabolites were extracted at -20°C for 15 minutes, and the filter was washed 10 times with the pooled solvent at the bottom of the petri dish. As much solvent and debris were collected into a 1.5-mL Eppendorf tube, and the samples were centrifuged at max speed, (21,130 × g) for 5 minutes at 4°C to pellet cell debris. The supernatant was transferred to a separate 1.5-mL Eppendorf tube and stored at -80°C.

3.3.3 Mass spectrometry for acetyl-CoA, CoA, and nicotinamide

Quantitation of nicotinamide (NAM) coenzyme A (CoA), and acetyl-coenzyme A (AcCoA) was performed by LC/MS/MS using an MRM approach. HPLC separation used an Agilent 1100 Binary Pump including column compartment, automated liquid sampler and autosampler thermostat with a Waters Atlantis T3 column, 2.1 mM x 150 mM containing 3µm particles. A binary gradient using 25 mM ammonium formate, pH 7.5 in water (solvent A) and neat acetonitrile (solvent B), was developed over 30 minutes at a flow rate of 200µL/min. The gradient was as follows: initial composition of 0%B held for 3 minutes, then increased to 70%B over 17 minutes, held at 70%B for 3 minutes, then returning to 0% B over 1 minute and holding at 0% B for 6 minutes, with a post-gradient re-equilibration for 12 minutes. The column was maintained at 25°C throughout. MS/MS detection was performed on a Thermo TSQ Quantum Discovery Max triple quadrupole instrument with positive ion electrospray ionization. The ESI source was a HESI-II probe with a vaporizer temperature of 300°C and ionization voltage of 4200V. The sheath gas was set to 35 (arbitrary units), ion sweep gas of 5 and auxiliary gas of 10. The inlet capillary was held at 300°C with a capillary offset of 35V. MS/MS precursor and product ions are shown in table 3.1.

Table 3.3 MS/MS precursor and product ions in duplicate

	Q1 m/z	Q3 m/z	Collision energy (CE)
NAM	123.0	78.1	22
	123.0	53.1	33
CoA	768.1	261.1	30
	768.1	428.0	27
AcCoA	810.1	303.1	32
	810.1	428.0	27

Sample preparation

Neat standards acetyl-CoA (cat # A2056-5mg), CoA (cat # C3144-10mg, and nicotinamide (cat # 72340-100g) were obtained from Sigma. A 5-standard mix was made in water at 100uM for each compound and serial dilutions to 10 μ M and 1uM were made in water. For calibration curves, one sample was used to provide a matrix and 20 μ L of sample was mixed with 60 μ L of water (0 μ M spike), 40 μ L 1 μ M standard and 20 μ L water (2 μ M spike), or 40 μ L 10 μ M standard and 20 μ L water (20 μ M spike). For sample analysis, 20 μ L of sample was diluted with 60 μ L water. Samples with water or samples with standard spikes and water were vortexed and spun down prior to being loaded into autosampler vials for injection. Injections were 5 μ L. Water blanks were analyzed between each sample to reduce carryover.

Data analysis was performed using Quantitative Analysis software (Thermo Fisher) to integrate peak areas for each analyte. Peak areas consisted of the summed signal for all MRM transitions for each analyte. Calibration curves were created from the spiked matrix samples in Excel to obtain the slope of the best-fit line. This was then used to calculate analyte concentrations from the remaining samples.

3.3.4 NAD:NADH assay

Cells were grown for at least 8 doublings in 700 mL YPD in a 2-L flask at 200 rpm, 25°C from a saturated culture to a final OD₆₀₀ between 0.5-0.7. 100 mL was aliquoted into 5, 500 mL flasks, to which 100 mL of prewarmed 55°C YPD was added. Flasks were placed in a 37°C, 200 rpm incubator for stress. Remaining unstressed cells were collected via vacuum filtration using a 90 mM filtration apparatus (VWR KT953755-0090) and 90 mm, 0.45 µM nylon membrane (VWR 76018-846) and scraping into liquid nitrogen. The remaining samples were collected at 5, 15, 30, 60, and 120 minutes. Cells were thawed on ice, suspend cells in lysis buffer (50% PBS and 50% 0.2 N NaOH, 3x protease inhibitor cocktail (VWR A32963)) and pipetted into liquid nitrogen to freeze. Cells were then ground into a fine powder with a mortar and pestle, adding liquid nitrogen to keep frozen. The powder was collected in a 50-mL conical tube, thawed on ice, and 1 mL was transferred to a 1.5-mL microcentrifuge tube. Following centrifugation at max speed (21,130 x g) for 5 minutes at 4°C to pellet debris, protein concentration was determined via Bradford assay, and samples were diluted to 10 µg/mL in 200 µl lysis buffer.

One hundred µL of each was transferred to a 1.5-mL tube for and 50 µL of 0.4 N HCl was added for acid treatment. The remaining 100 µL is the base treated sample. All samples were incubated for 15 minutes at 60°C. NAD⁺ is selectively destroyed by heating in a basic solution, while NADH is not stable in an acidic solution. Thus, luminescence from acid-treated samples is proportional to the amount of NAD⁺, and luminescence from the base-treated samples is proportional to the amount of NADH. Samples were equilibrated for 10 minutes at room temperature and 50 µL of 0.5 M Tris base was added to each tube of acid-treated cells to neutralize the acid. One-hundred µl of HCl/Tris solution was added to each tube containing base-treated samples, bring both samples to 200 µL in identical solutions. Fifty µL of each sample was transferred to one well in a white-walled 96-well plate containing 50 µL of NAD/NADH-Glo™ Detection Reagent prepared according to manufacturer protocol (Promega PAG9071). This was incubated for 30 minutes at room temperature in a microplate incubator

shaking at 600 rpm. Luminescence was recorded using a Synergy H1 microplate reader (Biotek).

3.3.5 TAP purification

Cells were grown for at least 8 doublings in 850 mL YPD in a 4-L flask at 125 rpm, 25°C from a saturated culture to a final OD₆₀₀ between 0.4 and 0.6. One-hundred and fifty milliliters of culture were aliquoted into 4, 1-L flasks, to which 150 mL of prewarmed 55°C YPD was added. Flasks were placed in a 37°C, 125 rpm incubator for stress. Remaining 250 mL unstressed cells were collected via vacuum filtration using a 90 mM filtration apparatus (VWR KT953755-0090) and 90 mM, 0.45 µM nylon membrane (VWR 76018-846) and scraping into liquid nitrogen. The remaining samples were collected at 15, 45, 90, and 120 minutes.

TAP purification was based on the protocol from Mitchell et al. 2008. Cells were thawed on ice in 500 µL lysis buffer (20 mM HEPES, pH 7.4, 0.1% Tween 20, 2 mM MgCl₂, 300 mM NaCl, protease inhibitor cocktail (VWR A32963), transferred to a 2-mL screw-top tube, and centrifuged at 4,500 rcf for 1 minute to remove supernatant containing residual media. Cells were then suspended in 300 µL lysis buffer, 500 µL acid-washed glass beads and lysed by vortexing for 6 cycles of 1 minute vortexing, 2 minutes on ice. The lysate was removed and transferred to a 1.5-mL microcentrifuge tube, and the beads were washed with 300 µL of fresh buffer. The lysate was cleared by centrifugation at 14,000 rpm for 20 minutes at 4°C, and protein was quantified via Bradford assay.

Ten milligrams of sample in 1 mL lysis buffer were incubated with 25 µL of magnetic Dynabeads (Fisher, 14301) crossed-linked to rabbit immunoglobulin G (IgG) (Sigma, I5006), for 2 hours with end-over-end incubation at 4°C. After 5 washes with 1 mL cold lysis buffer, Dynabeads were suspended in 25 µL loading buffer (50 mM Tris, pH 6.8, 2% sodium dodecyl sulfate [SDS], 0.1% bromophenol blue, 10% glycerol) and proteins were eluted at 65°C for 10 min. Loading buffer was transferred to a new 1.7-mL microcentrifuge tube and 2-β-

mercaptoethanol was added to a final concentration of 200 mM. This was then boiled for 5 minutes, and 20 μ L was resolved on a 4 to 12% polyacrylamide gradient gel (Biorad, 4561093). Proteins were fixed in 50% methanol, 40% ddH₂O, 10% acetic acid and visualized by blue-silver staining (0.12% Coomassie Blue G-250, 10% ammonium sulfate, 10% phosphoric acid, 20% methanol), described in Candiano et al. 2004.

3.3.6 Fluorescence microscopy

Cells were grown for at least 8 doublings in 25 mL SC in a 125-mL flask at 270 rpm, 25°C from a saturated culture to an OD₆₀₀ of 0.3. Ten μ L of culture were transferred to a 5 mm x 5 mm agarose pad (3% agarose in SC). The agarose pad with yeast was flipped and attached to a clean coverslip (cleaned with sonication in 1 M NaOH, 100% ethanol, and ultrapure water sequentially). A chamber was then constructed by adhering the coverslip to a 35 mm Petri dish (Cell E&G, GBD00002-200) using epoxy. The sample was equilibrated at 25°C in a plate incubator for 10 mins. Heat shock was initiated by placing the sample in a plate incubator at 37°C for 5 mins before being transferred to the microscope. The cells were maintained at 37°C using an onstage incubator and imaged at 5, 15, 30, 45, 60, 90, and 120 minutes post heat-shock.

The fluorescence microscope was home built on an Olympus IX-73 inverted microscope with an Olympus TIRF 100 \times N.A. = 1.49 oil immersion objective. The microscope and data acquisition were controlled by Micro-Manager. A 488 nm laser from a multilaser system (iChrome MLE, TOPTICA Photonics, New York) was used to excite GFP proteins in yeast. Emissions from the fluorescent proteins were collected by the objective and imaged on an EMCCD camera (Andor, Massachusetts) with an exposure time of 30 ms. The effective pixel size of the acquired images was 160 nm.

3.4 Results and Discussion

3.4.1 Metabolite changes occur early in the response to heat stress

Due to the critical role metabolites play in protein acetylation enzymatic processes, we began by looking at the levels of acetyl-CoA, the acetyl donor in KAT acetylation reactions, CoA, a byproduct of acetylation that can inhibit KAT activity, nicotinamide, a byproduct of sirtuin deacetylation that can act as a feedback inhibitor, and the NAD:NADH ratio, as NAD⁺ is consumed by sirtuins. For the first three, cells were harvested at 5, 15, 30, 60, and 120 minutes of heat shock and metabolite levels were analyzed via mass spectrometry in biological triplicate. Cellular levels of the acetyl donor acetyl-CoA showed an initial decrease averaging around 40% by the 60-minute mark before beginning to rebound (Fig. 3.2a). It is important to note that in live-cell conditions acetyl-CoA levels are compartmentalized between the mitochondria and cytoplasm, and thus this trend may be different in those compartments separately, whereas this assay can only analyze the combined pool. Consequential to the decrease in acetyl-CoA, there is an inverse trend in CoA levels, though the maximum of a roughly 150% increase occurs earlier than acetyl-CoA at 30 minutes before rapidly returning to unstressed levels by 60 minutes (Fig. 3.2b). Both of these changes, however, are occurring much earlier than the maximal changes in protein acetylation at 90 minutes, suggesting that the levels of these metabolites are not playing a large regulatory role in this response, and it is likely that these metabolite level changes are due to metabolic shifts focusing on energy production.

Next, we looked at nicotinamide, a product of the sirtuin deacetylation reaction that acts as a feedback inhibitor. We see a slight increase in nicotinamide levels within the first 5 minutes of heat shock, coinciding with possible histone deacetylation events beginning the transcriptional response, followed by an overall decrease in nicotinamide levels to 30% below unstressed levels at 30 minutes (Fig. 3.2c). Again, this response is occurring much earlier than global protein acetylation changes, suggesting it also is not playing a significant regulatory role.

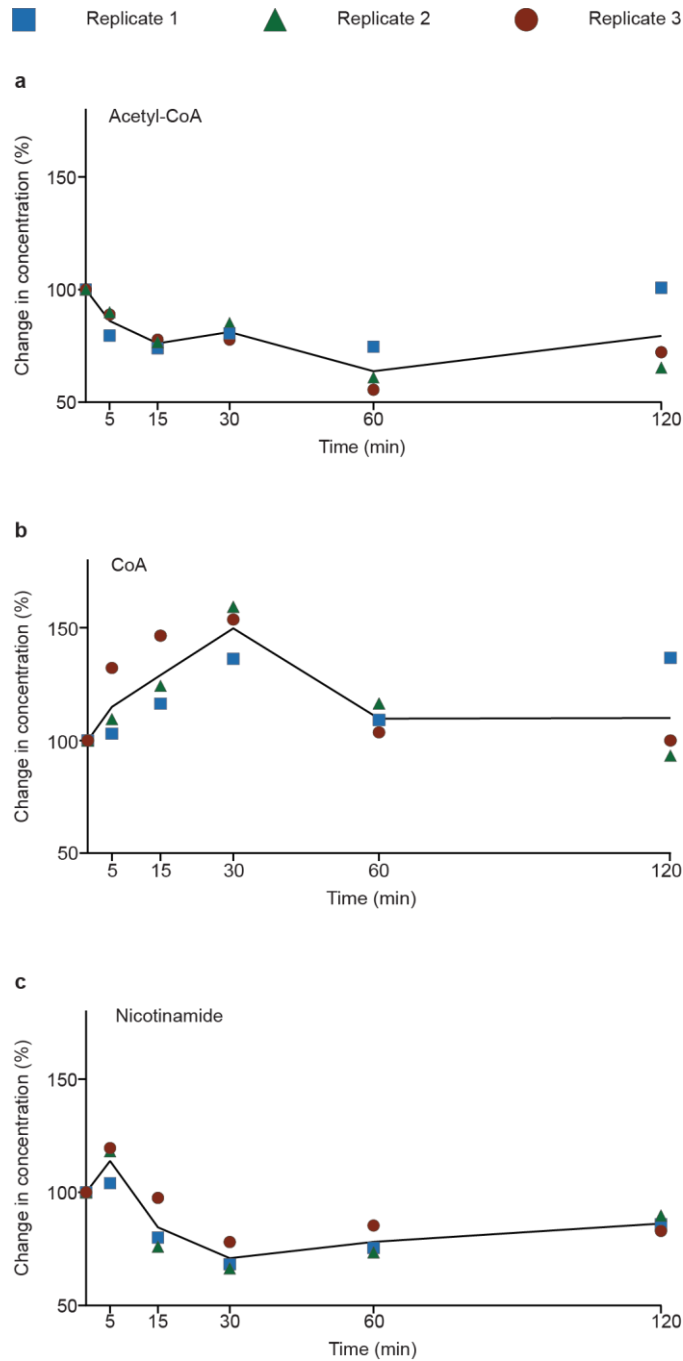


Figure 3.2 Concentrations of acetyl-CoA, CoA, and nicotinamide in response to heat shock. Concentrations of **A)** acetyl-CoA, **B)** CoA, and **C)** nicotinamide were determined across 120 minutes of heat shock using LC-MS/MS.

Finally, we looked at the ratio of NAD⁺ to NADH. NAD⁺ is consumed by sirtuins, and thus levels of NAD⁺ directly impact sirtuin activity. While we were able to obtain a somewhat consistent trend for the NAD⁺ to NADH ratio (Fig. 3.3a), each replicate showed wildly variable dynamics for NAD⁺ levels (Fig. 3.3b). Though the ratio is vital for understanding redox capabilities in the cell, sirtuins do not oxidize NAD⁺, but rather consume it to produce O-acetyl-ADP-ribose and nicotinamide (Figure 3.1), and thus the concentration of NAD⁺ is more informative. It is also very difficult to measure NAD⁺ and NADH in a biologically significant manner, as levels of these metabolites are highly compartmentalized and also exist in protein-bound forms that would not otherwise be available. While our ratios are similar to other whole-cell ratios, this measurement is significantly different from other forms of measurement that determine free cytosolic NAD:NADH using thermodynamic analysis of glycolytic metabolites (Canelas, van Gulik and Heijnen 2008).

3.4.2 KAT and KDAC complexes show little component changes

All of the KATs and KDACs perform their functions in complexes with other proteins that modulate the enzymatic efficiency and substrate specificity of the enzymatic subunit. To determine if there were any obvious changes in binding partners in response to heat stress, we performed TAP purification of each of the KAT and KDAC catalytic subunits that showed a significant enrichment for physical interactions with proteins we previously identified to be changing in acetylation in response to heat stress (Tables 3.4 And 3.5) across a heat shock time course at 37°C and analyzed for protein species that appear to change in abundance. Of the 11 enzymes, three KATs showed visual interaction changes during the time course: Esa1 (Fig. 3.4 and Table 3.6), Hpa3 (Fig. 3.5), and Taf1 (Fig. 3.6 And Table 3.7). Remaining immunoprecipitations can be found in figure 3.A.1.

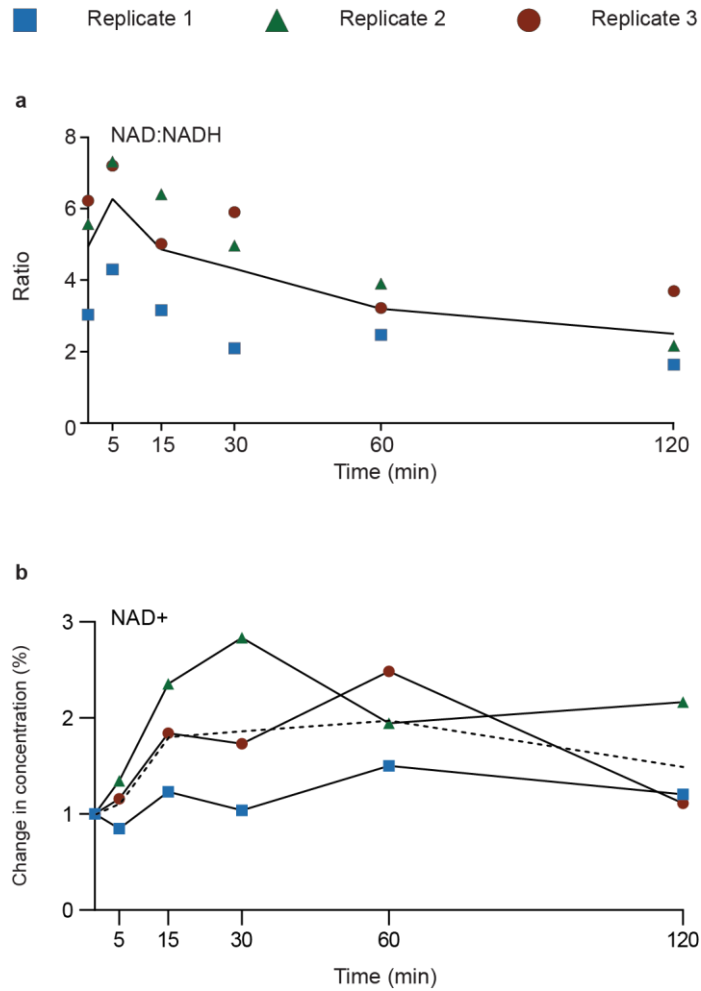


Figure 3.3 NAD:NADH ratio and NAD⁺ fold change in response to heat shock. A) The NAD:NADH ratio was monitored across a 120-minute heat shock using a NAD/NADH-Glo™ luminescence assay in which NAD⁺ was selectively destroyed by heating in a basic solution, while NADH was selectively destroyed in an acidic solution. Thus, luminescence from acid-treated samples is proportional to the amount of NAD⁺, and luminescence from the base-treated samples is proportional to the amount of NADH. **B)** Fold change in NAD⁺ levels calculated from the base treated sample described in **A**).

Table 3.4 Hypergeometric p-values for KATs and increasing acetylation clusters

KAT	Cluster		
	1	2	3
Eco1	--	--	--
Elp3	--	--	0.17547
Esa1	0.12959	0.23259	0.00459
Gcn5	0.00015	2.40162E-05	1.61560E-10
Hat1	0.12689	0.17923	0.00033
Hpa2	--	--	0.06702
Hpa3	--	--	0.58089
Rtt109	0.05390	--	0.12964
Sas2	--	0.11799	0.19437
Sas3	--	--	--
Spt10	0.24136	--	0.21214
Taf1	0.29324	--	0.08131

Table 3.5 Hypergeometric p-values for KDACs and decreasing acetylation clusters

KDAC	Cluster				
	4	5	6	7	8
Hda1	0.10023	0.00380	0.01016	0.00728	0.15357
Hos1	--	--	--	--	--
Hos2	--	--	0.09620	--	--
Hos3	--	0.07437	0.00702	--	--
Hst1	--	--	--	--	--
Hst2	0.02513	--	0.00057	0.03086	0.03939
Hst3	0.04619	--	0.00206	0.05657	0.07194
Hst4	--	--	--	--	--
Rpd3	0.27518	0.24771	0.01107	0.05831	0.00152
Set3	--	--	0.12466	--	--
Sir2	0.00241	0.02373	0.00714	0.00032	0.35117

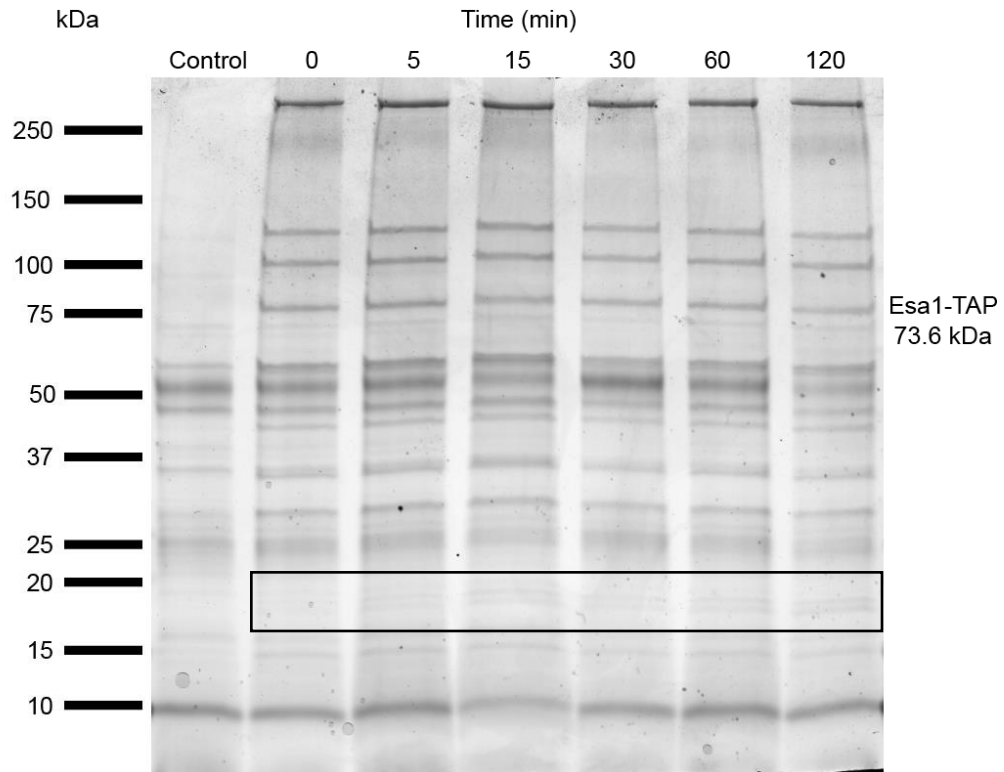


Figure 3.4 Co-Immunoprecipitation of Esa1-TAP. Co-immunoprecipitation of Esa1 and interacting proteins using a TAP-tagged Esa1 and visualized with blue-silver staining. Two bands appeared to change in abundance and were identified as the ribosomal protein Rpl12A and vesicle membrane receptor protein Snc2.

Table 3.6 Fold change in Rpl12A and Snc2 interacting with Esa1 compared to control

Time (min)	Rpl12A Fold Change	Snc2 Fold Change
5	0.90	0.94
15	2.51	2.12
30	1.74	1.23
60	1.81	2.09
120	2.72	2.98

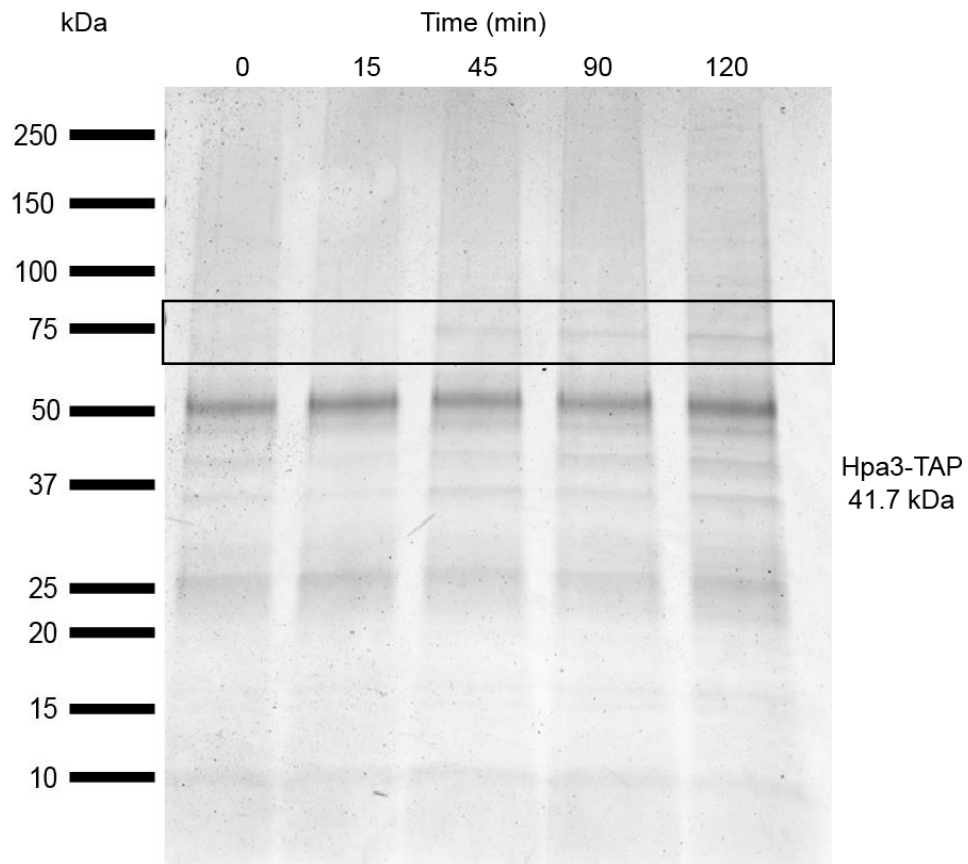


Figure 3.5 Co-Immunoprecipitation of Hpa3-TAP. Co-immunoprecipitation of Hpa3 and interacting proteins using a TAP-tagged Hpa3 and visualized with blue-silver staining. One band appeared to change in abundance, but we were unable to reproduce the result sufficiently for identification.

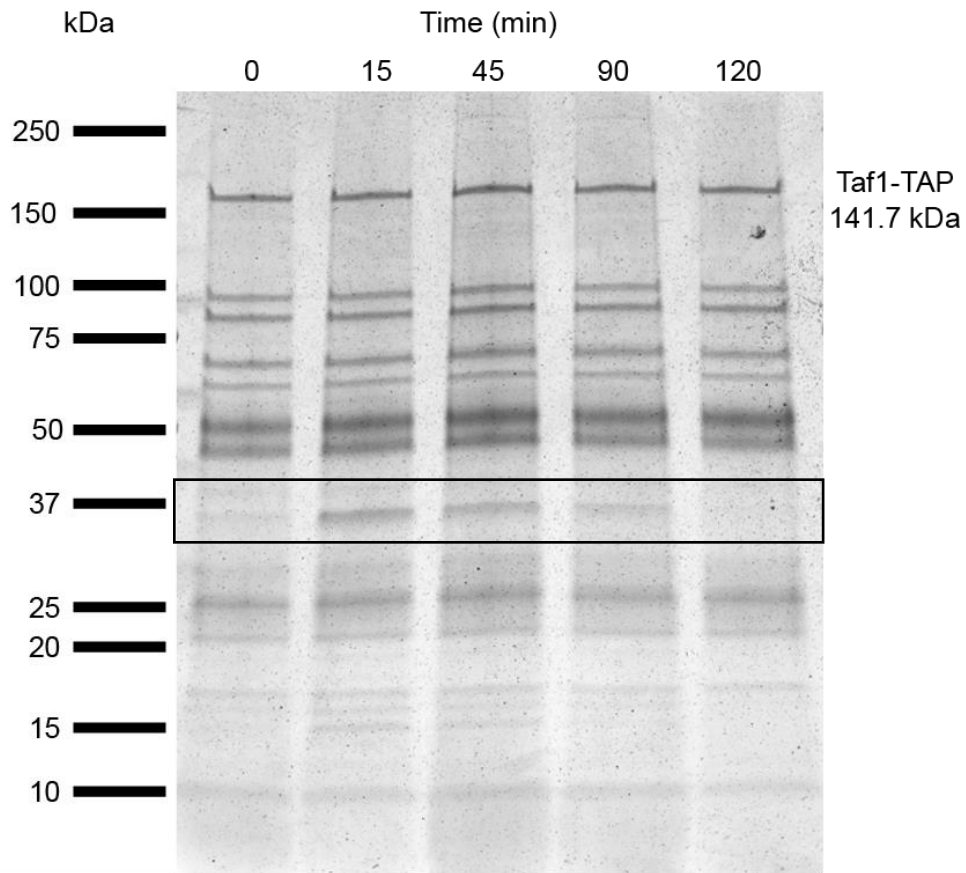


Figure 3.6 Co-Immunoprecipitation of Taf1-TAP. Co-immunoprecipitation of Taf1 and interacting proteins using a TAP-tagged Taf1 and visualized with blue-silver staining. One band changing in abundance was identified as the glyceraldehyde-3-phosphate dehydrogenase isoform Tdh3,

Table 3.7 Fold change of Tdh3 interacting with Taf1 compared to control

Time (min)	Fold change
15	4.32
45	2.08
90	1.23
120	0.17

Due to the high sensitivity of mass spectrometer, all bands came back with over 250 identified proteins, but based on highest total spectral counts, the two bands identified in the Esa1 samples are most likely the ribosomal protein Rpl12A, a constituent of the 60s ribosomal subunit, and the vesicle membrane receptor protein Snc2. While we were not able to identify Snc2 in our previous study, we did identify Rpl12A as an acetylated protein, though the levels of acetylation did not appear to be significantly changing in response to heat stress. It is likely that these interactions are simply substrate interactions, and not affecting the activity of Esa1. The Hpa3 co-immunoprecipitated band was not visible when the purification was repeated for identification. This could mean that the first purification was spurious, but in both attempts, the levels of Hpa3 were very low, which may explain why the changing band was not visible the second time.

The changing species purified with Taf1 is the glyceraldehyde-3-phosphate dehydrogenase Tdh3. Tdh3 was found to be highly acetylated in our time course data as well as in other studies (Henriksen et al. 2012). Interestingly, Tdh3 serves a variety of moonlighting functions. It plays a vital role as a labile heme chaperone (Sweeny et al. 2018) and Tdh3 peptides have been found to accumulate on the surface of cells and serve as an antimicrobial agent upon cell to cell contact (Branco et al. 2017). Most relevant to this study, Tdh3 is critical for the proper assembly of the major KAT SAGA. While it is not found in the final SAGA complex, it is instead found in other small complexes with Gcn5, the SAGA enzymatic subunit. Further studies concluded that Tdh3 contributed to Gcn5 incorporation into SAGA by protecting newly produced Spt20 from cleavage allowing Spt20 to co-translationally associate with Ada2, a necessary step in SAGA formation (Kassem, Villanyi and Collart 2017). Ada2 is critical for Gcn5 incorporation into SAGA and activates Gcn5's acetyltransferase activity (Sun et al. 2018). While we do not know whether the association of Tdh3 with Taf1 is a part of its moonlighting functions or as a substrate, it is likely that this is not a coincidence, especially considering the >4-fold increase in association following heat shock, and further study is needed.

3.4.3 Hda1 translocates from the nucleus to the cytoplasm

In our final experiment to identify mechanisms regulating acetyl dynamics, we wanted to see if any of the significantly enriched KAT and KDAC enzymatic subunits showed localization changes in response to heat. Most of these enzymes are known to be in the nucleus where they are involved in transcription control, but the majority of proteins that we found to be experiencing changes in acetylation are in the cytoplasm. To test if any of these proteins are translocating into the cytoplasm, we monitored the GFP-tagged proteins in live cells across 2 hours of incubation at 37°C, imaging at 5, 15, 30, 45, 60, 90, and 120 minutes (Table 3.8, Fig 3.7 and Supplemental Fig. 3.A.2). With this approach, we identified the KDAC Hda1 as a possible candidate for translocation. This response also appears to occur late in the response, after 60 minutes (Figs. 3.7 and 3.8), similar to when we see the majority of deacetylation events. Hda1 has been shown to be involved in the regulatory deacetylation of the cytoplasmic Hsp90, a key player in the heat stress response (Robbins et al. 2012). This suggests that Hda1 may be a contributor to non-nuclear protein deacetylation in response to heat shock.

3.5 Conclusion

While we were not able to definitively identify a major regulatory mechanism for the acetylation dynamics identified in the yeast response to heat shock, it is apparent that regulation likely occurs on multiple levels to finely tune this response. While the majority of metabolite levels relevant to acetylation appear to show their largest fluctuations earlier in the response than the bulk of the acetylation changes, it is possible that localized metabolite concentrations have differing effects on proteins in that region of the cell, such as in the nucleus or the mitochondria. With few exceptions, we were not able to detect large KAT or KDAC localization changes or complex remodeling, but it is very likely that this is occurring at levels below our level of detection, and that even at these lower levels these changes could have significant

Table 3.8 Known KAT and KDAC localization

KAT/KDAC	Molecules/cell ^a	Localization ^a
Esa1	1170	nucleus
Gcn5	1180	nucleus
Hat1	not visualized	n/a
Hda1	3050	nucleus
Hst2	5260	cytoplasm
Hst3	319	nucleus
Rpd3	3850	nucleus and cytoplasm
Rtt109	1140	nucleus
Sir2	3350	nucleus
Taf1	1500	nucleus

a. Obtained from the yeast GFP-fusion localization database (Huh et al. 2003)

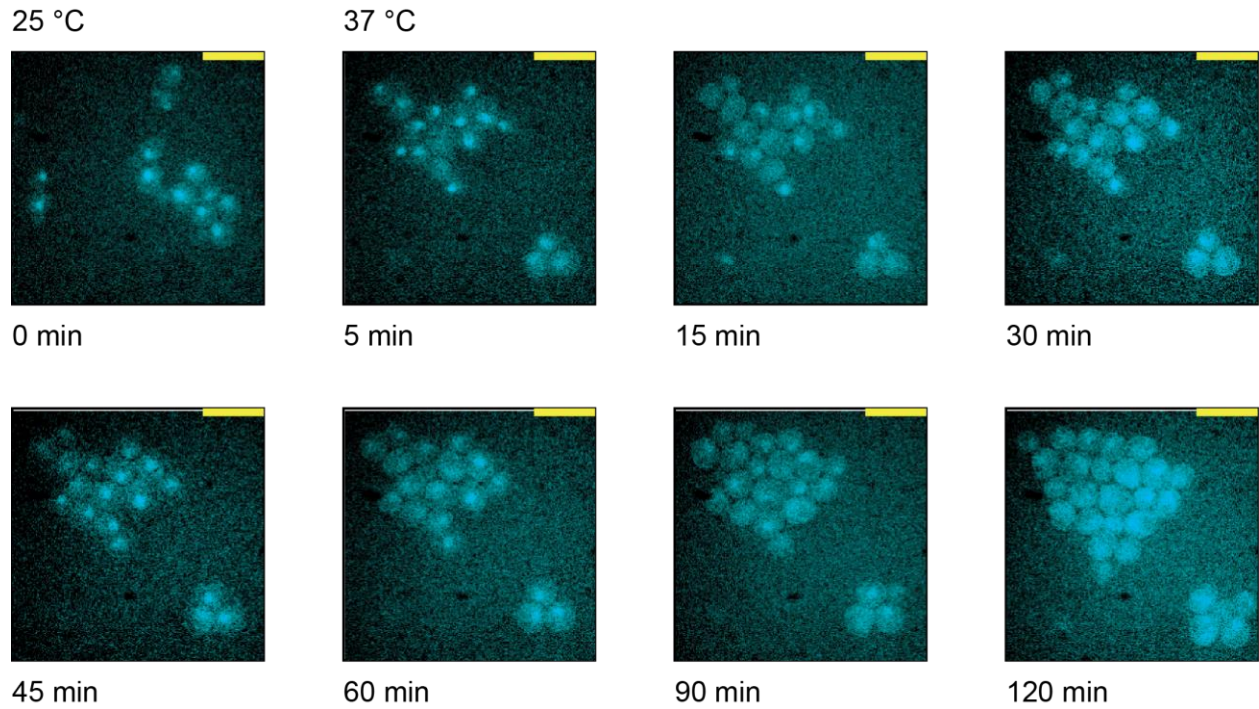


Figure 3.7 Hda1 relocates to the cytoplasm after 45 minutes of heat shock at 37°C. Strains carrying a GFP-tagged Hda1 were visualized at 37°C for 2 hours to determine possible changes in Hda1 localization. Hda1 appears to move out of the nucleus and into the cytosol after an hour, exposing it to a different substrate pool. Scale bar = 10 μ m

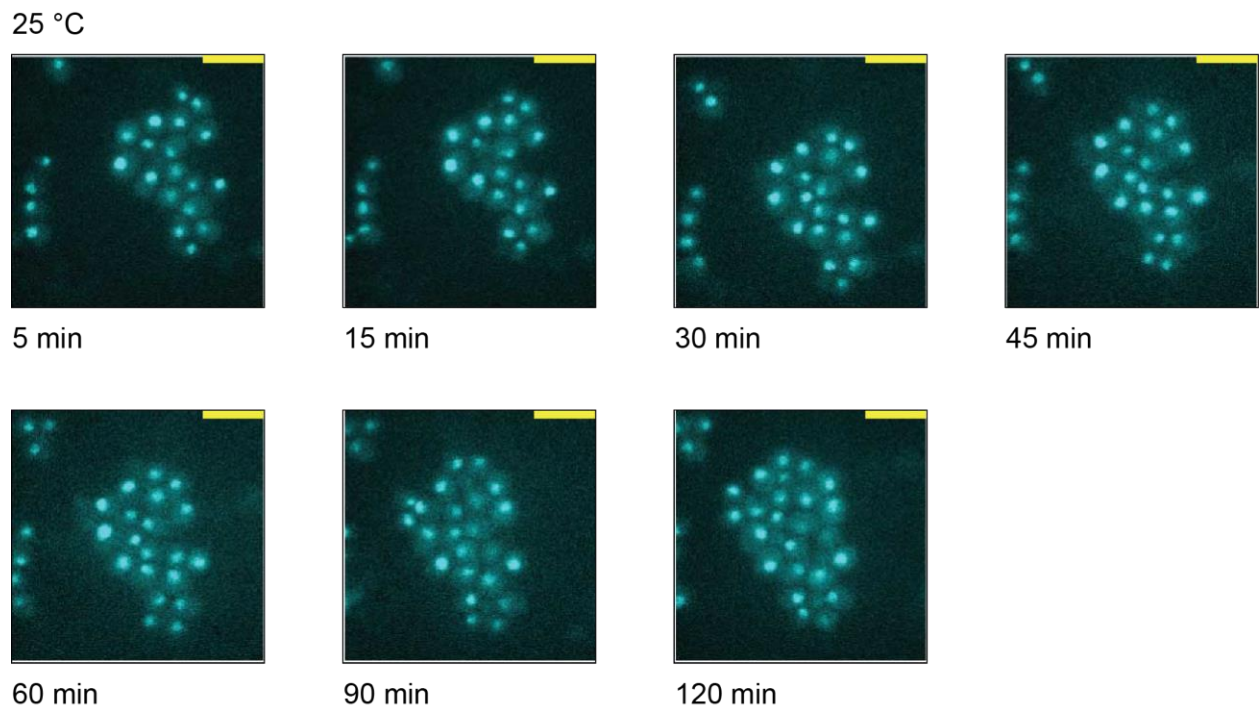


Figure 3.8 Hda1 resides in the nucleus in unstressed conditions at 25°C.

effects. Further, more specific methods of analysis will be needed to better understand the multiple levels of regulation that are likely occurring in this response.

3.6 Acknowledgements

We would like to thank Dr. Andrew Alverson and Dr. Elizabeth Ruck for equipment use and advice, Dr. Kristen Baetz and Dr. Michael Downey for providing Esa1-GFP, and for general advice from Dr. Downey.

3.7 References

- Albaugh, B. N., K. M. Arnold & J. M. Denu (2011) KAT(ching) Metabolism by the Tail: Insight into the links between lysine acetyltransferases and metabolism. *Chembiochem*, 12, 290-8.
- Albaugh, B. N., E. M. Kolonko & J. M. Denu (2010) Kinetic mechanism of the Rtt109-Vps75 histone acetyltransferase-chaperone complex. *Biochemistry*, 49, 6375-85.
- Balasubramanian, R., M. G. Pray-Grant, W. Selleck, P. A. Grant & S. Tan (2002) Role of the Ada2 and Ada3 transcriptional coactivators in histone acetylation. *J Biol Chem*, 277, 7989-95.
- Berndsen, C. E., B. N. Albaugh, S. Tan & J. M. Denu (2007) Catalytic mechanism of a MYST family histone acetyltransferase. *Biochemistry*, 46, 623-9.
- Boffa, L. C., G. Vidali, R. S. Mann & V. G. Allfrey (1978) Suppression of histone deacetylation in vivo and in vitro by sodium butyrate. *J Biol Chem*, 253, 3364-6.
- Branco, P., V. Kemsawasd, L. Santos, M. Diniz, J. Caldeira, M. G. Almeida, N. Arneborg & H. Albergaria (2017) *Saccharomyces cerevisiae* accumulates GAPDH-derived peptides on its cell surface that induce death of non-*Saccharomyces* yeasts by cell-to-cell contact. *FEMS Microbiol Ecol*, 93.
- Candiano, G., M. Bruschi, L. Musante, L. Santucci, G. M. Ghiggeri, B. Carnemolla, P. Orecchia, L. Zardi & P. G. Righetti (2004) Blue silver: a very sensitive colloidal Coomassie G-250 staining for proteome analysis. *Electrophoresis*, 25, 1327-33.
- Canelas, A. B., W. M. van Gulik & J. J. Heijnen (2008) Determination of the cytosolic free NAD/NADH ratio in *Saccharomyces cerevisiae* under steady-state and highly dynamic conditions. *Biotechnol Bioeng*, 100, 734-43.

- Cherry, J. M., E. L. Hong, C. Amundsen, R. Balakrishnan, G. Binkley, E. T. Chan, K. R. Christie, M. C. Costanzo, S. S. Dwight, S. R. Engel, D. G. Fisk, J. E. Hirschman, B. C. Hitz, K. Karra, C. J. Krieger, S. R. Miyasato, R. S. Nash, J. Park, M. S. Skrzypek, M. Simison, S. Weng & E. D. Wong (2012) Saccharomyces Genome Database: the genomics resource of budding yeast. *Nucleic Acids Res*, 40, D700-5.
- Crutchfield, C. A., W. Lu, E. Melamud & J. D. Rabinowitz (2010) Mass spectrometry-based metabolomics of yeast. *Methods Enzymol*, 470, 393-426.
- Galdieri, L., T. Zhang, D. Rogerson, R. Lleshi & A. Vancura. 2014. Protein Acetylation and Acetyl Coenzyme A Metabolism in Budding Yeast. In *Eukaryot Cell*, 1472-83.
- Henriksen, P., S. A. Wagner, B. T. Weinert, S. Sharma, G. Bacinskaja, M. Rehman, A. H. Juffer, T. C. Walther, M. Lisby & C. Choudhary (2012) Proteome-wide analysis of lysine acetylation suggests its broad regulatory scope in *Saccharomyces cerevisiae*. *Mol Cell Proteomics*, 11, 1510-22.
- Huh, W. K., J. V. Falvo, L. C. Gerke, A. S. Carroll, R. W. Howson, J. S. Weissman & E. K. O'Shea (2003) Global analysis of protein localization in budding yeast. *Nature*, 425, 686-91.
- Kassem, S., Z. Villanyi & M. A. Collart (2017) Not5-dependent co-translational assembly of Ada2 and Spt20 is essential for functional integrity of SAGA. *Nucleic Acids Res*, 45, 1186-1199.
- Kouzarides, T. (2000) Acetylation: a regulatory modification to rival phosphorylation? *EMBO J*, 19, 1176-9.
- Menzies, K. J., H. Zhang, E. Katsyuba & J. Auwerx (2016) Protein acetylation in metabolism - metabolites and cofactors. *Nat Rev Endocrinol*, 12, 43-60.
- Mitchell, L., J. P. Lambert, M. Gerdes, A. S. Al-Madhoun, I. S. Skerjanc, D. Figeys & K. Baetz (2008) Functional dissection of the NuA4 histone acetyltransferase reveals its role as a genetic hub and that Eaf1 is essential for complex integrity. *Mol Cell Biol*, 28, 2244-56.
- Robbins, N., M. D. Leach & L. E. Cowen (2012) Lysine deacetylases Hda1 and Rpd3 regulate Hsp90 function thereby governing fungal drug resistance. *Cell Rep*, 2, 878-88.
- Sekhavat, A., J. M. Sun & J. R. Davie (2007) Competitive inhibition of histone deacetylase activity by trichostatin A and butyrate. *Biochem Cell Biol*, 85, 751-8.
- Sun, J., M. Paduch, S. A. Kim, R. M. Kramer, A. F. Barrios, V. Lu, J. Luke, S. Usatyuk, A. A. Kossiakoff & S. Tan (2018) Structural basis for activation of SAGA histone acetyltransferase Gcn5 by partner subunit Ada2. *Proc Natl Acad Sci U S A*, 115, 10010-10015.
- Sweeny, E. A., A. B. Singh, R. Chakravarti, O. Martinez-Guzman, A. Saini, M. M. Haque, G. Garee, P. D. Dans, L. Hannibal, A. R. Reddi & D. J. Stuehr (2018) Glyceraldehyde-3-phosphate dehydrogenase is a chaperone that allocates labile heme in cells. *J Biol Chem*, 293, 14557-14568.

Tanner, K. G., M. R. Langer, Y. Kim & J. M. Denu (2000) Kinetic mechanism of the histone acetyltransferase GCN5 from yeast. *J Biol Chem*, 275, 22048-55.

3.8 Appendix

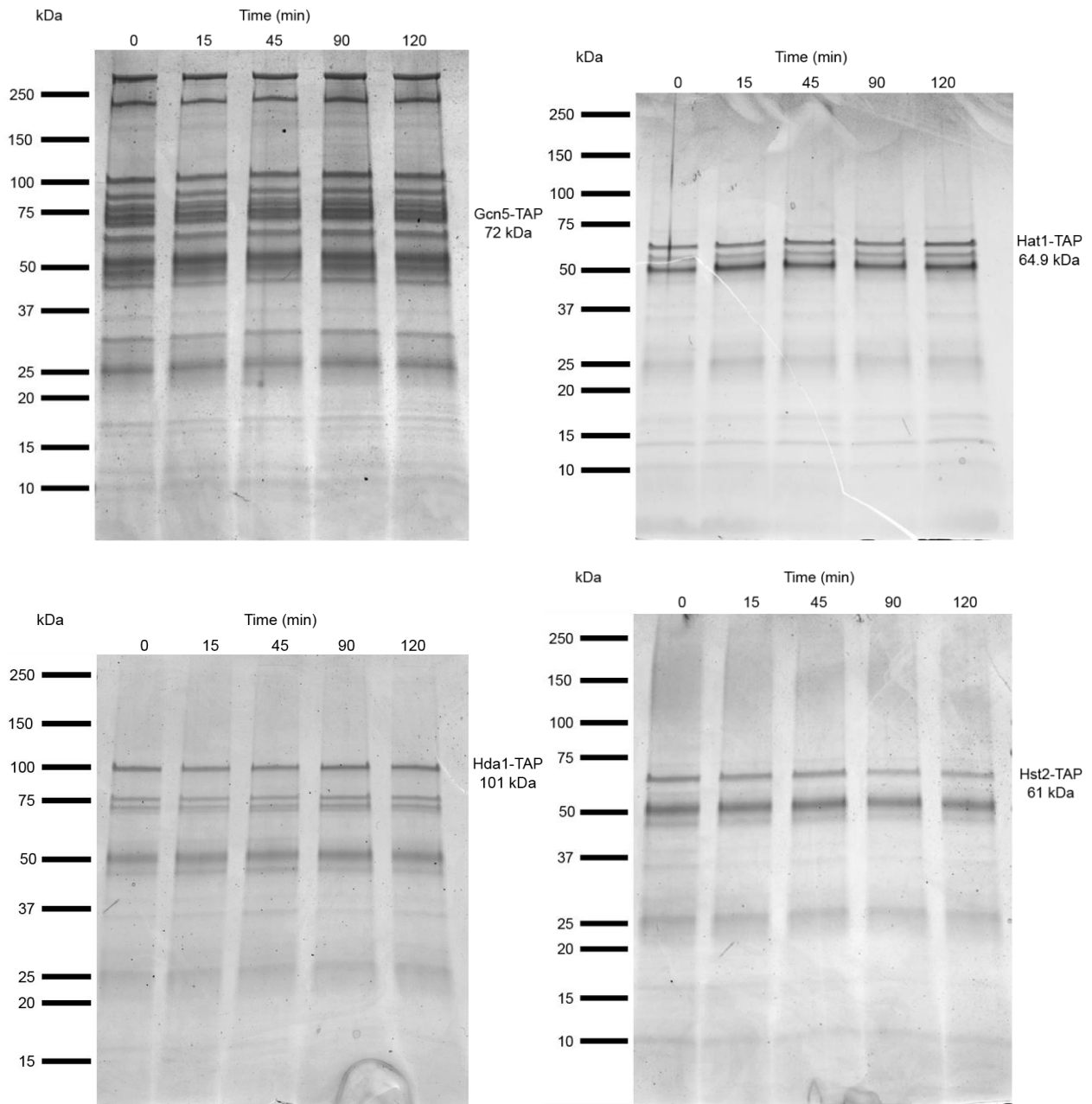


Figure 3.A.1 Tap co-immunoprecipitations of KAT and KDAC enzymes and interacting proteins. Identified KAT and KDAC enzymes and interacting proteins were co-immunoprecipitated and visualized with blue-silver staining. No interaction changes were visualized.

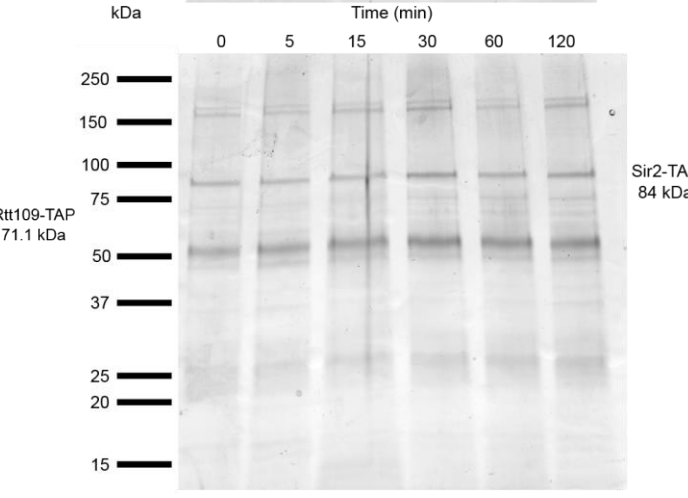
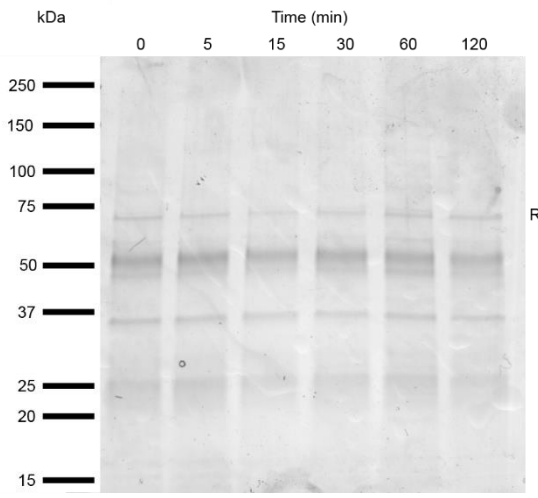
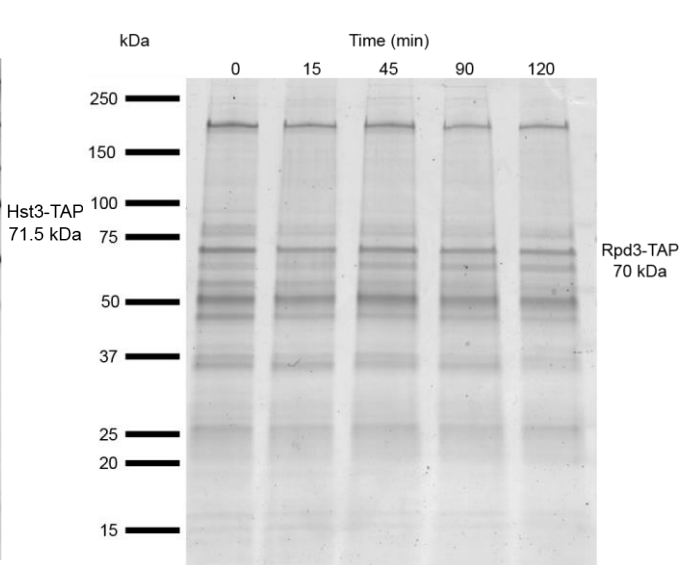
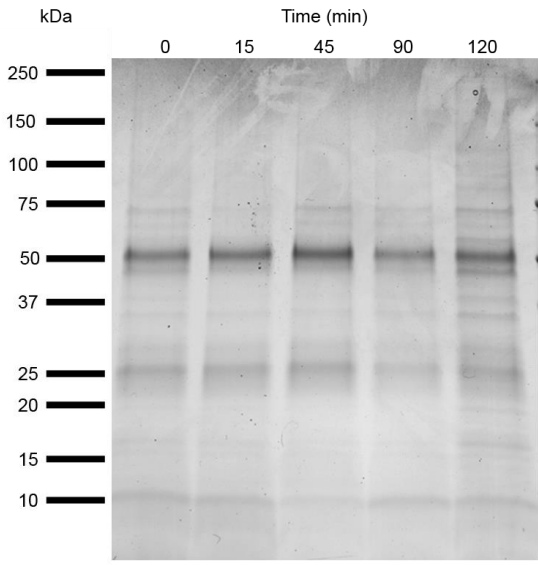
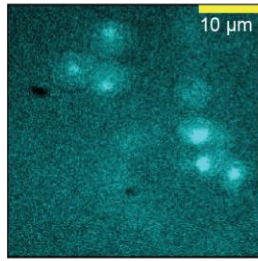
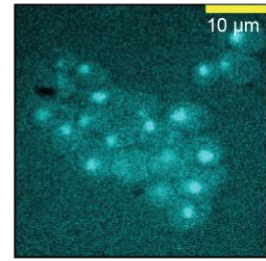
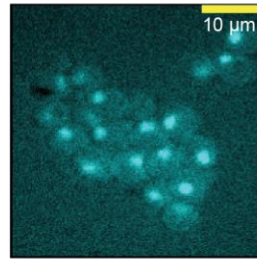
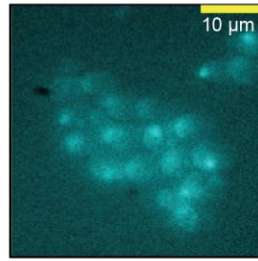


Figure 3.A.1 (cont.)

Esa1-GFP
25 °C



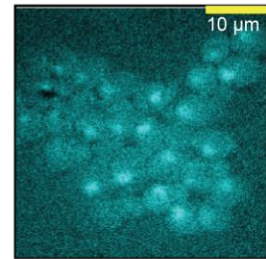
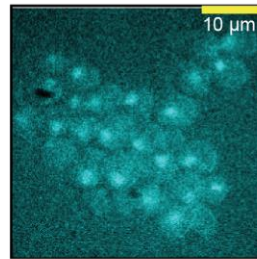
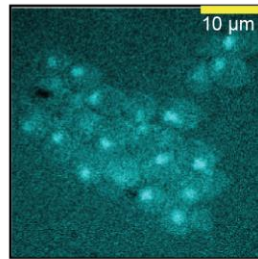
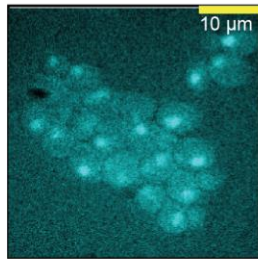
37 °C



5 min

15 min

30 min



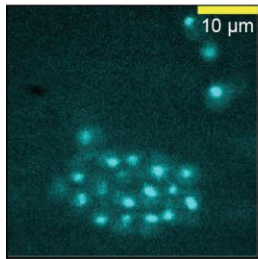
45 min

60 min

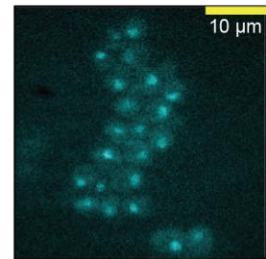
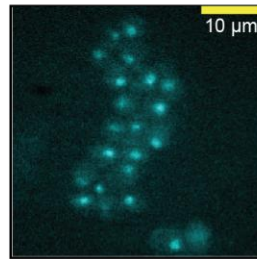
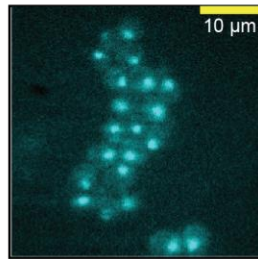
90 min

120 min

Gcn5-GFP
25 °C



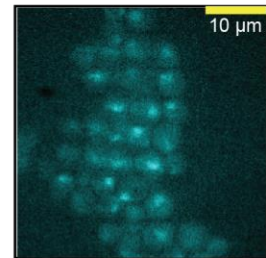
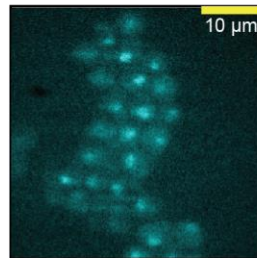
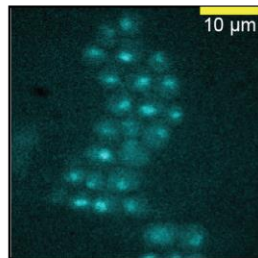
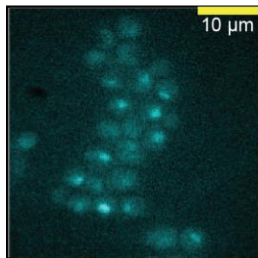
37 °C



5 min

15 min

30 min



45 min

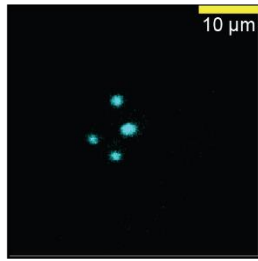
60 min

90 min

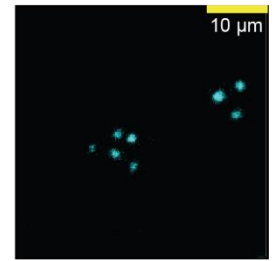
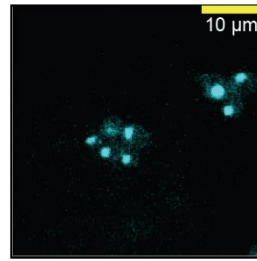
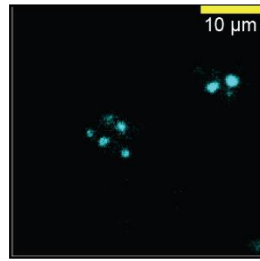
120 min

Figure 3.A.2 Localization of KATs and KDACs during heat shock. Localization of enriched KATs and KDACs was monitored using a GFP-tagged across a 120-minute heat shock.

Hat1-GFP
25 °C



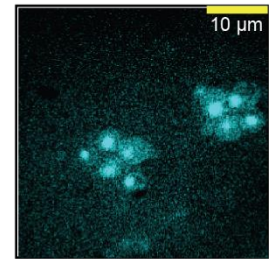
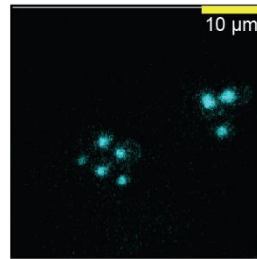
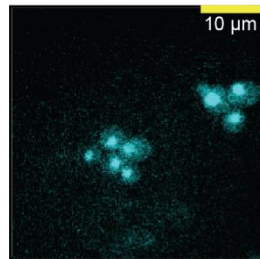
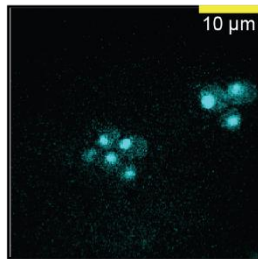
37 °C



5 min

15 min

30 min



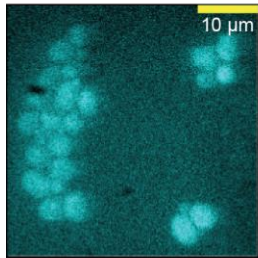
45 min

60 min

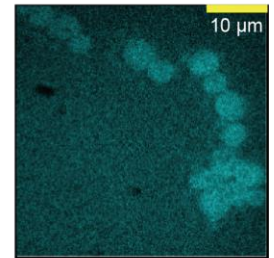
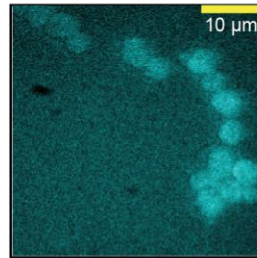
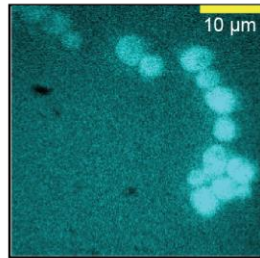
90 min

120 min

Hpa3-GFP
25 °C



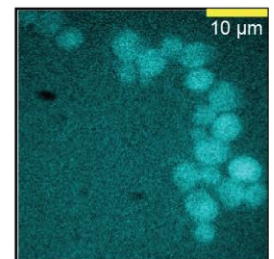
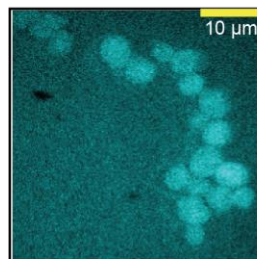
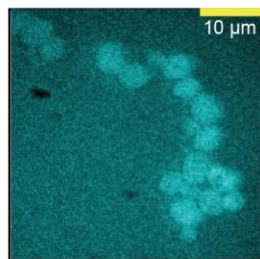
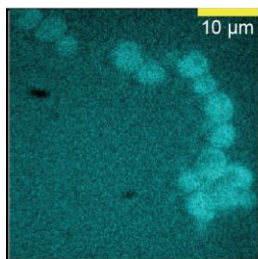
37 °C



5 min

15 min

30 min



45 min

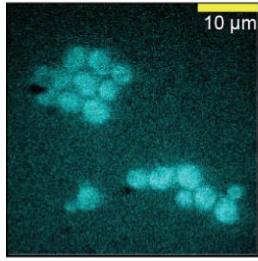
60 min

90 min

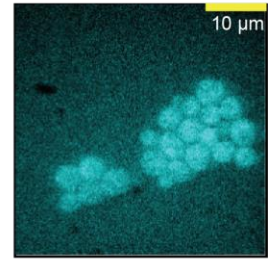
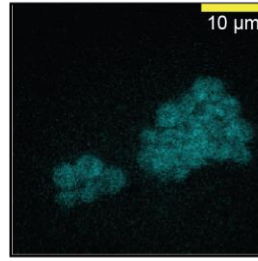
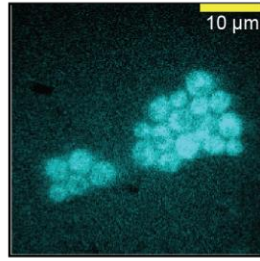
120 min

Figure 3.A.2 (cont.)

Hst2-GFP
25 °C



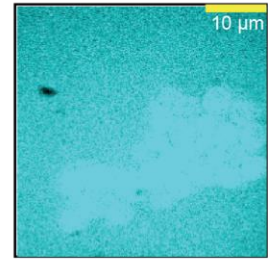
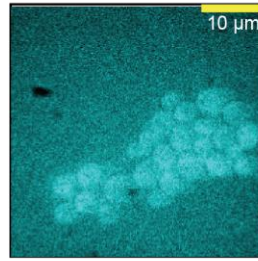
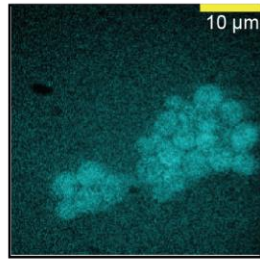
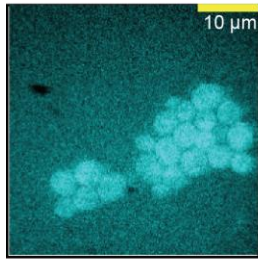
37 °C



5 min

15 min

30 min



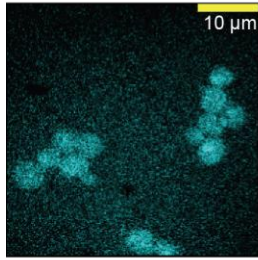
45 min

60 min

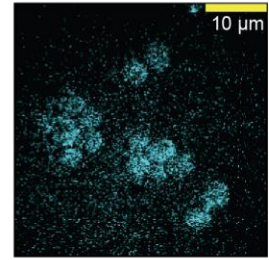
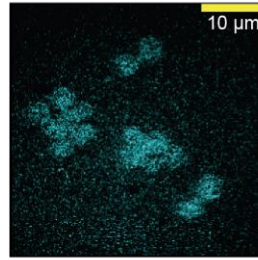
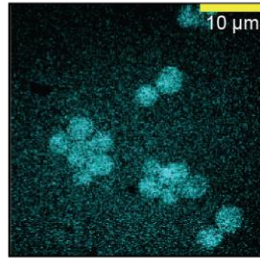
90 min

120 min

Hst3-GFP
25 °C



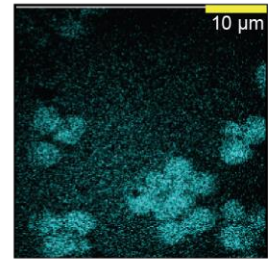
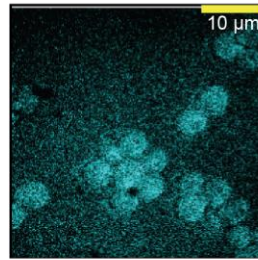
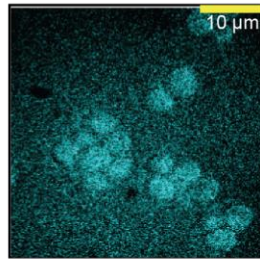
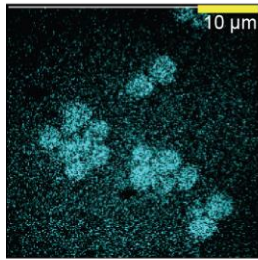
37 °C



5 min

15 min

30 min



45 min

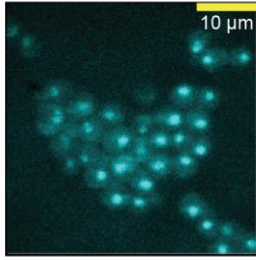
60 min

90 min

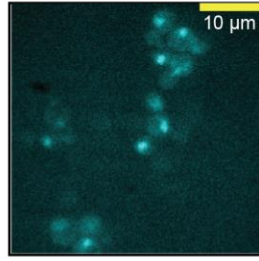
120 min

Figure 3.A.2 (cont.)

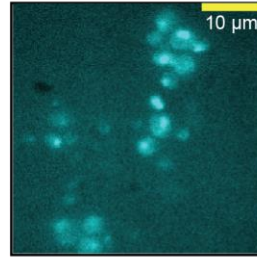
Rpd3-GFP
25 °C



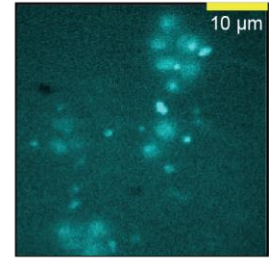
37 °C



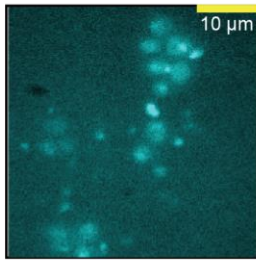
5 min



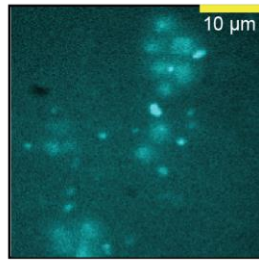
15 min



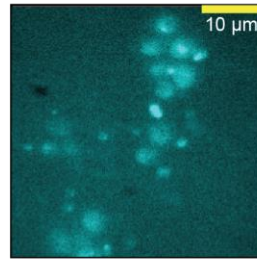
30 min



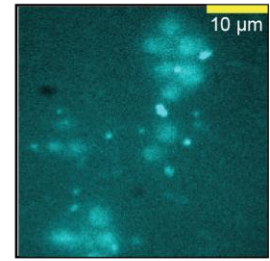
45 min



60 min

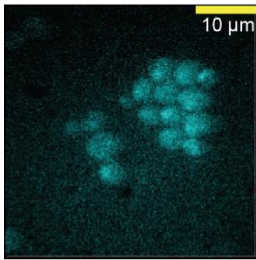


90 min

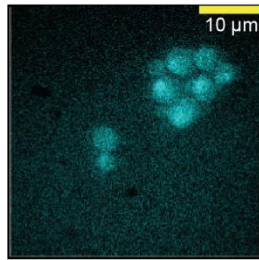


120 min

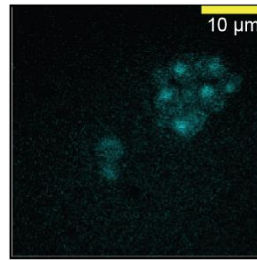
Rtt109-GFP
25 °C



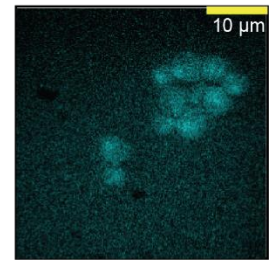
37 °C



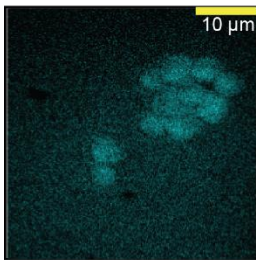
5 min



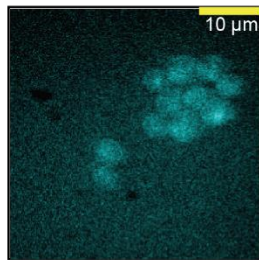
15 min



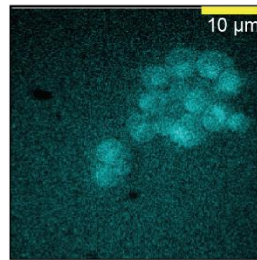
30 min



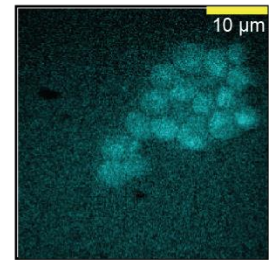
45 min



60 min



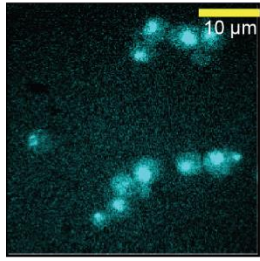
90 min



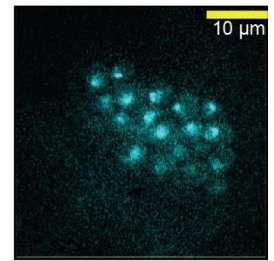
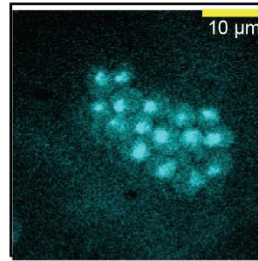
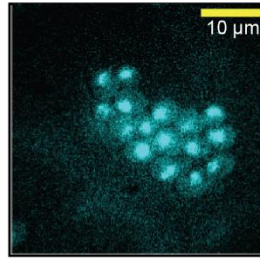
120 min

Figure 3.A.2 (cont.)

Sir2-GFP
25 °C



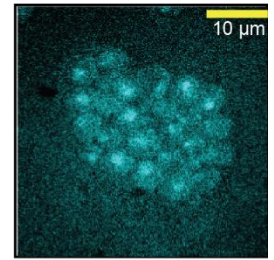
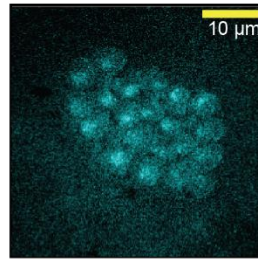
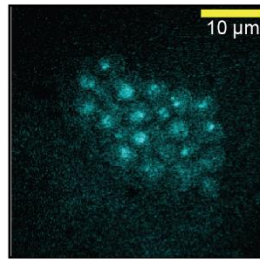
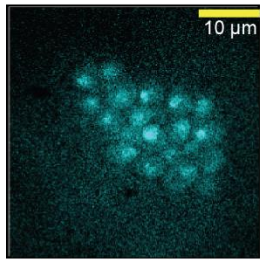
37 °C



5 min

15 min

30 min



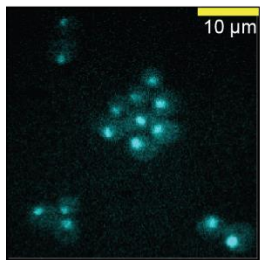
45 min

60 min

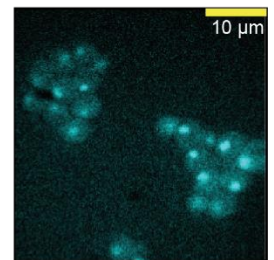
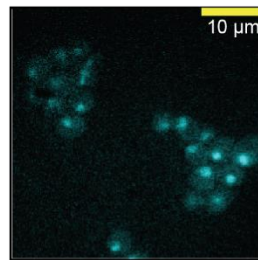
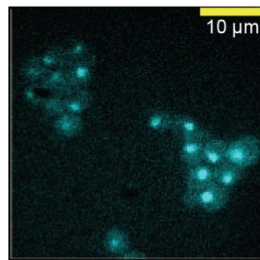
90 min

120 min

Taf1-GFP
25 °C



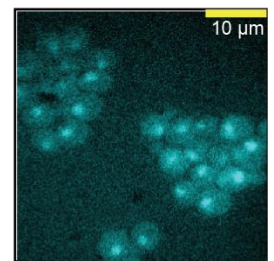
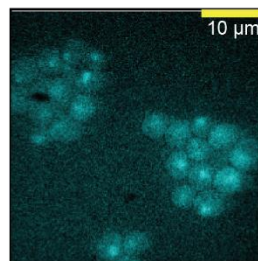
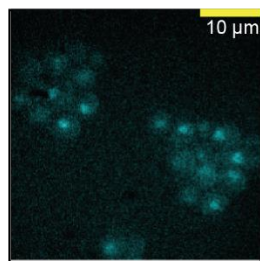
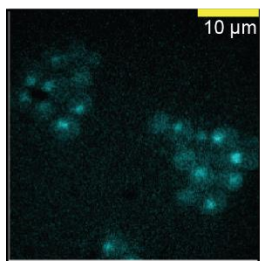
37 °C



5 min

15 min

30 min



45 min

60 min

90 min

120 min

Figure 3.A.2 (cont.)

Chapter 4 Conclusions and Future Directions

4.1 Conclusions

4.1.1 The yeast acetylome is highly dynamic in response to heat stress

Recent studies have identified thousands of acetyl sites across all domains of life, but few of these studies looked at global acetylation changes in response to changing environmental conditions. To identify acetyl marks that are potentially serving a regulatory role, we analyzed global acetylation dynamics in the heat shock response of *Saccharomyces cerevisiae* at 37°C over four hours. In total, we identified 1473 acetylated peptides representing 596 proteins. Of those, 387 residues representing 207 unique proteins showed a significant fold change (Benjamini-Hochberg corrected p-value <0.05) in acetylation in at least one time point compared to t0. The majority of these significantly changing marks (74%) occurred at 90 minutes of heat shock, the same time at which the majority of significant protein level changes are occurring. This was surprising to us, as we had hypothesized that acetylation changes would occur earlier in the response as a rapid mechanism for protein regulation before transcriptional and translational changes could take effect.

Analyzing the dynamics of these changes we clustered the data and identified peptides with distinct dynamics. Proteins with lysines showing increased acetylation during heat shock were strongly enriched protein folding and refolding, carbohydrate and small molecule metabolism, and the response to heat. Proteins with decreasing lysine acetylation were functionally enriched for translation, ribosome biogenesis, and nitrogen and peptide metabolism. In the increasing peptides we also noticed a generally weaker but still significant enrichment for translation and the same was true for decreasing peptides with protein (re) folding, and intrigued as to why these processes were enriched in both increasing and decreasing clusters we looked for proteins that experienced both significant increasing and decreasing acetylation on different lysines. We identified 36 non-histone proteins that fall into this category, and almost half were involved in translation including 14 ribosome constituents. The fact that we see increasing and

decreasing acetylation on the same protein suggests that this process may be dynamically regulated. 64 proteins also experienced significant acetyl changes without showing significant changes in protein level, furthering the evidence for regulation and not just increased or decreased likelihood of random interactions with acetyltransferases or deacetylases.

4.1.2 Multiple KATs and KDACs are enriched for physical interactions with proteins experiencing significant acetylation changes

The two classes responsible for protein acetylation changes are lysine acetyltransferases (KATs) and lysine deacetylases (KDACs). To determine which of the 12 KATs and 11 KDACs in yeast are most likely to be involved in the dynamics we identified, we examined whether they were significantly enriched for physical interactions for each of these enzymes. Among proteins with increasing acetylation, there was strong enrichment for Gcn5 in all clusters, as well as enrichment for Esa1 and Hat1 in one of the three. We also identified the KATs Taf1 and Hpa3 as enriched across all increasing acetylated proteins. In the decreasing clusters, we found a wide variety of enrichments totaling six different KDACs, Rpd3, Hda1, Sir2, Hst2, Hst3, and Hos3.

To further evaluate possible regulatory mechanisms for these enzymes, we looked for possible changes in binding partners through TAP co-immunoprecipitation and localization changes using GFP. We identified changing binding partners with three KATs: Esa1, Hpa3, and Taf1. Mass spectrometry identified the changing proteins binding Esa1 to be the ribosomal protein Rpl12A and the vesicle membrane receptor protein Snc2. The dramatically changing protein interacting with Taf1 is the glyceraldehyde 3-phosphate isomer Tdh3. While the effect of this binding is unknown, Tdh3 is known to perform many moonlighting functions in the cell, and further investigation is warranted. We were unable to identify the protein associating with Hpa3 due to low abundance. Looking at localization changes, the only enzyme that appeared to be

relocalizing in response to stress was the KDAC Hda1, which translocated from the nucleus to the cytoplasm after 60 minutes at 37°C.

4.1.3 Acetylation dynamics are not likely due to metabolite concentration changes

To determine possible mechanisms by which these acetylation dynamics are being regulated we began by measuring metabolite level fluctuation in response to heat stress. In all known enzymatic acetylation reactions, the acetyl donor is acetyl-CoA and CoA is released. It then stands to reason that acetyl-CoA levels could regulate these dynamics. Our data, however, indicates that the maximum decrease of acetyl-CoA and the corresponding increase of CoA fluctuations occur much earlier, 60 minutes and 30 minutes respectively, than the majority of acetyl changes at 90 minutes, suggesting that these levels are not having much of a regulatory effect. Looking at metabolites regulating deacetylation, we focused on NAD⁺, which is consumed by sirtuins, and nicotinamide, a product of sirtuin deacetylation that acts as a feedback inhibitor. Similar to the previous metabolites, however, changes in these metabolites are occurring much earlier than deacetylation changes. Nicotinamide displays a slight increase within the first 5 minutes followed by a maximum decrease at 30 minutes. Monitoring NAD⁺ as a ratio between its oxidized and reduced form as NADH also shows a brief increase at 5 minutes, followed by a steady decrease through the remaining two hours that we monitored. NAD⁺ levels alone did not show a reproducible trend.

4.2 Future Directions

4.2.1 Effect of acetylation changes on protein activity and function

Now that we have identified a number of proteins that are experiencing acetylation changes in response to heat stress, the next big question is what consequence these changes have on protein activity and function. The addition of the acetyl group on a lysine residue negates the positive charge, and this can have dramatic effects on how that region of the

protein interacts with its environment. A well-known example of this is in the regulation of transcription via histone acetylation. Positively charged histone residues interact strongly with the negatively charged phosphate backbone of DNA, making it inaccessible for transcription. Following acetylation, however, this interaction is weakened, allowing transcription factor binding and transcription initiation. Two possible techniques to determine the effect of acetylation on protein function are mimetics and non-canonical amino acid incorporation.

In the first method, lysine residues that are identified as significantly changing in acetylation can be genetically mutated to arginine, chemically mimicking an unacetylated lysine, or glutamine, mimicking an acetylated lysine (Dormeyer, Ott and Schnölzer 2005, Kim et al. 2006). Mutation to alanine is also performed to determine the effect of a neutrally charged mutation in that region of the protein as a control. These strains can then be subjected to phenotypic analysis in which wild-type and deletion strains show differing phenotypes. If the mimetic behaves similarly to the wild type strain, then the protein most likely has wild-type activity, and if the mimetic strain is more phenotypically similar to the deletion strain, then it does not. In the case that the alanine, arginine, and glutamine mutations all behave similarly to the deletion strain, then it is likely that mutation of that residue is not tolerated, a major caveat of this technique.

For proteins in which an activity assay is feasible, a second alternative to test the effect of acetylation on specific residues is by incorporating acetyllysine into the protein as it is being translated in *E. coli*, followed by purification [Reviewed in Chen et al. 2018]. This involves mutating the codon for the target lysine to an amber stop codon (UAG) and expressing an engineered archaeal Pyrrolysyl-tRNA synthetase (PylRS) and tRNA^{Pyl} to create acetyllysine tRNA molecules with the UAG anticodon (Neumann, Peak-Chew and Chin 2008, Venkat et al. 2017). This approach, however, cannot be done *in vivo*, where other factors are likely regulating protein function.

Based on the known activity of the proteins we identified during the stress response, I suspect that the majority of the acetylation marks identified in this study serve as activating marks. The proteins that experienced the strongest increase acetylation are well known to be involved in the response to heat stress including protein chaperones and genes involved in glucose and ergosterol metabolism. The proteins experiencing the strongest decreases in acetylation, however, are those known to be repressed in the response to heat shock such as ribosomal proteins. It would then make sense that the increasing acetylation marks are activating stress defense proteins while removing acetylation marks are repressing the unfavorable activity of others.

4.2.2 Determine KATs and KDACs involved in the acetyl dynamics of the heat shock response

While this study identified hundreds of changing acetylation marks, we were only able to speculate on which KATs and KDACs were responsible for these changes based on known physical interactions. These known interactions, however, were identified by other groups and in most cases in different conditions. Using the same TMT time-course method in KAT and KDAC deletion strains would provide a more accurate depiction of the KATs and KDACs regulating these dynamics. For example, we would compare peptides that are deacetylated in the wild-type background to those that are not in a KDAC deletion background. Peptides that are no longer deacetylated in the latter can assume to be targets of that KDAC. One major caveat of this approach is redundancy among these enzymes. It is very likely that these enzymes share substrates, and multiple deletions may be required. This approach would also not be suitable for identifying Esa1 targets, as this protein is essential (Smith et al. 1998).

4.2.3 Conservation of changing acetyllysine residues

A previous study by Henriksen et al. (2012) showed that acetylated lysines in yeast were highly conserved among higher eukaryotes including drosophila and humans. This suggests that these residues are important for protein function, causing them to be maintained throughout evolutionary history. We can use this approach to make similar conclusions about lysine residues that are changing in acetylation. This will also suggest which residues are more likely to have significant regulatory roles for further biochemical and genetic analysis.

4.3 Future of acetylproteomics

As it is now well established that protein acetylation is a widespread and conserved modification, further work is needed to understand how this process is regulated. The enzymes involved in this process are well known and studied for their roles in transcription regulation, but substrate recognition outside of histones is still in its infancy. By identifying larger substrate pools for these enzymes, we will be able to generate more specific binding motifs, allowing for better prediction of acetylation sites especially among proteins showing lower acetylation stoichiometry. This will require technological advances as well, as the current methods using antibodies for enrichment show distinct biases for specific recognition sequences and more highly abundant proteins/proteins which are highly acetylated.

It has also become more important to look more closely at multiple modifications, as there appears to be significant cross-talk (Beltrao et al. 2013, Soufi et al. 2012). For example, phosphorylation of a protein may be necessary for the subsequent acetylation of a nearby lysine residue. Modification competition may also play a significant role in protein regulation. Of the hundreds of known PTMs, the majority occur on a small number of residues, namely those with charges side chains such as serine, tyrosine, threonine, arginine, and lysine. Three of the most abundant PTMs, acetylation, methylation, and ubiquitination, all occur on lysine residues. Once a residue is modified with one chemical group, this sufficiently blocks the addition of another. An

example of this is acetylation of p53, which leads to stabilization and activation, inhibiting repression of p53-mediated transcription activation, by blocking ubiquitination and methylation (Meek and Anderson 2009, Li et al. 2002)

Another aspect of regulation that is still unknown for acetylation is whether there are signaling cascades such as those seen with phosphorylation. Many proteins involved in protein acetylation are acetylated themselves either by KATs or through autoacetylation. It is possible that changing acetylation sites affect substrate specificity, leading to changing acetyl dynamics in the cell. To test this hypothesis, future work needs to be conducted looking at protein acetylation in changing conditions. Thus far, the majority of acetylation studies have looked in static conditions, or researchers are only looking at a very small number of proteins of interest. Global, non-biased studies monitoring acetylation dynamics during various cellular responses will provide deeper insight into which acetyl marks are more likely to be serving a regulatory function, and highlight which pathways are being most affected.

The above discussion also highlights the importance of model organism research in the field. Following the discovery that KDAC inhibitors were potential candidates for cancer treatment, a large portion of acetylation studies focused on acetylation in disease states (Hassell 2019, Auburger et al. 2014, Narita et al. 2018). However, we still do not have a deep understanding of the basic biology of protein acetylation, which can be better addressed in simpler eukaryotic organisms for which there are a plethora of biochemical and genetic tools such as yeast and *Drosophila*.

4.4 References

- Auburger, G., S. Gispert & M. Jendrach (2014) Mitochondrial acetylation and genetic models of Parkinson's disease. *Prog Mol Biol Transl Sci*, 127, 155-82.
- Beltrao, P., P. Bork, N. J. Krogan & V. van Noort (2013) Evolution and functional cross-talk of protein post-translational modifications. *Mol Syst Biol*, 9, 714.

- Chen, H., S. Venkat, P. McGuire, Q. Gan & C. Fan (2018) Recent Development of Genetic Code Expansion for Posttranslational Modification Studies. *Molecules*, 23.
- Dormeyer, W., M. Ott & M. Schnölzer (2005) Probing lysine acetylation in proteins: strategies, limitations, and pitfalls of in vitro acetyltransferase assays. *Mol Cell Proteomics*, 4, 1226-39.
- Hassell, K. N. (2019) Histone Deacetylases and their Inhibitors in Cancer Epigenetics. *Diseases*, 7.
- Henriksen, P., S. A. Wagner, B. T. Weinert, S. Sharma, G. Bacinskaja, M. Rehman, A. H. Juffer, T. C. Walther, M. Lisby & C. Choudhary (2012) Proteome-wide analysis of lysine acetylation suggests its broad regulatory scope in *Saccharomyces cerevisiae*. *Mol Cell Proteomics*, 11, 1510-22.
- Kim, S. C., R. Sprung, Y. Chen, Y. Xu, H. Ball, J. Pei, T. Cheng, Y. Kho, H. Xiao, L. Xiao, N. V. Grishin, M. White, X. J. Yang & Y. Zhao (2006) Substrate and functional diversity of lysine acetylation revealed by a proteomics survey. *Mol Cell*, 23, 607-18.
- Li, M., J. Luo, C. L. Brooks & W. Gu (2002) Acetylation of p53 inhibits its ubiquitination by Mdm2. *J Biol Chem*, 277, 50607-11.
- Meek, D. W. & C. W. Anderson (2009) Posttranslational Modification of p53: Cooperative Integrators of Function. *Cold Spring Harb Perspect Biol*, 1.
- Narita, T., B. T. Weinert & C. Choudhary (2018) Functions and mechanisms of non-histone protein acetylation. *Nat Rev Mol Cell Biol*.
- Neumann, H., S. Y. Peak-Chew & J. W. Chin (2008) Genetically encoding N(epsilon)-acetyllysine in recombinant proteins. *Nat Chem Biol*, 4, 232-4.
- Smith, E. R., A. Eisen, W. Gu, M. Sattah, A. Pannuti, J. Zhou, R. G. Cook, J. C. Lucchesi & C. D. Allis (1998) ESA1 is a histone acetyltransferase that is essential for growth in yeast. *Proc Natl Acad Sci U S A*, 95, 3561-5.
- Soufi, B., N. C. Soares, V. Ravikumar & B. Macek (2012) Proteomics reveals evidence of cross-talk between protein modifications in bacteria: focus on acetylation and phosphorylation. *Curr Opin Microbiol*, 15, 357-63.
- Venkat, S., C. Gregory, K. Meng, Q. Gan & C. Fan (2017) A Facile Protocol to Generate Site-Specifically Acetylated Proteins in *Escherichia Coli*. *J Vis Exp*.

Supplemental Chapter 1 Accurate and Sensitive Quantitation of the Dynamic Heat Shock Proteome using Tandem Mass Tags

Aaron J. Storey¹, Rebecca E. Hardman^{2,4}, Stephanie D. Byrum¹, Samuel G. Mackintosh¹, Rick D. Edmondson³, Wayne P. Wahls¹, Alan J. Tackett¹, and Jeffrey A. Lewis^{4,*}

¹ Department of Biochemistry and Molecular Biology, University of Arkansas for Medical Sciences, Little Rock, Arkansas 72205, United States of America

² Interdisciplinary Graduate Program in Cell and Molecular Biology, University of Arkansas, Fayetteville, Arkansas 72701, United States of America

³ College of Medicine, University of Arkansas for Medical Sciences, Little Rock, Arkansas 72205, United States of America

⁴ Department of Biological Sciences, University of Arkansas, Fayetteville, Arkansas 72701, United States of America

Author contributions: A.J.S. performed TMT 2 sample preparation and all mass spectrometry and data analysis. R.E.H. performed TMT10 sample preparation and western blot validation. J.A.L. performed data analysis and wrote the following manuscript.

This work has been deposited to the preprint server BioRxiv and submitted for publication

Abstract

Cells respond to environmental perturbations and insults through modulating protein abundance and function. However, the majority of studies have focused on changes in RNA abundance because quantitative transcriptomics has historically been more facile than quantitative proteomics. Modern Orbitrap mass spectrometers now provide sensitive and deep proteome coverage, allowing direct, global quantification of not only protein abundance, but also post-translational modifications (PTMs) that regulate protein activity. We implemented and validated using the well-characterized heat shock response of budding yeast, a tandem mass tagging (TMT), triple-stage mass spectrometry (MS3) strategy to measure global changes in the proteome during the yeast heat shock response over nine time points. We report that basic pH, ultra-high performance liquid chromatography (UPLC) fractionation of tryptic peptides yields super fractions of minimal redundancy, a crucial requirement for deep coverage and quantification by subsequent LC-MS3. We quantified 2,275 proteins across 3 biological replicates and found that differential expression peaked near 90 minutes following heat shock (with 868 differentially expressed proteins at 5% FDR). The sensitivity of the approach also allowed us to detect changes in the relative abundance of ubiquitination and phosphorylation PTMs over time. Remarkably, relative quantification of post-translationally modified peptides revealed striking evidence of regulation of the heat shock response by protein PTMs. These data demonstrate that the high precision of TMT-MS3 enables peptide-level quantification of samples, which can reveal important regulation of protein abundance and regulatory PTMs under various experimental conditions.

Introduction

Cells employ a diverse array of regulatory strategies to maintain homeostasis in the face of environmental challenges. These regulatory strategies exist on a number of physiological timescales. For instance, rapid responses (i.e. seconds to minutes) necessitate changing the activity of proteins that are already present in the cell and can include changing concentrations of regulatory metabolites (e.g. allosteric inducers or inhibitors) or covalent post-translational protein modifications (PTMs). Over longer time scales (i.e. minutes to hours), cells can respond to stressful environments by remodeling gene expression. For example, the model eukaryote *Saccharomyces cerevisiae* responds to stress by globally remodeling gene expression to shift translational capacity towards the production of stress defense proteins that increase cellular fitness in the face of stress (Gasch et al. 2000a, Causton et al. 2001, Lee et al. 2011).

While changes in protein abundance and activities are the ultimate mediators of biological responses, the majority of studies have historically focused on transcriptional changes. This was largely due to technical challenges related to accurately quantifying protein abundance (Zhou et al. 2013). Independent of sequence, nucleic acids are chemically homogeneous enough to allow for the common hybridization chemistry used for microarrays (Shalon, Smith and Brown 1996), and subsequently for high-throughput sequencing (Bentley et al. 2008). In contrast, proteins are much more heterogeneous and diverse in their chemistries, limiting our ability to design “one-size fits all” approaches to proteomics. Furthermore, it was generally assumed that while imperfect, mRNA levels were an adequate proxy for protein level estimates. However, early studies comparing the transcriptome and proteome in multiple organisms showed extremely poor correlations between mRNA and protein levels (Gygi et al. 1999, Griffin et al. 2002, Nie, Wu and Zhang 2006, Washburn et al. 2003), creating a real doubt about whether mRNA levels were really a good proxy for protein levels. Some of this discrepancy may be due to experimental noise (Csardi et al. 2015), highlighting both the challenge and importance of being able to accurately quantitate peptide abundance. However,

while the correlation between mRNA and protein levels is not as poor as initially thought (Schwanhausser et al. 2011, Csardi et al. 2015), substantial regulation of protein levels still occurs post-transcriptionally. For example, detailed comparisons between mRNA and protein levels during the yeast response to hyperosmotic shock revealed that ~80% of the variation in induced proteins can be explained by changes in mRNA abundance, with the remaining variation possibly explained by translational or post-translational regulation (Lee et al. 2011). Similarly, ribosomal profiling experiments have identified widespread changes in mRNA translational efficiency under a number of conditions ranging from meiosis to stress (Brar et al. 2012, Halbeisen and Gerber 2009, Lackner et al. 2012). Finally, it is well established that protein stability and degradation play an important role in regulated protein turnover during environmental shifts (Medicherla and Goldberg 2008, Martin-Perez and Villen 2017). Indeed, because proteins have longer half-lives than RNAs (Belle et al. 2006), lack of translation alone is generally insufficient to reduce protein levels. Thus, regulated proteolysis is a key mechanism for ridding the cell of irrevocably damaged proteins and proteins that are maladaptive to a new environment (Ho, Baryshnikova and Brown 2018a, Rutkowski et al. 2006).

In addition to protein abundance changes, PTMs are well known to regulate protein activity and/or stability during environmental shifts. For example, stress-activated protein kinases coordinate phospho-signal transduction cascades that are largely conserved from yeast through humans (Brewster et al. 1993, Proft et al. 2001, Han et al. 1998, Rouse et al. 1994). Acetylation and methylation of histones and transcription factors also facilitate transcriptional reprogramming during stress (Shivaswamy and Iyer 2008, Wang et al. 2007, Xie et al. 2012, Westerheide et al. 2009a, Magraner-Pardo et al. 2014). During stress, damaged proteins are frequently targeted for proteasomal degradation via ubiquitination (Medicherla and Goldberg 2008, Wang et al. 2010). Additionally, global changes in SUMOylation play an important role in heat stress adaptation (Miller et al. 2013, Golebiowski et al. 2009), providing further support for the notion that global PTM remodeling is a broad regulatory strategy during stress adaptation.

Thus, an integrated view of stress physiology requires the ability to sensitively and accurately measure relative protein abundance and PTMs.

Here, we describe a workflow for using a tandem mass tagging (TMT) strategy to measure global proteomic changes during environmental shifts. The key advantage is that this approach supports simultaneous analyses of multiple samples in the same MS run. As a proof-of-concept, we measured protein abundance changes in yeast before and after heat shock. The response to elevated temperature is arguably the best-studied environmental response across diverse organisms, with many important evolutionary features conserved from bacteria to humans (Lindquist and Craig 1988, Verghese et al. 2012a). Heat stress affects a number of cellular targets including increasing membrane fluidity (Swan and Watson 1997) (which leads to disruption of nutrient uptake (Mishra and Prasad 1987), pH balance (Coote, Cole and Jones 1991, Panaretou and Piper 1992), and ROS production due to “leaking” of electrons from the mitochondrial electron transport chain (Davidson and Schiestl 2001)), and protein unfolding (leading to induction of heat shock protein (HSP) chaperones and other protectants such as trehalose (Glover and Lindquist 1998, Jakob et al. 1993, Singer and Lindquist 1998a)).

While many studies have characterized the global transcriptional response to heat shock in yeast (Causton et al. 2001, Gasch et al. 2000a, Eng et al. 2010, Wohlbach et al. 2014, Yoon and Brem 2010, Yassour et al. 2010), relatively few studies have examined proteomic changes (Nagaraj et al. 2012, Jarnuczak et al. 2018). Moreover, these previous studies used either stable isotope labeling of amino acids in cell culture (SILAC) or label-free proteomics, which may have disadvantages compared to the multiplexing capacity of TMT. We used a MultiNotch triple-stage mass spectrometry (MS3) workflow to quantify peptides, which mitigates interference of nearly isobaric contaminant ions that cause an underestimate of differential expression (Ting et al. 2011, McAlister et al. 2014). We tested our workflow using a 10-plex design comparing the proteome of unstressed cells to heat-shocked cells over 9 time points, with three biological replicates.

Our TMT-MS3 workflow, which included pre-fractionation of peptide mixtures to reduce sample complexity and increase coverage of identifications, identified over 3000 proteins and quantified over 2000 proteins between a heat shock and unstressed control sample. In addition to providing insight into the dynamics of protein abundance changes during heat shock, we also identified post-translationally modified peptides whose relative abundance also changed dynamically. These data demonstrate that the high precision of TMT-MS3 enables peptide-level quantification of samples, which can reveal important regulation of protein post-translational modifications under various experimental conditions.

Experimental Procedures

Sample Preparation for TMT-Labeling and LC-MS/MS

Yeast Growth Conditions

We first performed a pilot TMT 2-plex experiment comparing unstressed cells to heat-stressed cells at a single time point, followed by a TMT-10 heat shock timecourse that was performed with three independent biological replicates. For both experiments, yeast strain BY4741 (S288c background; MATa his3 Δ 1 leu2 Δ 0 met15 Δ 0 ura3 Δ 0) was grown >7 generations to mid-exponential phase (OD₆₀₀ of 0.3 to 0.6) at 25°C and 125 rpm in YPD medium (1% yeast extract, 2% peptone, 2% dextrose). For the TMT-2 experiment, 500-ml of starting culture was divided in half, collected by centrifugation at 1,500 x g for 3 minutes, resuspended in either pre-warmed 25°C medium (unstressed sample) or 37°C medium (heat shocked sample), and then incubated for 1 hour at 25°C or 37°C, respectively. Following incubation, samples were collected by centrifugation at 1500 x g for 3 minutes, the media was decanted, and the pellet was flash-frozen in liquid nitrogen and stored at -80°C until processing. For the TMT-10 experiment, two 1 L cultures of exponentially growing cells were pooled, and then the culture was split across three flasks. Two flasks received 500-ml culture, while the third flask received 250-ml culture plus 250-ml 25°C YPD (to maintain exponential growth at the 90, 120, and 240

minute time points). Heat shock was performed by adding an equal amount of 55°C preheated media to immediately bring the final temperature to 37°C followed by continued incubation at 37°C. One-hundred twenty ml of cells were collected on cellulose nitrate filters by vacuum filtration from an unstressed sample and samples exposed to heat shock for 5, 10, 15, 30, 45, 60, 90, 120, and 240 minutes. Cells were immediately scraped from the filters into liquid nitrogen and stored at -80°C until processing.

TMT 2-Plex Sample Preparation

For the TMT-2 experiment, cell pellets were resuspended in 3 ml of lysis buffer (20 mM HEPES, 150 mM potassium acetate, 2 mM magnesium acetate, pH 7.4) plus EDTA-free Protease Inhibitor Tablets (Pierce catalog number 88266), and frozen dropwise into liquid nitrogen. Samples were lysed by cryogrinding using a Retsch MM 400 Mixer Mill (5 cycles of 30 Hz for 3 minutes), returning the chamber to liquid nitrogen between rounds. Proteins were thawed in cold water and precipitated with 4 volumes of ice-cold acetone overnight, and resuspended in 5 ml of buffer containing 8 M urea, 5 mM dithiothreitol, and 1 M ammonium bicarbonate, pH 8.0. Ammonium bicarbonate was included to reduce protein carbamylation that occurs in urea-containing buffers (Sun et al. 2014). Samples were divided into 1 ml aliquots, flash-frozen in liquid nitrogen, and stored at -80°C until further processing.

Protein samples were reduced by incubating with 5 mM tris(2-carboxyethyl)phosphine (TCEP) at 37°C for 1 hour and alkylated with 15 mM iodoacetamide at room temperature for 30 minutes. Protein samples were extracted with chloroform-methanol (Wessel and Flugge 1984), resuspended in 100 mM triethylammonium bicarbonate (TEAB) pH 8.0 with 1 µg Trypsin per 50 µg protein, and incubated at 37°C for 16 hours. Tryptic peptides were desalted with Sep Pak C18 columns (Waters) according to the manufacturer's instructions and lyophilized. Peptides were resuspended in 100 mM TEAB pH 8.0, quantified using a Pierce Quantitative Colorimetric Peptide Assay Kit (ThermoFisher Scientific), and equal amounts of peptide samples were

labeled with Tandem Mass Tag (TMT) 2-plex reagents (ThermoFisher Scientific) according to the manufacturer's instructions.

TMT 10-Plex Sample Preparation

For the TMT-10 experiment, samples were processed as described (Hebert et al. 2018). Briefly, previously flash-frozen cell pellets were resuspended in fresh 6 M guanidine HCl, 100 mM Tris-HCl, pH 8.0, and cells were lysed by incubation at 100°C for 5 minutes, 25°C for 5 minutes, and 100°C for 5 minutes. The rapid lysis via boiling in the presence of strong denaturants has been previously used to stabilize PTMs in the absence of specific inhibitors (Batth et al. 2018). Proteins were precipitated by adding 9 volumes of 100% methanol, vortexing, and centrifuging at 9,000 x g for 5 minutes. The supernatant was carefully decanted, the protein pellets were air-dried for 5 minutes and then resuspended in 8 M urea.

Protein samples (~5 mg total) were diluted to 2M urea with 100mM Tris pH 8.0 and digested with a 1:50 ratio of Trypsin overnight at 25°C with gently mixing in the presence of 2.5mM TCEP and 10mM chloroacetamide. Tryptic digestion was performed at 25°C to prevent carbamylation of free amines (Poulsen et al. 2013, Sun et al. 2014), with alkylation performed with chloroacetamide to prevent artifacts that can be falsely identified as diglycine (ubiquitination) (Nielsen et al. 2008). Digestion was quenched with 0.6% TFA to a pH less than 2, and peptides were desalted with Sep Pak C18 columns (Waters) according to the manufacturer's instructions and lyophilized. A detailed protocol for the peptide desalting step can be found on the protocols.io repository under DOI [dx.doi.org/10.17504/protocols.io.3hegj3e](https://doi.org/10.17504/protocols.io.3hegj3e). Peptides were resuspended in 200mM TEAB to a final concentration of ~8 µg, quantitated with Pierce Colorimetric Peptide Assay, and diluted to 5 µg/µl in TEAB. We labeled 500 µg of each sample in 100 µl total volume and used 50 µg for fractionation (with the "excess" TMT material being used for a separate immuno-enrichment study). Each sample was mixed with a separate TMT label reconstituted in 50µl acetonitrile. Samples were incubated at RT for 1 hour. Labeling

was quenched with 8 μ l 5% hydroxylamine for 15 minutes and samples were combined, desalted, and lyophilized. Labeling efficiency was monitored by performing Mascot searches with the TMT-10 modification mass as a variable modification instead of fixed. The labeling efficiencies (96.3%, 97.4%, and 97.5% for Reps 1, 2, 3, respectively). The detailed step-by-step TMT labeling workflow can be found on protocols.io under DOI dx.doi.org/10.17504/protocols.io.3g9gjz6.

LC-MS/MS Data Analysis

For both TMT-2 and TMT-10, 50 μ g of pooled peptides were fractionated (with the exception of TMT-10 replicate 2, where sample was lost in transit and a backup sample of 10 μ g was fractionated) using a 100 mm x 1.0 mm Acquity BEH C18 column (Waters) using an UltiMate 3000 UHPLC system (ThermoFisher Scientific) with a 40-min gradient from 99:1 to 60:40 buffer A:B ratio under basic (pH = 10) conditions (buffer A = 0.05% acetonitrile, 10 mM NH₄OH; buffer B = 100% acetonitrile, 10 mM NH₄OH). The 96 individual fractions were then consolidated into 24 super fractions using a concatenation scheme as described (Wang et al. 2011) (1+25+49+73, 2+26+50+74, etc.).

Super-fractions from the TMT 2-plex experiment were loaded on a Jupiter Proteo resin (Phenomenex) on an in-line 150 mm x 0.075 mm column using a nanoAcquity UPLC system (Waters). Peptides were eluted using a 45-min gradient from 97:3 to 65:35 buffer A:B ratio (buffer A = 0.1% formic acid; buffer B = acetonitrile, 0.1% formic acid) into an Orbitrap Fusion Tribrid mass spectrometer (ThermoFisher Scientific). MS acquisition consisted of a full MS scan at 240,000 resolution in profile mode of scan range 375-1500, maximum injection time of 400 ms, and AGC target of 5×10^5 , followed by CID MS/MS scans of the N most abundant ions of charge state +2-7 within a 3-second duty cycle. Precursor ions were isolated with a 2 Th isolation window in the quadrupole, fragmented with CID at 35%, and analyzed in the ion trap with a maximum injection time of 35 ms and a scan setting of Rapid. Dynamic exclusion was set

to 20 seconds with a 10 ppm tolerance. MS2 scans were followed by synchronous precursor selection and HCD (65%) fragmentation of the 10 most abundant fragment ions. MS3 scans were performed at 30,000 resolution with a maximum injection time of 200 ms and AGC target of 100,000.

For the TMT 10-plex experiment, super fractions were loaded on a 150 mm x 0.075 mm column packed with Waters C18 CSH resin. Peptides were eluted using a 45-min gradient from 96:4 to 75:25 buffer A:B ratio into an Orbitrap Fusion Lumos mass spectrometer (ThermoFisher Scientific). MS acquisition consisted of a full scan at 120,000 resolution, maximum injection time of 50 ms, and AGC target of 7.5×10^5 . Selection filters consisted of monoisotopic peak determination, charge state 2-7, intensity threshold of 2.0×10^4 , and mass range of 400-1200 m/z. Dynamic exclusion length was set to 15 seconds. Data-dependent cycle time was set for 2.5 seconds. Isolation widths were 0.7 Da for MS2 and 2 Da for the MS3 scans. Selected precursors were fragmented using CID 35% with an AGC target of 5.0×10^3 and a maximum injection time of 50 ms. MS2 scans were followed by synchronous precursor selection of the 10 most abundant fragment ions, which were fragmented with HCD 65% and scanned in the Orbitrap at 50,000 resolution, AGC target of 5.0×10^4 and maximum injection time of 86 ms.

Proteins were identified by database search using MaxQuant (Cox and Mann 2008) (Max Planck Institute) using the Uniprot *S. cerevisiae* database from October 2014, (The UniProt Consortium 2018) with a parent ion tolerance of 3 ppm and a fragment ion tolerance of 0.5 Da. Carbamidomethylation of cysteine residues was used as a fixed modification. Acetylation of protein N-termini and oxidation of methionine were selected as variable modifications. Mascot searches were performed using the same parameters as above, but with peptide N-terminal fixed modification of TMT 2-plex (+225.16) or TMT 10-plex (+229.16), and variable modifications of diglycine (+334.20 (114.04 + TMT-10)) and TMT 2- or 10-plex on lysine residues, and phosphorylation (+79.97) of serine and threonine. Mascot search results were imported into Scaffold software (v4) (Searle 2010) and filtered for protein and peptide false

discovery rates (FDR) of 1%. For the TMT-10 experiment, the 1% FDR was applied to the entire dataset (i.e. all 3 biological replicates together). Across the TMT-10 replicates 1-3, the success rates for peptide identification were 17.8%, 17.0%, and 23.3%, respectively. Data normalization and analyses were performed using R, and all R scripts for analysis are provided in File S1. Spectra containing missing values in any channel were excluded from the quantitative analysis. Spectra were further filtered to include only high-scoring peptide-spectrum matches (Mascot Ion Score cutoff of >15) for quantitation. For the TMT-10 experiments, the entire dataset for all replicates was normalized and analyzed together. Reporter ion intensities were log₂ transformed, mean-centered for each spectrum, then median-centered for each channel to control for mixing. Peptide abundance for each time point was calculated using the average abundance for all spectra mapping to the protein. The overlap between peptides quantified in each TMT-10 replicate experiment is shown in Figure S1. Unstressed (time 0) cells were used as a reference within each TMT-10 biological replicate experiment to calculate relative log₂ abundance changes during heat shock across each stress timepoint, which is a strategy that has been successfully used to identify changes in relative abundance across multiple TMT experiments (Lee et al. 2011). All raw mass spectrometry data and MaxQuant search results have been deposited to the ProteomeXchange Consortium via the PRIDE (Perez-Riverol et al. 2019) partner repository with the dataset identifier PXD014552 and 10.6019/PXD014552.

Proteins with significant abundance differences in response to heat at each time point relative to the unstressed control were identified by performing an empirical Bayes moderated t-test using the BioConductor package Limma v 3.36.2 and Benjamini-Hochberg FDR correction (Ritchie et al. 2015). Unless otherwise stated, we applied an FDR cutoff of 0.05 (see File S2 for the Limma output). Protein or peptide clustering was performed with Cluster 3.0 (<http://bonsai.hgc.jp/~mdehoon/software/cluster/software.htm>) using hierarchical clustering and Euclidian distance as the metric (Eisen et al. 1998). Timepoints were weighted using a cutoff value of 0.4 and an exponent value of 1. Functional enrichments of gene ontology (GO)

categories were performed using GO-TermFinder (<https://go.princeton.edu/cgi-bin/GOTermFinder>), (Boyle et al. 2004a) with Bonferroni-corrected P-values < 0.01 taken as significant. Complete lists of enriched categories can be found in File S3. Significantly enriched regulatory associations were identified using the YEAsT Search for Transcriptional Regulators And Consensus Tracking (YEASTRACT) database (Teixeira et al. 2018), using documented DNA binding plus expression evidence. Significant associations can be found in File S4.

Quantitative Western Blotting

Validation of LC-MS/MS was performed using the yeast TAP Tagged ORF collection (GE Dharmacon) in biological triplicate. Cells were collected and heat-shocked exactly as described for the TMT-2 sample preparation, with the duration of the 37°C heat shock being 1 hour. The OD600 for the heat-shocked and unstressed control samples were recorded for subsequent normalization. Fifteen ml of each sample was collected by centrifugation at 1500 x g for 3 minutes, the media was decanted, and the pellet was flash-frozen in liquid nitrogen and stored at -80°C until processing. Sample processing for western blotting was performed as described (von der Haar 2007) with the following modifications. Samples were thawed and resuspended in 1 ml of sterile water, and then an equal number of cells (~ 1 x 10⁷) was removed and collected by centrifugation at 10,000 x g for 1 minute. Cells were resuspended in 200 µl lysis buffer (0.1 M NaOH, 50 mM EDTA, 2% SDS, 2% β-mercaptoethanol plus EDTA-free Protease Inhibitor Tablets (Pierce catalog number 88265)). Samples were then incubated at 90°C for 10 minutes, 5 µl of 4 M acetic acid was added, and the sample was vortexed at maximum speed for 30 seconds. Samples were then incubated at 90°C for an additional 10 minutes to complete lysis. Fifty µl of loading buffer (0.25 M Tris-HCl pH 6.8, 50% glycerol, 0.05% bromophenol blue) was added to each sample, and samples were centrifuged at 21,130 x g for 5 minutes to pellet cellular debris. Twenty µl of each sample was loaded onto a 4 - 20% gradient acrylamide gel (Bio-Rad), separated by SDS-PAGE, and transferred for 1 hour onto an

Amersham Protran Premium 0.45 nitrocellulose membrane (GE Healthcare). Western blotting was performed using a mixture of mouse anti-actin antibodies (VWR catalog number 89500-294) and rabbit anti-TAP antibodies (ThermoFisher catalog number CAB1001) to simultaneously detect Act1p and the Tap-tagged protein of interest. Anti-TAP and anti-actin antibodies were used at a dilution of 1:1000 and 1:2500, respectively. IRDye® 680RD-conjugated anti-rabbit IgG (LI-COR Biosciences catalog number 926-68073) and IRDye® 800CW-conjugated anti-mouse IgG (LI-COR Biosciences catalog number 926-32212) were used as secondary antibodies at a dilution of 1:10,000. Detection was performed with a LI-COR Odyssey Imaging System using Image Studio v2.0. Densitometry was performed using ImageJ (Schneider, Rasband and Eliceiri 2012), and log₂ fold changes upon heat shock were calculated for each TAP-tagged protein following normalization to actin. Raw images and pixel densities can be found in Files S5 and S6.

Results and Discussion

Precision of MultiNotch MS3

We first sought to measure the precision of our TMT-MS3 workflow by characterizing the yeast response to elevated temperatures. One of the great advantages of TMT is the ability to multiplex, though there are mixed reports concerning whether increased multiplexing comes at the expense of protein identification and/or accuracy (Pichler et al. 2010, Pottiez et al. 2012). Thus, we first compared the accuracy and total protein identification of TMT-2 plex vs. TMT-10 plex. For our pilot TMT-2 experiment, we measured changes in protein abundance before and after 60 minutes of a 25°C to 37°C heat shock. We then performed a TMT-10 plex experiment designed to capture proteome dynamics of cells responding to heat shock over 9 timepoints using biological triplicates (Figure 1).

For both sets of experiments, cells were harvested and lysed, and then protein samples were prepared using a standard bottom-up proteomics workflow with in-solution trypsin

digestion, TMT 2-plex or 10-plex labeling, peptide fractionation, and analysis via MultiNotch MS3 on an Orbitrap Fusion (TMT-2) or Orbitrap Fusion Lumos (TMT-10).

One of the major challenges in quantitative proteomics is that peptides exist across a broad dynamic range of abundances, with high-abundance peptides dominating the signal of complex samples (Corthals et al. 2000). Reducing sample complexity through fractionation improves the ability to detect and quantify low abundance peptides (Chen et al. 2006). In an ideally-resolved sample, peptides are found within a single fraction. One widely used workflow for offline sample fractionation is the separation of proteins by SDS-PAGE prior to trypsin digestion. However, this workflow is incompatible with TMT labeling, as proteins must be digested and labeled prior to fractionation. An alternative fractionation procedure is to separate peptide species by high-performance liquid chromatography (HPLC), with fractionation via basic-pH reversed-phase HPLC showing the best peptide coverage for complex human proteomes (Wang et al. 2011, Mertins et al. 2013).

Thus, we fractionated our samples using basic-pH ultra-high performance liquid chromatography (UPLC) into 96 fractions, which were pooled into 24 super fractions. To measure the resolving power of basic-pH UPLC, we used the TMT 2-plex experiment to analyze the number of super fraction(s) in which each unique peptide was found (Figure 2A). By this analysis, 84% of peptides were found within a single super fraction, and 97% of peptides were found in two or fewer fractions. Additionally, peptides were evenly distributed across super fractions, with each super fraction yielding approximately 900 unique peptides (Figure 2B). Thus, basic-pH UPLC fractionation suitably reduces the number of redundant MS2 and MS3 scans and increases the depth of unique peptide and protein identifications, which is important because the MultiNotch MS3 method has a slightly slower duty cycle than MS2-based reporter ion quantitation.

We next tested the precision of the MultiNotch MS3 method. As a first measure of the precision of TMT proteomics, we used the TMT 2-plex experiment to analyze the coefficient of

variation (CV) of log₂ fold changes in response to heat stress for each unique peptide (7,129 total) identified by MaxQuant (Figure 3A). The CV values for 85% of quantified peptides were below 30% (6,070 / 7,129). The distribution of both standard deviations and CV% was lowest for peptides with two spectral counts, which represented the largest class of peptides (4,759 / 7,129), and this trend was also observed across all biological replicates for the TMT-10 experiment (Figure S2). We hypothesized that peptides with lower numbers of spectral counts were more likely to be lowly expressed in cells. Indeed, we found a strong correlation between estimated protein copy number per cell (from Ho et al. 2018a) and the number of peptide spectral counts (Figure S3). Thus, we have a somewhat counterintuitive result in that peptides with lower numbers of spectral counts tend to have lower CVs, whereas CV is often inversely proportional to sample size. This result had little to do with ion intensity, as we found poor correlation between CV and MS1 ($r = -0.06$) or MS3 ($r = -0.15$) ion intensities (Figure S4). Overall, the data suggests that our TMT proteomic workflow yields reliable measurements for low abundance proteins, which we sought to examine in more detail.

To further examine the precision of low-abundance peptides in the TMT 2-plex dataset, we filtered the data for peptides with 2 spectral counts and analyzed the precision of the two peptide measurements. The data followed a right-skewed distribution, with the majority (95%) of peptides showing good agreement between measurements ($r^2 = 0.87$, Figure 3B). Including the values from the remaining 5% of peptides markedly decreases the goodness-of-fit for all data points ($r^2 = 0.54$), indicating that a small frequency of outlier measurements pose a challenge in this workflow. Thus, our interpretation for the counterintuitive result that peptides with lower numbers of spectral counts have lower CVs is that the majority of reporter ion scans yield reproducible quantitative measurements, but a small portion of scans are distorted by co-isolation of contaminant peptides. Peptides with a larger number of spectral counts are more likely to encounter this problem, and thus have higher CVs on average. Ultimately, we conclude that the MultiNotch method yields high-quality data for the vast majority (95%) of peptide-level

measurements, while there remains a need to predict the quality of measurement in the absence of technical replicates, possibly through measuring the proportion of SPS ion intensity which did not map to the matched peptide. Finally, we should note that when we compare to the TMT-2 experiment, we identified a larger number of unique peptides (29467, 18118, 39993 for Replicates 1-3) and similar number of total proteins (3312, 3018, 3351 for Replicates 1-3) in the TMT-10 experiment, suggesting that both high accuracy and multiplexing are achievable without a large tradeoff in peptide identification. We also note that the inclusion of LysC in the protein digestion and longer on-line gradients (e.g. 3 hours) could improve peptide identification.

Using Increased Multiplexing to Characterize the Dynamic Heat Shock Proteome.

To determine whether our TMT workflow was able to recapitulate known biology while providing new insights, we examined the dynamic response to heat stress across 9 time points (from 5 – 240 minutes post heat shock) using TMT 10-plex reagents and three independent biological replicates. Out of 2,276 proteins with at least duplicate data using a stringent quality cutoff (see Methods), 1,148 proteins were differentially expressed (FDR < 0.05) in at least one time point. We used quantitative western blotting on 7 significantly induced proteins at the 60-minute time point, and all 7 proteins independently validated the proteomic data (Figure S5). We also compared our data to two yeast heat shock proteomic studies. First, we compared our dataset to a SILAC study from Nagaraj et al. that looked at a 30-minute heat shock (Nagaraj et al. 2012). Compared to the SILAC experiment, we identified fewer differentially expressed proteins at 30 minutes post heat shock (150 vs. 234, Figure S6). This is likely due to a larger number of proteins quantified by Nagaraj et al. (3,152 vs. 2,276) combined with more statistical power due to an additional biological replicate. Notably, the proportion of proteins identified as significantly differentially expressed was similar across both studies (7.4% in Nagaraj et al. vs. 6.6% in this study). We next compared our data to a recent label-free study from Jarnuczak et al. that measured the heat shock response over 5 time points (Jarnuczak et al. 2018),

specifically their time point with the highest number of differentially expressed proteins (240 minutes). While their study had more statistical power due to an additional biological replicate, we still identified more proteins as differentially expressed (Figure S6), and at a higher proportion (20.1% in Jarnuczak et al. vs. 27.0% in this study). Some of these differences in the ability to identify differentially expressed proteins are likely due to differences in experimental design (e.g. choice of heat shock temperature). However, some of the differences are likely due to the increased precision and lower variance of TMT-MS3, as smaller fold changes were more likely to be called significant in our dataset.

Examining the most up- and down-regulated processes (>1.5-fold) during heat shock revealed processes likely important for acclimation to elevated temperatures. Proteins with significantly higher expression (>1.5-fold) following heat shock were enriched for functions known to be important for tolerating elevated temperatures. These included processes related to protein refolding ($p = 3 \times 10^{-14}$), oxidative stress response ($p = 3 \times 10^{-5}$), and metabolism of the known stress protectant molecule trehalose ($p = 3 \times 10^{-3}$). Other metabolic processes were also induced, including those related to redox chemistry ($p = 3 \times 10^{-21}$), amino acid metabolism ($p = 2 \times 10^{-6}$), and nucleotide metabolism ($p = 5 \times 10^{-6}$). In contrast, proteins repressed during heat shock were enriched for functions related to ribosomal biogenesis ($p = 1 \times 10^{-22}$), RNA processing ($p = 8 \times 10^{-14}$), and gene expression ($p = 2 \times 10^{-7}$).

We next sought to take advantage of our time series data to analyze the dynamics of the heat shock response in more detail. The maximal response occurred between 60 and 90 minutes post heat shock based on both the number of differentially expressed genes and the magnitude of the changes (Figures 4 and 5C). We identified 10 proteins with significantly higher abundance within 10 minutes post heat shock that likely reflect increased stabilization of key proteins. Of these 10 proteins with extremely early “induction,” four are heat shock protein chaperones (Hsp26p, Hsp42p, Hsp78p, Hsp104p), two are ribosomal proteins (Rps29bp, Rpl35ap), two are metabolic enzymes (Ura1p, Gre3p), and two are involved in protein targeting

(Btn2p, Vac8). Intriguingly, the protein sorting protein Btn2p—the only protein with significantly increased abundance at the 5 min time point—works with the chaperone Hsp42p to regulate compartmentalization of protein aggregates for later repair or removal (Miller, Mogk and Bukau 2015), Btn2p is known to be rapidly degraded by the proteasome during unstressed conditions (Malinovska et al. 2012), suggesting that changes in protein stability may play an important role in the early stages of the heat shock response.

To better identify temporal patterns in our data, we hierarchically clustered the 1,148 proteins with differential expression (Figure 4B). Induced proteins could be roughly categorized into three clusters: rapid and strong responders (41 proteins with a peak response of 60 minutes, average \log_2 fold change of 2.33), moderately induced responders (81 proteins with a peak response of 90 minutes, average \log_2 fold change of 1.18), and a broad cluster of mildly induced responders (469 proteins with a 90-min peak response, average \log_2 fold change of 0.50). The 41 rapid responders included several proteins known to be involved in the first line of heat stress defense including several key chaperones (Hsp26p, Hsp42p, Hsp78p, Hsp104p), glycogen and trehalose metabolic enzymes (Glc3p, Gsy2p, Tsl1p, Gph1p), and aromatic amino acid catabolic enzymes (Aro9p, Aro10p). Additionally, there were several induced aldehyde dehydrogenases (Ald2p, Ald3p, Ald4p) and proteins involved in carbohydrate metabolism (Glk1p, Hxk2p, Gre3p, Sol3p, Yjr096wp, Pgm2p). The second wave of moderate responders also included additional chaperones or co-chaperones (Aha1p, Cpr1p, Cpr3p, Cpr6p, Hsp60p, Hsp82p, Sis1p, Ssa3p, Ssa4p, Sti1p) and trehalose metabolic enzymes (Nth1p and Tps2p). The broad mildly-induced responders included heat shock chaperones (Hsc82p, Ssa1p, Ecm10p, Ssc1p, Ssa2p, Kar2p, Sse2p, Mdj1p), but was also enriched for diverse metabolic functions including nitrogen metabolism ($p = 3 \times 10^{-14}$), nucleotide metabolism ($p = 5 \times 10^{-14}$), phosphorus metabolism ($p = 1 \times 10^{-9}$), and glucose metabolism ($p = 4 \times 10^{-5}$).

We hypothesized that the rapid responders may largely represent proteins that directly respond to heat shock, while the mildly induced responders may reflect indirect responses. To

test this, we used the YEASTRACT database to identify transcription factors that may be regulating gene expression for each cluster. The two major transcription factors that regulate the heat shock response in yeast include the heat shock transcription factor Hsf1p (Sorger and Pelham 1987), and the paralogous general stress-responsive transcription factors Msn2p and Msn4p (Martinez-Pastor et al. 1996). Genes encoding rapid responders were more likely to be regulated by Hsf1p (83%) than either the moderately (59%) or mildly induced (36%) genes (File S4). Similarly, the rapid response genes were also more likely to be regulated by Msn2p/4p (95%) than the moderately (84%) and mildly (60%) induced genes. Additionally, we identified several transcription factors that regulate the mildly-induced genes that are themselves either Msn2/4p targets (Rdr1p, Xbp1p, Oaf1p) or both Msn2/4 and Hsf1 targets (Rap1p, Tup1p, Pho4p, Ino2p, Tye7p, Reb1p, Mth1p, Prs1p). These transcription factors regulate diverse processes that are likely indirectly impacted by heat shock, including cell cycle progression and lipid, glucose, and phosphate metabolism.

Lastly, we examined the relationship between mRNA induction during heat shock and the proteomic response. Jarnuczak et al. also measured the correlation of mRNA and protein level changes, and found a modest correlation ($r = 0.49$ for the pairwise comparison with the highest correlation). We performed a similar analysis using a heat shock microarray time course (5, 15, 30, 45, 60, and 120 minutes) from Eng et al. (2010) and we found a stronger correlation between changes in the heat shock transcriptome and proteome ($r = 0.71$). We explored the relationship between mRNA and protein further, which revealed some fundamental differences between how mRNAs and proteins are regulated during heat shock. First, in contrast with mRNA expression—where more mRNAs are repressed than induced during heat shock—we found that more proteins had increasing rather than decreasing abundance changes. This likely reflects the fact that proteins are more stable than mRNAs and that targeted protein degradation may be necessary to rapidly decrease protein levels (Belle et al. 2006, Liu, Beyer and Aebersold 2016). Similar to Lee and colleagues³, we found that changes in mRNA abundance

for induced transcripts correlated rather well with protein induction, while protein abundances changes were showed poor correlation with repressed mRNAs. This is consistent with proposed models suggesting the function of transcript repression is not to reduce protein abundance for those transcripts, but instead frees ribosomes and increases translation of the induced transcripts (Lee et al. 2011, Ho et al. 2018b). Intriguingly, despite the apparent lack of correlation for repressed mRNAs and their corresponding proteins, we did find that the functional enrichments for repressed mRNAs and repressed proteins were similar (i.e. ribosome biogenesis and translation). The poor correlation of repressed mRNAs and proteins occurs largely because repressed mRNAs show a wide range of repression values, while repressed proteins largely cluster around 1.5-fold repression (Figure S7). This “buffering” of repressed protein-level changes could be due to the increased stability of proteins vs. mRNAs (Belle et al. 2006). The repressed proteins are strongly enriched for the pre-ribosome complex ($p = 3 \times 10^{-37}$), thus the buffering of repressed proteins towards similar relative levels may help maintain proper subunit stoichiometry during stress.

Analysis of protein post-translational modifications

The proteomics community uses several different peptide search engines for peptide spectrum matching, with each search engine having various strengths and weaknesses. Software with high-performance PTM identification may not be compatible with TMT-MS3 quantitation, and software with TMT-MS3 quantitation may fail to identify modified peptides in a sample. For example, we have previously used Mascot Distiller to search for post-translational modifications (Byrum et al. 2012), which does not currently offer MS3 quantitation. Likewise, MaxQuant is also unable to naively handle SPS-MS3 data when searching for variable modifications on lysine residues. To circumvent this, phosphorylation and ubiquitination PTMs were searched using the Mascot database, and this information was used to manually extract MS3 intensities from raw files using the R package mzR (Chambers et al. 2012). We manually

validated to ensure quality spectral matches, which yielded 22 ubiquitinated lysines and 67 phosphorylated serines or threonines—each with high-confidence spectra across the entire time course. Using scan number and m/z values of MS2 from the Mascot results, we extracted intensity values from the matched MS3 scans. The Mascot and MaxQuant datasets were joined, and we normalized changes in peptide-level PTMs to underlying changes in total protein abundance.

We saw striking evidence of PTM changes following heat shock. Consistent with the findings of Kanshin et al. (2015), we saw evidence for dynamic changes in protein phosphorylation levels (Figure 6A). Proteins with at least 1.5-fold increased phosphorylation were enriched for endocytosis ($p < 3 \times 10^{-3}$), cellular important ($p < 8 \times 10^{-3}$), and notably, response to stress ($p < 8 \times 10^{-3}$). These latter proteins included an enzyme (Tps2p) and regulatory submit (Tps3p) of trehalose biosynthetic complex, both of which are known to be regulated by phosphorylation during stress (Trevisol et al. 2014). We also observed several proteins with increased or decreased lysine ubiquitination (Figure 6B). While we cannot distinguish between mono and polyubiquitination with tryptic digestion, both can target proteins for proteasomal degradation (Braten et al. 2016, Rutkowski et al. 2006), with polyubiquitination being the canonical signal (Pickart and Fushman 2004). Intriguingly—and consistent with ubiquitination playing a role as a regulator of protein degradation during heat stress—we observed an inverse relationship ($r^2 = 0.42$) between total protein abundance at 90 minutes post-heat shock and fold-change in lysine ubiquitination at 15 minutes post-heat shock (Figure 6D). Notably, there was no correlation between protein abundance changes and protein phosphorylation changes ($R^2 = 0.03$; Figure 6C), suggesting that the ubiquitination trend is likely biologically meaningful. Overall, our TMT-MS3 workflow is precise enough to delineate protein-level and PTM-level changes in biological samples.

Conclusions

In this study, we present a TMT-MS3 proteomics workflow that yields precise and accurate measurements of peptide and protein abundance, using the well-studied yeast heat shock response as a test case. At the protein abundance level, our Multinotch MS3 analysis method for TMT proteomics was robust to detect differential expression, even in the case of a single replicate. Proteins with significant induction or repression largely recapitulated expectations, with HSP chaperones amongst the most strongly induced proteins, and proteins related to cell growth and protein synthesis among the most strongly repressed. Our method also performed particularly well in the quantification of low abundance peptides. Compared to SILAC and label-free methods, the TMT Multinotch MS3 workflow affords a significant increase in multiplexing capacity and technical precision for peptide-level quantitative measurements, which is necessary for designing high-power experiments to study temporal dynamics of changing PTMs in a variety of biological contexts. In fact, our analysis of PTMs suggests an additional layer of regulation that has been largely understudied in the context of the yeast heat shock response. While PTMs are known to play key regulatory roles during the adaptation to stress, to date there has been only a single study examining PTM changes during the yeast heat shock response (in this case phosphorylation) (Kanshin et al. 2015). In this study, we identified both phospho- and ubiquitin-modified peptides whose abundance changed during heat shock even following normalization to abundance changes of unmodified peptides for the same protein. We hypothesize that several of the other dynamic PTMs may be important and understudied components of heat shock adaptation. That these were identified without specific enrichment steps suggests that MultiNotch MS3 datasets can be mined for PTMs that change in abundance during environmental perturbation.

Acknowledgments

We thank Nilda Burgos and Reiofeli Salas for the use and assistance with the bead mill, and Shannon Servoss and Neda Mahmoudi for the use and assistance with the lyophilizer, and Alex Heber for helpful conversations on TMT proteomic sample processing. This work was supported by a grant from the National Science Foundation (IOS-1656602) to JAL, by a grant from the National Institutes of Health (GM081766) to WPW, and by the Arkansas Biosciences Institute (Arkansas Settlement Proceeds Act of 2000). REH was partially supported by the University of Arkansas Cell and Molecular Biology Graduate Program. AJT acknowledges support from the National Institutes of Health (R01GM118760, P20GM121293, UL1TR000039, P20GM103625, S10OD018445, and P20GM103429).

Figures

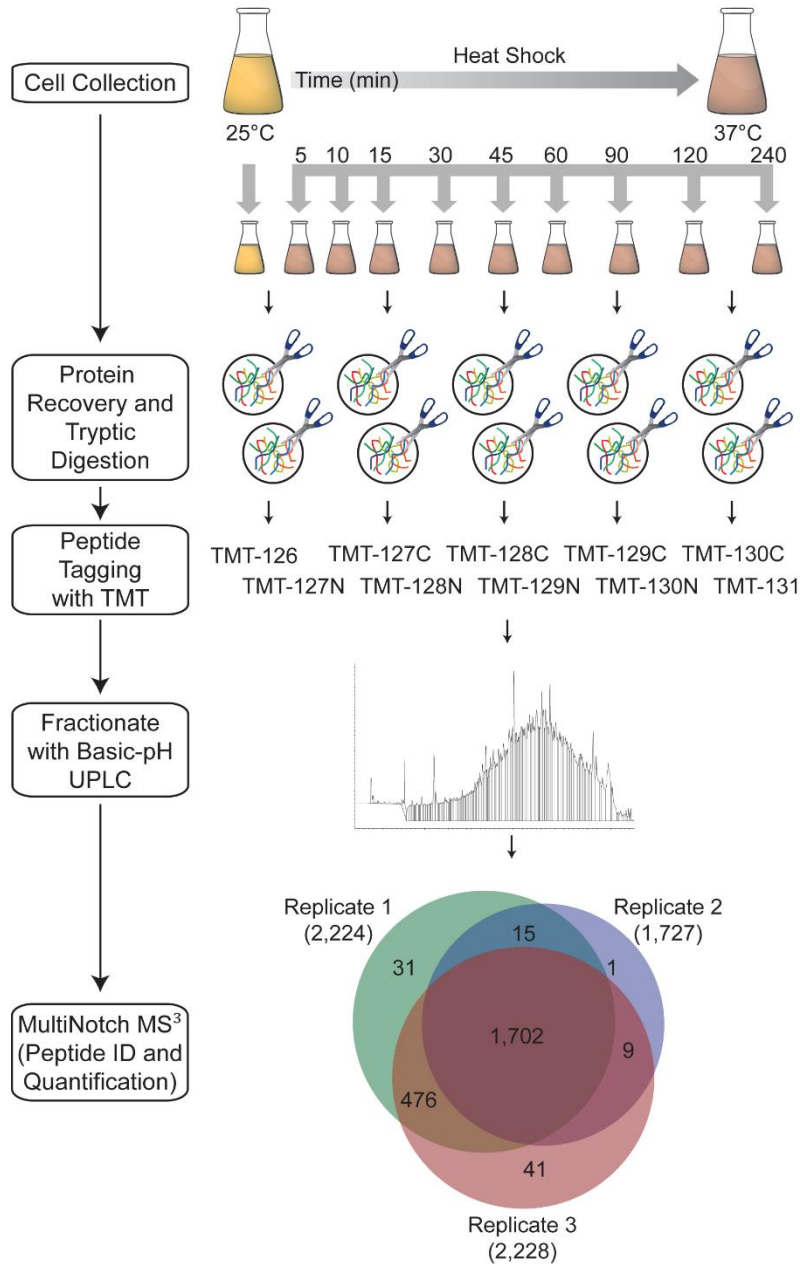


Figure 1. Schematic of Proteomic Workflow. Yeast cells were grown to mid-exponential phase at 25°C, an unstressed control sample was collected, and then cells were subjected to a 37°C heat shock, with samples collected at the indicated time points. Protein samples were digested with trypsin, labeled with one of the 10-plex tandem mass tags (TMT-10), pooled and fractionated by high-pH UPLC, and analyzed by MultiNotch LC-MS³. The Venn diagram depicts the overlap for proteins identified in each biological replicate.

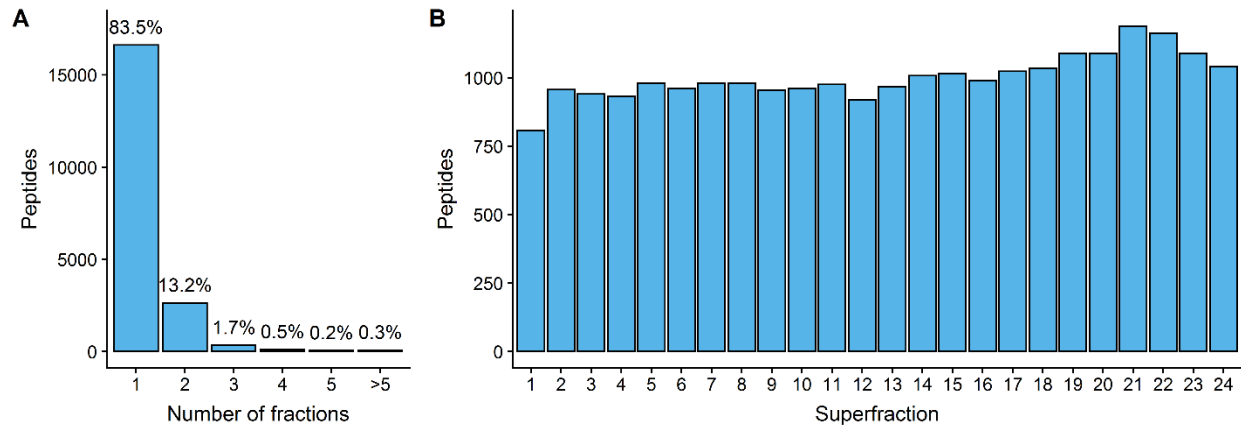


Figure 2. High pH UPLC fractionation efficiently separates TMT-labeled peptides. Protein samples were digested with trypsin, TMT 2-plex labeled, and then fractionated by UPLC under basic conditions, and the fractions were concatenated into 24 super fractions. Each super fraction was then analyzed by LC-MS3. A) Resolution of high pH fractionation. The X-axis shows the number of super fractions in which a given peptide was detected (bins); the histogram (Y-axis) shows the number and frequency of peptides in each bin. Note that the vast majority of peptides partition within only one or two of the 24 super fractions, greatly reducing sample complexity and increasing depth of coverage by LC-MS3. B) Sampling depth for each fractionation. The bar graph shows the number of peptides identified (Y-axis) in each super fraction (X-axis).

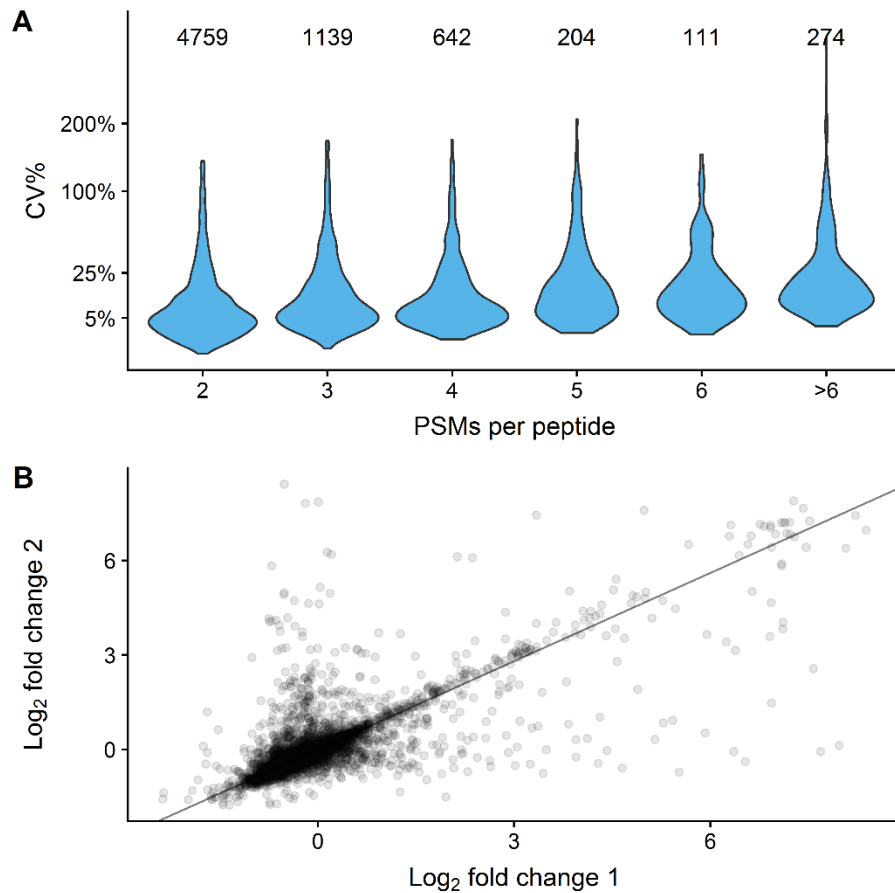


Figure 3. TMT-MS3 measurements of peptides are highly precise, even for low-abundance species. An underlying principle of quantitative proteomics is that high-abundance proteins yield more peptide spectral counts or measurements (PSMs) than low-abundance proteins. The differential abundance of peptides (fold change) following 60 minutes heat shock was used to determine the precision of PSM measurements for TMT-2. A) Precision of measurements as a function of PSM number. Violin plots showing the coefficient of variation (CV) of fold change measurements for peptides with different numbers of PSMs. The number above each plot shows the number of data points in each plot. B) Precision of measurements for low-abundance peptides. Scatter plot shows log₂ fold changes for 4,759 peptides with two spectral counts.

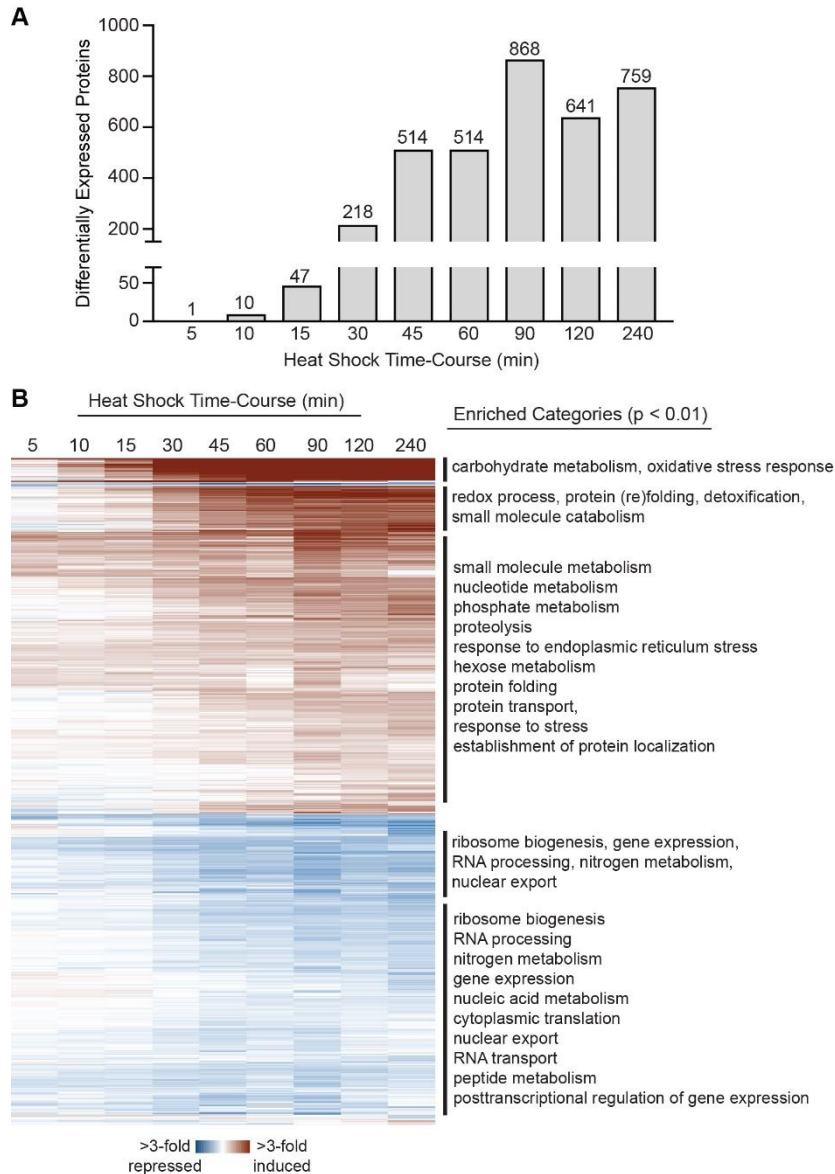


Figure 4. The temporal dynamics of the heat shock proteome. A) The number of differentially expressed proteins (FDR < 0.05) for each time point. B) The heat map depicts the hierarchical clustering of 1,148 proteins whose change in abundance was statistically significant (FDR < 0.05) at any time point. Each row represents a unique protein, and each column represents the average expression change of heat-stressed vs. unstressed cells at each time point. Red indicates induced and blue indicates repressed expression in response to heat. Enriched functional groups (Bonferroni-corrected $P < 0.01$, see Methods) are annotated to the right. Complete Gene Ontology (GO) enrichments for each cluster can be found in File S3.

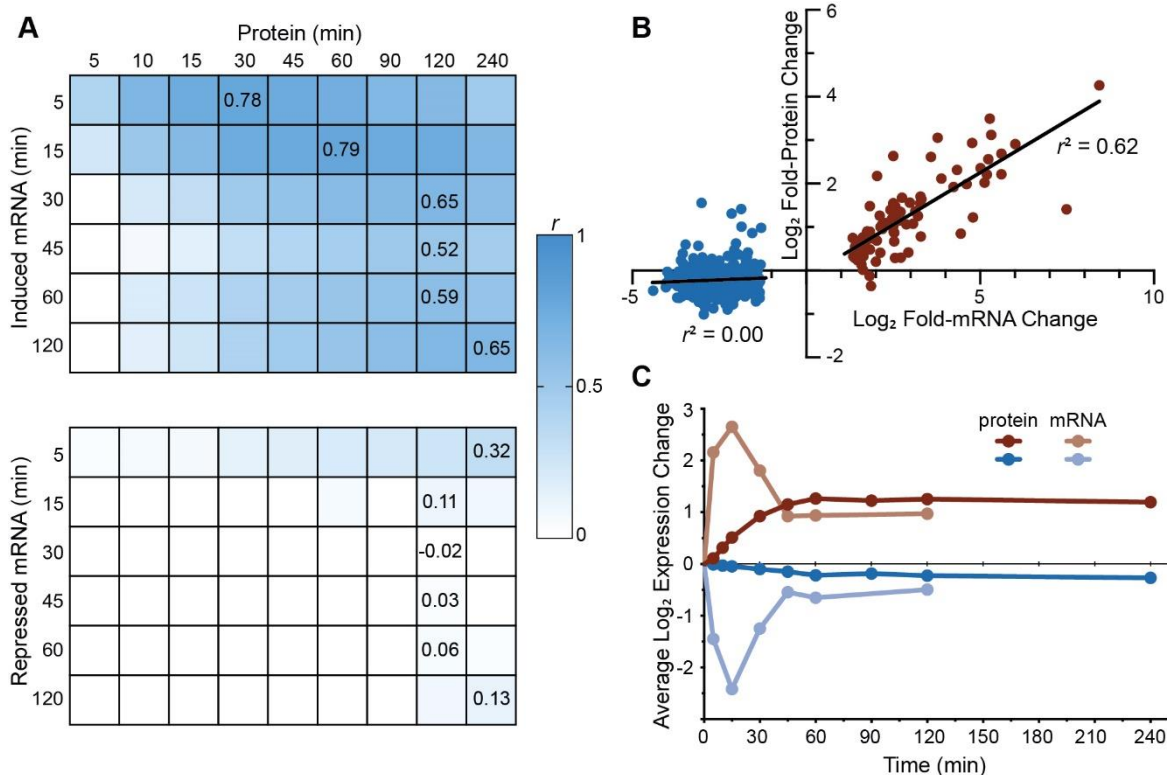


Figure 5. Heat shock responsive mRNAs correlate with protein induction but not repression. A) The tables compare changes in protein abundance at each time point following heat shock to mRNAs that significantly increased (top) or decreased (bottom) in expression reported by Eng et al. (Eng et al. 2010) (at FDR < 0.05). Shading indicates Pearson correlation coefficients (r) between the two datasets, with values of maximal concordance reported. B) Plot of the correlation between induced (red) and repressed (blue) mRNAs at 15 minutes vs. their corresponding proteins at 60 minutes. C) The temporal dynamics for all significantly induced or repressed mRNAs and their corresponding proteins.

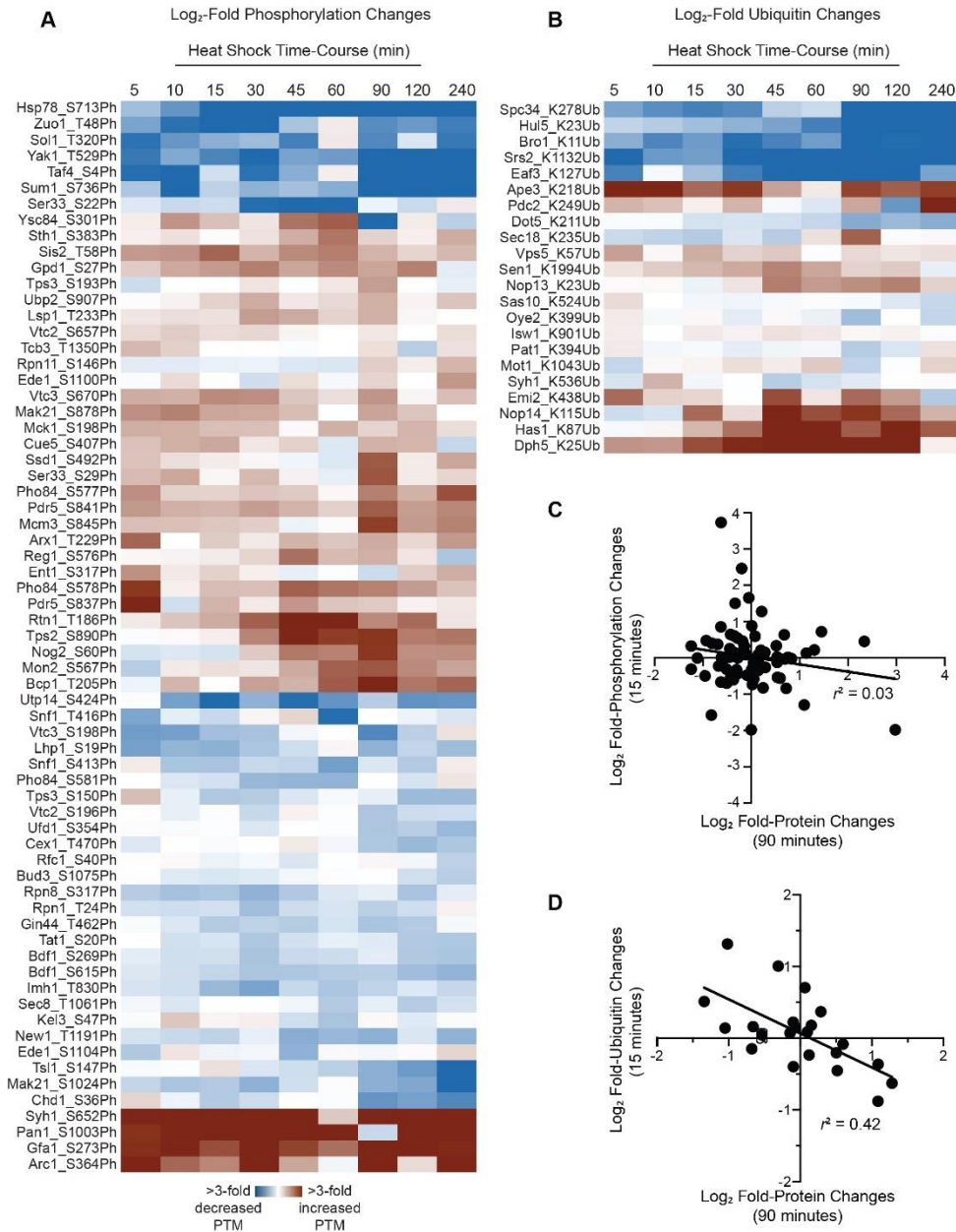


Figure 6. TMT-MS3 reveals dynamic changes in the abundance of protein PTMs during heat shock. Modified peptides were identified by searches of MS data using Mascot Distiller and were manually validated as described in the Methods. PTM abundance was normalized to overall abundance changes of the corresponding protein. The heat maps depict heat shock-dependent increases (red) or decreases (blue) in A) phosphorylation or B) ubiquitination. Plot of the correlation between fold-changes in total protein levels and fold changes in A) phosphorylation or B) ubiquitination.

References

- Batth, T. S., M. Papetti, A. Pfeiffer, M. A. X. Tollenaere, C. Francavilla & J. V. Olsen (2018) Large-Scale Phosphoproteomics Reveals Shp-2 Phosphatase-Dependent Regulators of Pdgf Receptor Signaling. *Cell Rep*, 22, 2784-2796.
- Belle, A., A. Tanay, L. Bitincka, R. Shamir & E. K. O'Shea (2006) Quantification of protein half-lives in the budding yeast proteome. *Proc Natl Acad Sci U S A*, 103, 13004-13009.
- Bentley, D. R., S. Balasubramanian, H. P. Swerdlow, G. P. Smith, J. Milton, C. G. Brown, K. P. Hall, D. J. Evers, C. L. Barnes, H. R. Bignell, J. M. Boutell, J. Bryant, R. J. Carter, R. Keira Cheetham, A. J. Cox, D. J. Ellis, M. R. Flatbush, N. A. Gormley, S. J. Humphray, L. J. Irving, M. S. Karbelashvili, S. M. Kirk, H. Li, X. Liu, K. S. Maisinger, L. J. Murray, B. Obradovic, T. Ost, M. L. Parkinson, M. R. Pratt, I. M. Rasolonjatovo, M. T. Reed, R. Rigatti, C. Rodighiero, M. T. Ross, A. Sabot, S. V. Sankar, A. Scally, G. P. Schroth, M. E. Smith, V. P. Smith, A. Spiridou, P. E. Torrance, S. S. Tzonev, E. H. Vermaas, K. Walter, X. Wu, L. Zhang, M. D. Alam, C. Anastasi, I. C. Aniebo, D. M. Bailey, I. R. Bancarz, S. Banerjee, S. G. Barbour, P. A. Baybayan, V. A. Benoit, K. F. Benson, C. Bevis, P. J. Black, A. Boodhun, J. S. Brennan, J. A. Bridgham, R. C. Brown, A. A. Brown, D. H. Buermann, A. A. Bundu, J. C. Burrows, N. P. Carter, N. Castillo, E. C. M. Chiara, S. Chang, R. Neil Cooley, N. R. Crake, O. O. Dada, K. D. Diakoumakos, B. Dominguez-Fernandez, D. J. Earnshaw, U. C. Egbujor, D. W. Elmore, S. S. Etchin, M. R. Ewan, M. Fedurco, L. J. Fraser, K. V. Fuentes Fajardo, W. Scott Furey, D. George, K. J. Gietzen, C. P. Goddard, G. S. Golda, P. A. Granieri, D. E. Green, D. L. Gustafson, N. F. Hansen, K. Harnish, C. D. Haudenschild, N. I. Heyer, M. M. Hims, J. T. Ho, A. M. Horgan, et al. (2008) Accurate whole human genome sequencing using reversible terminator chemistry. *Nature*, 456, 53-59.
- Boyle, E. I., S. Weng, J. Gollub, H. Jin, D. Botstein, J. M. Cherry & G. Sherlock (2004) GO:TermFinder--open source software for accessing Gene Ontology information and finding significantly enriched Gene Ontology terms associated with a list of genes. *Bioinformatics*, 20, 3710-3715.
- Brar, G. A., M. Yassour, N. Friedman, A. Regev, N. T. Ingolia & J. S. Weissman (2012) High-resolution view of the yeast meiotic program revealed by ribosome profiling. *Science*, 335, 552-557.
- Braten, O., I. Livneh, T. Ziv, A. Admon, I. Kehat, L. H. Caspi, H. Gonen, B. Bercovich, A. Godzik, S. Jahandideh, L. Jaroszewski, T. Sommer, Y. T. Kwon, M. Guharoy, P. Tompa & A. Ciechanover (2016) Numerous proteins with unique characteristics are degraded by the 26S proteasome following monoubiquitination. *Proc Natl Acad Sci U S A*, 113, 4639-4647.
- Brewster, J. L., T. de Valoir, N. D. Dwyer, E. Winter & M. C. Gustin (1993) An osmosensing signal transduction pathway in yeast. *Science*, 259, 1760-1763.
- Byrum, S. D., A. Raman, S. D. Taverna & A. J. Tackett (2012) ChAP-MS: a method for identification of proteins and histone posttranslational modifications at a single genomic locus. *Cell Rep*, 2, 198-205.

- Causton, H. C., B. Ren, S. S. Koh, C. T. Harbison, E. Kanin, E. G. Jennings, T. I. Lee, H. L. True, E. S. Lander & R. A. Young (2001) Remodeling of yeast genome expression in response to environmental changes. *Mol Biol Cell*, 12, 323-337.
- Chambers, M. C., B. Maclean, R. Burke, D. Amodei, D. L. Ruderman, S. Neumann, L. Gatto, B. Fischer, B. Pratt, J. Egertson, K. Hoff, D. Kessner, N. Tasman, N. Shulman, B. Frewen, T. A. Baker, M. Y. Brusniak, C. Paulse, D. Creasy, L. Flashner, K. Kani, C. Moulding, S. L. Seymour, L. M. Nuwaysir, B. Lefebvre, F. Kuhlmann, J. Roark, P. Rainer, S. Detlev, T. Hemenway, A. Huhmer, J. Langridge, B. Connolly, T. Chadick, K. Holly, J. Eckels, E. W. Deutsch, R. L. Moritz, J. E. Katz, D. B. Agus, M. MacCoss, D. L. Tabb & P. Mallick (2012) A cross-platform toolkit for mass spectrometry and proteomics. *Nat Biotechnol*, 30, 918-920.
- Chen, E. I., J. Hewel, B. Felding-Habermann & J. R. Yates, 3rd (2006) Large scale protein profiling by combination of protein fractionation and multidimensional protein identification technology (MudPIT). *Mol Cell Proteomics*, 5, 53-56.
- Coote, P. J., M. B. Cole & M. V. Jones (1991) Induction of increased thermotolerance in *Saccharomyces cerevisiae* may be triggered by a mechanism involving intracellular pH. *J Gen Microbiol*, 137, 1701-8.
- Corthals, G. L., V. C. Wasinger, D. F. Hochstrasser & J. C. Sanchez (2000) The dynamic range of protein expression: a challenge for proteomic research. *Electrophoresis*, 21, 1104-1115.
- Cox, J. & M. Mann (2008) MaxQuant enables high peptide identification rates, individualized p.p.b.-range mass accuracies and proteome-wide protein quantification. *Nat Biotechnol*, 26, 1367-1372.
- Csardi, G., A. Franks, D. S. Choi, E. M. Airoidi & D. A. Drummond (2015) Accounting for experimental noise reveals that mRNA levels, amplified by post-transcriptional processes, largely determine steady-state protein levels in yeast. *PLoS Genet*, 11, e1005206.
- Davidson, J. F. & R. H. Schiestl (2001) Mitochondrial respiratory electron carriers are involved in oxidative stress during heat stress in *Saccharomyces cerevisiae*. *Mol Cell Biol*, 21, 8483-9.
- Eisen, M. B., P. T. Spellman, P. O. Brown & D. Botstein (1998) Cluster analysis and display of genome-wide expression patterns. *Proc Natl Acad Sci U S A*, 95, 14863-14868.
- Eng, K. H., D. J. Kvitek, S. Keles & A. P. Gasch (2010) Transient genotype-by-environment interactions following environmental shock provide a source of expression variation for essential genes. *Genetics*, 184, 587-593.
- Gasch, A. P., P. T. Spellman, C. M. Kao, O. Carmel-Harel, M. B. Eisen, G. Storz, D. Botstein & P. O. Brown (2000) Genomic expression programs in the response of yeast cells to environmental changes. *Mol Biol Cell*, 11, 4241-4257.
- Glover, J. R. & S. Lindquist (1998) Hsp104, Hsp70, and Hsp40: a novel chaperone system that rescues previously aggregated proteins. *Cell*, 94, 73-82.

- Golebiowski, F., I. Matic, M. H. Tatham, C. Cole, Y. Yin, A. Nakamura, J. Cox, G. J. Barton, M. Mann & R. T. Hay (2009) System-wide changes to SUMO modifications in response to heat shock. *Sci Signal*, 2, ra24.
- Griffin, T. J., S. P. Gygi, T. Ideker, B. Rist, J. Eng, L. Hood & R. Aebersold (2002) Complementary profiling of gene expression at the transcriptome and proteome levels in *Saccharomyces cerevisiae*. *Mol Cell Proteomics*, 1, 323-333.
- Gygi, S. P., Y. Rochon, B. R. Franza & R. Aebersold (1999) Correlation between protein and mRNA abundance in yeast. *Mol Cell Biol*, 19, 1720-1730.
- Halbeisen, R. E. & A. P. Gerber (2009) Stress-dependent coordination of transcriptome and translome in yeast. *PLoS Biol*, 7, e1000105.
- Han, S. J., K. Y. Choi, P. T. Brey & W. J. Lee (1998) Molecular cloning and characterization of a *Drosophila* p38 mitogen-activated protein kinase. *J Biol Chem*, 273, 369-374.
- Hebert, A. S., S. Prasad, M. W. Belford, D. J. Bailey, G. C. McAlister, S. E. Abbatiello, R. Huguet, E. R. Wouters, J. J. Dunyach, D. R. Brademan, M. S. Westphall & J. J. Coon (2018) Comprehensive Single-Shot Proteomics with FAIMS on a Hybrid Orbitrap Mass Spectrometer. *Anal Chem*, 90, 9529-9537.
- Ho, B., A. Baryshnikova & G. W. Brown (2018a) Unification of Protein Abundance Datasets Yields a Quantitative *Saccharomyces cerevisiae* Proteome. *Cell Syst*, 6, 192-205 e3.
- Ho, Y. H., E. Shishkova, J. Hose, J. J. Coon & A. P. Gasch (2018b) Decoupling Yeast Cell Division and Stress Defense Implicates mRNA Repression in Translational Reallocation during Stress. *Curr Biol*, 28, 2673-2680 e4.
- Jakob, U., M. Gaestel, K. Engel & J. Buchner (1993) Small heat shock proteins are molecular chaperones. *J Biol Chem*, 268, 1517-20.
- Jarnuczak, A. F., M. G. Albornoz, C. E. Eyers, C. M. Grant & S. J. Hubbard (2018) A quantitative and temporal map of proteostasis during heat shock in *Saccharomyces cerevisiae*. *Mol Omics*, 14, 37-52.
- Kanshin, E., P. Kubiniok, Y. Thattikota, D. D'Amours & P. Thibault (2015) Phosphoproteome dynamics of *Saccharomyces cerevisiae* under heat shock and cold stress. *Mol Syst Biol*, 11, 813.
- Lackner, D. H., M. W. Schmidt, S. Wu, D. A. Wolf & J. Bahler (2012) Regulation of transcriptome, translation, and proteome in response to environmental stress in fission yeast. *Genome Biol*, 13, R25.
- Lee, M. V., S. E. Topper, S. L. Hubler, J. Hose, C. D. Wenger, J. J. Coon & A. P. Gasch (2011) A dynamic model of proteome changes reveals new roles for transcript alteration in yeast. *Mol Syst Biol*, 7, 514.
- Lindquist, S. & E. A. Craig (1988) The heat-shock proteins. *Annu Rev Genet*, 22, 631-677.

- Liu, Y., A. Beyer & R. Aebersold (2016) On the Dependency of Cellular Protein Levels on mRNA Abundance. *Cell*, 165, 535-550.
- Magraner-Pardo, L., V. Pelechano, M. D. Coloma & V. Tordera (2014) Dynamic remodeling of histone modifications in response to osmotic stress in *Saccharomyces cerevisiae*. *BMC Genomics*, 15, 247.
- Malinowska, L., S. Kroschwald, M. C. Munder, D. Richter & S. Alberti (2012) Molecular chaperones and stress-inducible protein-sorting factors coordinate the spatiotemporal distribution of protein aggregates. *Mol Biol Cell*, 23, 3041-3056.
- Martin-Perez, M. & J. Villen (2017) Determinants and Regulation of Protein Turnover in Yeast. *Cell Syst*, 5, 283-294 e5.
- Martinez-Pastor, M. T., G. Marchler, C. Schuller, A. Marchler-Bauer, H. Ruis & F. Estruch (1996) The *Saccharomyces cerevisiae* zinc finger proteins Msn2p and Msn4p are required for transcriptional induction through the stress response element (STRE). *EMBO J*, 15, 2227-2235.
- McAlister, G. C., D. P. Nusinow, M. P. Jedrychowski, M. Wuhr, E. L. Huttlin, B. K. Erickson, R. Rad, W. Haas & S. P. Gygi (2014) MultiNotch MS3 enables accurate, sensitive, and multiplexed detection of differential expression across cancer cell line proteomes. *Anal Chem*, 86, 7150-7158.
- Medicherla, B. & A. L. Goldberg (2008) Heat shock and oxygen radicals stimulate ubiquitin-dependent degradation mainly of newly synthesized proteins. *J Cell Biol*, 182, 663-673.
- Mertins, P., J. W. Qiao, J. Patel, N. D. Udeshi, K. R. Clauser, D. R. Mani, M. W. Burgess, M. A. Gillette, J. D. Jaffe & S. A. Carr (2013) Integrated proteomic analysis of post-translational modifications by serial enrichment. *Nat Methods*, 10, 634-637.
- Miller, M. J., M. Scalf, T. C. Rytz, S. L. Hubler, L. M. Smith & R. D. Vierstra (2013) Quantitative proteomics reveals factors regulating RNA biology as dynamic targets of stress-induced SUMOylation in *Arabidopsis*. *Mol Cell Proteomics*, 12, 449-463.
- Miller, S. B., A. Mogk & B. Bukau (2015) Spatially organized aggregation of misfolded proteins as cellular stress defense strategy. *J Mol Biol*, 427, 1564-1574.
- Mishra, P. & R. Prasad (1987) Alterations in fatty acyl composition can selectively affect amino acid transport in *Saccharomyces cerevisiae*. *Biochem Int*, 15, 499-508.
- Nagaraj, N., N. A. Kulak, J. Cox, N. Neuhauser, K. Mayr, O. Hoerning, O. Vorm & M. Mann (2012) System-wide perturbation analysis with nearly complete coverage of the yeast proteome by single-shot ultra HPLC runs on a bench top Orbitrap. *Mol Cell Proteomics*, 11, M111 013722.
- Nie, L., G. Wu & W. Zhang (2006) Correlation between mRNA and protein abundance in *Desulfovibrio vulgaris*: a multiple regression to identify sources of variations. *Biochem Biophys Res Commun*, 339, 603-610.

- Nielsen, M. L., M. Vermeulen, T. Bonaldi, J. Cox, L. Moroder & M. Mann (2008) Iodoacetamide-induced artifact mimics ubiquitination in mass spectrometry. *Nat Methods*, 5, 459-460.
- Panaretou, B. & P. W. Piper (1992) The plasma membrane of yeast acquires a novel heat-shock protein (hsp30) and displays a decline in proton-pumping ATPase levels in response to both heat shock and the entry to stationary phase. *Eur J Biochem*, 206, 635-40.
- Perez-Riverol, Y., A. Csordas, J. Bai, M. Bernal-Llinares, S. Hewapathirana, D. J. Kundu, A. Inuganti, J. Griss, G. Mayer, M. Eisenacher, E. Perez, J. Uszkoreit, J. Pfeuffer, T. Sachsenberg, S. Yilmaz, S. Tiwary, J. Cox, E. Audain, M. Walzer, A. F. Jarnuczak, T. Ternent, A. Brazma & J. A. Vizcaino (2019) The PRIDE database and related tools and resources in 2019: improving support for quantification data. *Nucleic Acids Res*, 47, D442-D450.
- Pichler, P., T. Kocher, J. Holzmann, M. Mazanek, T. Taus, G. Ammerer & K. Mechtler (2010) Peptide labeling with isobaric tags yields higher identification rates using iTRAQ 4-plex compared to TMT 6-plex and iTRAQ 8-plex on LTQ Orbitrap. *Anal Chem*, 82, 6549-6558.
- Pickart, C. M. & D. Fushman (2004) Polyubiquitin chains: polymeric protein signals. *Curr Opin Chem Biol*, 8, 610-616.
- Pottiez, G., J. Wiederin, H. S. Fox & P. Ciborowski (2012) Comparison of 4-plex to 8-plex iTRAQ quantitative measurements of proteins in human plasma samples. *J Proteome Res*, 11, 3774-3781.
- Poulsen, J. W., C. T. Madsen, C. Young, F. M. Poulsen & M. L. Nielsen (2013) Using guanidine-hydrochloride for fast and efficient protein digestion and single-step affinity-purification mass spectrometry. *J Proteome Res*, 12, 1020-1030.
- Proft, M., A. Pascual-Ahuir, E. de Nadal, J. Arino, R. Serrano & F. Posas (2001) Regulation of the Sko1 transcriptional repressor by the Hog1 MAP kinase in response to osmotic stress. *EMBO J*, 20, 1123-1133.
- Ritchie, M. E., B. Phipson, D. Wu, Y. Hu, C. W. Law, W. Shi & G. K. Smyth (2015) limma powers differential expression analyses for RNA-sequencing and microarray studies. *Nucleic Acids Res*, 43, e47.
- Rouse, J., P. Cohen, S. Trigon, M. Morange, A. Alonso-Llamazares, D. Zamanillo, T. Hunt & A. R. Nebreda (1994) A novel kinase cascade triggered by stress and heat shock that stimulates MAPKAP kinase-2 and phosphorylation of the small heat shock proteins. *Cell*, 78, 1027-1037.
- Rutkowski, D. T., S. M. Arnold, C. N. Miller, J. Wu, J. Li, K. M. Gunnison, K. Mori, A. A. Sadighi Akha, D. Raden & R. J. Kaufman (2006) Adaptation to ER stress is mediated by differential stabilities of pro-survival and pro-apoptotic mRNAs and proteins. *PLoS Biol*, 4, e374.
- Schneider, C. A., W. S. Rasband & K. W. Eliceiri (2012) NIH Image to ImageJ: 25 years of image analysis. *Nat Methods*, 9, 671-675.

- Schwanhausser, B., D. Busse, N. Li, G. Dittmar, J. Schuchhardt, J. Wolf, W. Chen & M. Selbach (2011) Global quantification of mammalian gene expression control. *Nature*, 473, 337-342.
- Searle, B. C. (2010) Scaffold: a bioinformatic tool for validating MS/MS-based proteomic studies. *Proteomics*, 10, 1265-1269.
- Shalon, D., S. J. Smith & P. O. Brown (1996) A DNA microarray system for analyzing complex DNA samples using two-color fluorescent probe hybridization. *Genome Res*, 6, 639-645.
- Shivaswamy, S. & V. R. Iyer (2008) Stress-dependent dynamics of global chromatin remodeling in yeast: dual role for SWI/SNF in the heat shock stress response. *Mol Cell Biol*, 28, 2221-2234.
- Singer, M. A. & S. Lindquist (1998) Multiple effects of trehalose on protein folding in vitro and in vivo. *Mol Cell*, 1, 639-48.
- Sorger, P. K. & H. R. Pelham (1987) Purification and characterization of a heat-shock element binding protein from yeast. *EMBO J*, 6, 3035-3041.
- Sun, S., J. Y. Zhou, W. Yang & H. Zhang (2014) Inhibition of protein carbamylation in urea solution using ammonium-containing buffers. *Anal Biochem*, 446, 76-81.
- Swan, T. M. & K. Watson (1997) Membrane fatty acid composition and membrane fluidity as parameters of stress tolerance in yeast. *Can J Microbiol*, 43, 70-7.
- The UniProt Consortium (2018) UniProt: the universal protein knowledgebase. *Nucleic Acids Res*, 46, 2699.
- Teixeira, M. C., P. T. Monteiro, M. Palma, C. Costa, C. P. Godinho, P. Pais, M. Cavalheiro, M. Antunes, A. Lemos, T. Pedreira & I. Sa-Correia (2018) YEASTRACT: an upgraded database for the analysis of transcription regulatory networks in *Saccharomyces cerevisiae*. *Nucleic Acids Res*, 46, D348-D353.
- Ting, L., R. Rad, S. P. Gygi & W. Haas (2011) MS3 eliminates ratio distortion in isobaric multiplexed quantitative proteomics. *Nat Methods*, 8, 937-940.
- Trevisol, E. T., A. D. Panek, J. F. De Mesquita & E. C. Eleutherio (2014) Regulation of the yeast trehalose-synthase complex by cyclic AMP-dependent phosphorylation. *Biochim Biophys Acta*, 1840, 1646-1650.
- Verghese, J., J. Abrams, Y. Wang & K. A. Morano (2012) Biology of the heat shock response and protein chaperones: budding yeast (*Saccharomyces cerevisiae*) as a model system. *Microbiol Mol Biol Rev*, 76, 115-158.
- von der Haar, T. (2007) Optimized protein extraction for quantitative proteomics of yeasts. *PLoS One*, 2, e1078.
- Wang, F., M. Nguyen, F. X. Qin & Q. Tong (2007) SIRT2 deacetylates FOXO3a in response to oxidative stress and caloric restriction. *Aging Cell*, 6, 505-514.

- Wang, X., J. Yen, P. Kaiser & L. Huang (2010) Regulation of the 26S proteasome complex during oxidative stress. *Sci Signal*, 3, ra88.
- Wang, Y., F. Yang, M. A. Gritsenko, Y. Wang, T. Clauss, T. Liu, Y. Shen, M. E. Monroe, D. Lopez-Ferrer, T. Reno, R. J. Moore, R. L. Klemke, D. G. Camp, 2nd & R. D. Smith (2011) Reversed-phase chromatography with multiple fraction concatenation strategy for proteome profiling of human MCF10A cells. *Proteomics*, 11, 2019-2026.
- Washburn, M. P., A. Koller, G. Oshiro, R. R. Ulaszek, D. Plouffe, C. Deciu, E. Winzeler & J. R. Yates, 3rd (2003) Protein pathway and complex clustering of correlated mRNA and protein expression analyses in *Saccharomyces cerevisiae*. *Proc Natl Acad Sci U S A*, 100, 3107-3112.
- Wessel, D. & U. I. Flugge (1984) A method for the quantitative recovery of protein in dilute solution in the presence of detergents and lipids. *Anal Biochem*, 138, 141-143.
- Westerheide, S. D., J. Anckar, S. M. Stevens, Jr., L. Sistonen & R. I. Morimoto (2009) Stress-inducible regulation of heat shock factor 1 by the deacetylase SIRT1. *Science*, 323, 1063-1066.
- Wohlbach, D. J., N. Rovinskiy, J. A. Lewis, M. Sardi, W. S. Schackwitz, J. A. Martin, S. Deshpande, C. G. Daum, A. Lipzen, T. K. Sato & A. P. Gasch (2014) Comparative genomics of *Saccharomyces cerevisiae* natural isolates for bioenergy production. *Genome Biol Evol*, 6, 2557-2566.
- Xie, Q., Y. Hao, L. Tao, S. Peng, C. Rao, H. Chen, H. You, M. Q. Dong & Z. Yuan (2012) Lysine methylation of FOXO3 regulates oxidative stress-induced neuronal cell death. *EMBO Rep*, 13, 371-377.
- Yassour, M., J. Pfiffner, J. Z. Levin, X. Adiconis, A. Gnirke, C. Nusbaum, D. A. Thompson, N. Friedman & A. Regev (2010) Strand-specific RNA sequencing reveals extensive regulated long antisense transcripts that are conserved across yeast species. *Genome Biol*, 11, R87.
- Yoon, O. K. & R. B. Brem (2010) Noncanonical transcript forms in yeast and their regulation during environmental stress. *RNA*, 16, 1256-1267.
- Zhou, F., Y. Lu, S. B. Ficarro, G. Adelmant, W. Jiang, C. J. Luckey & J. A. Marto (2013) Genome-scale proteome quantification by DEEP SEQ mass spectrometry. *Nat Commun*, 4, 2171.

Supplementary Figures

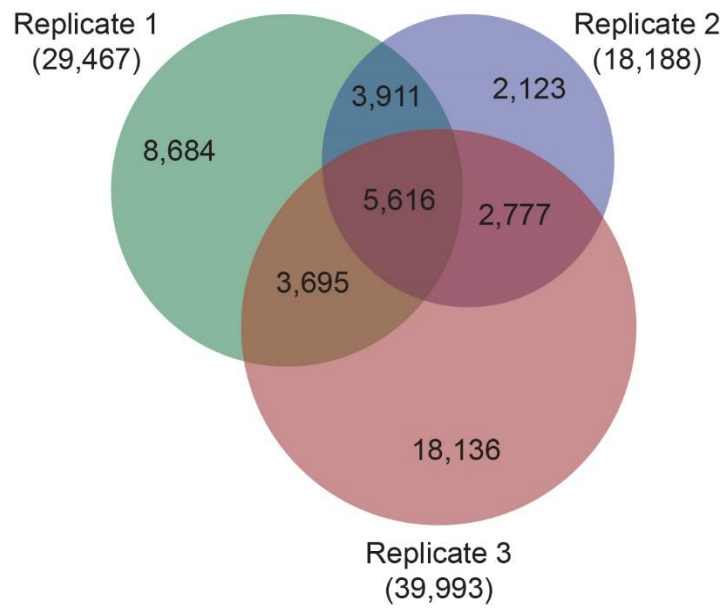


Figure S1: Overlap Between Identified Peptides Across Replicates. The Venn diagram depicts the overlap peptides identified in each biological replicate.

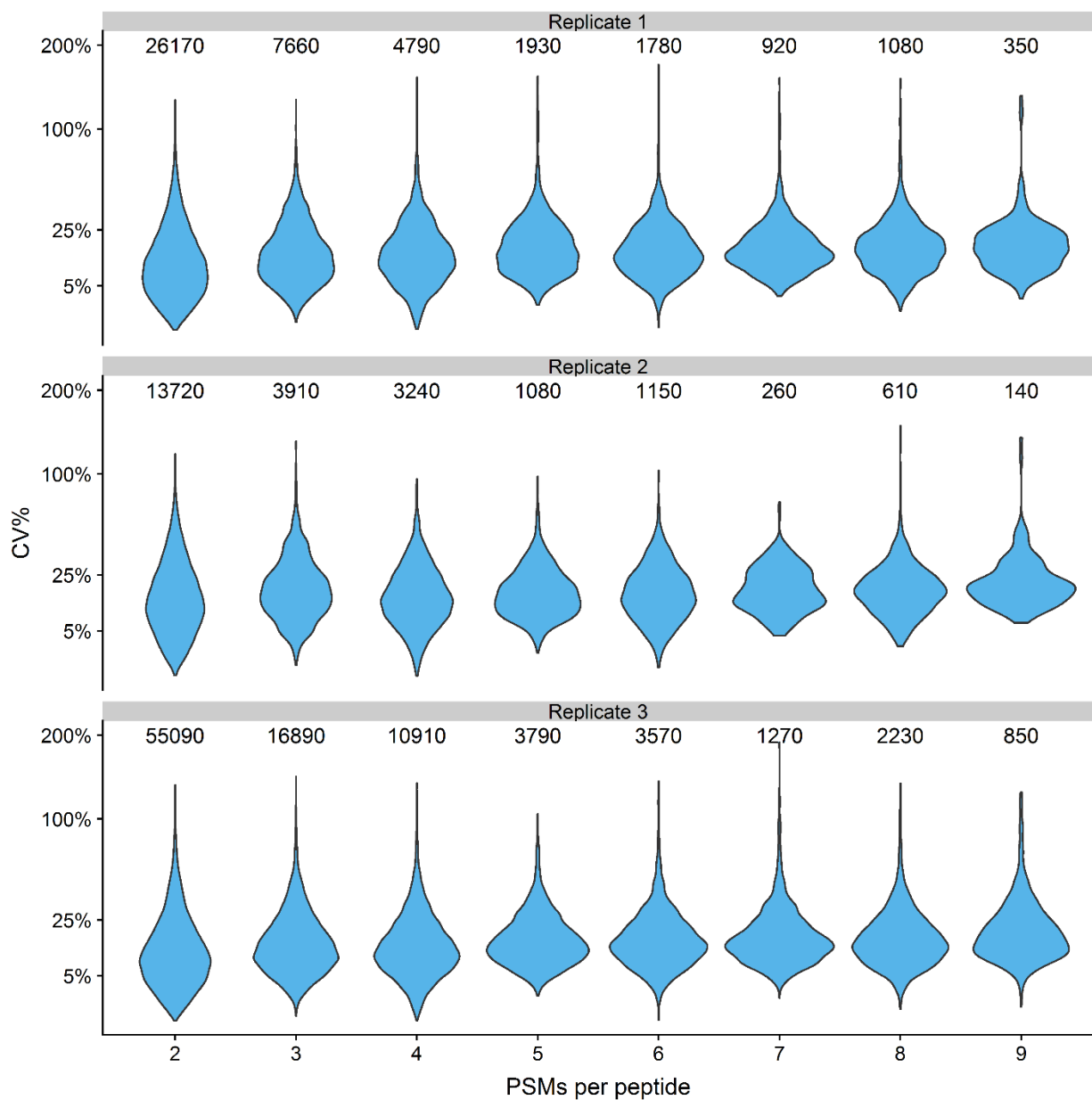


Figure S2: Highly precise, peptide-level measurements for three independent TMT 10-plex experiments. Reporter ion intensity data from three independent TMT 10-plex heat shock time-course experiments were used to calculate coefficient of variance as a function of PSM number.

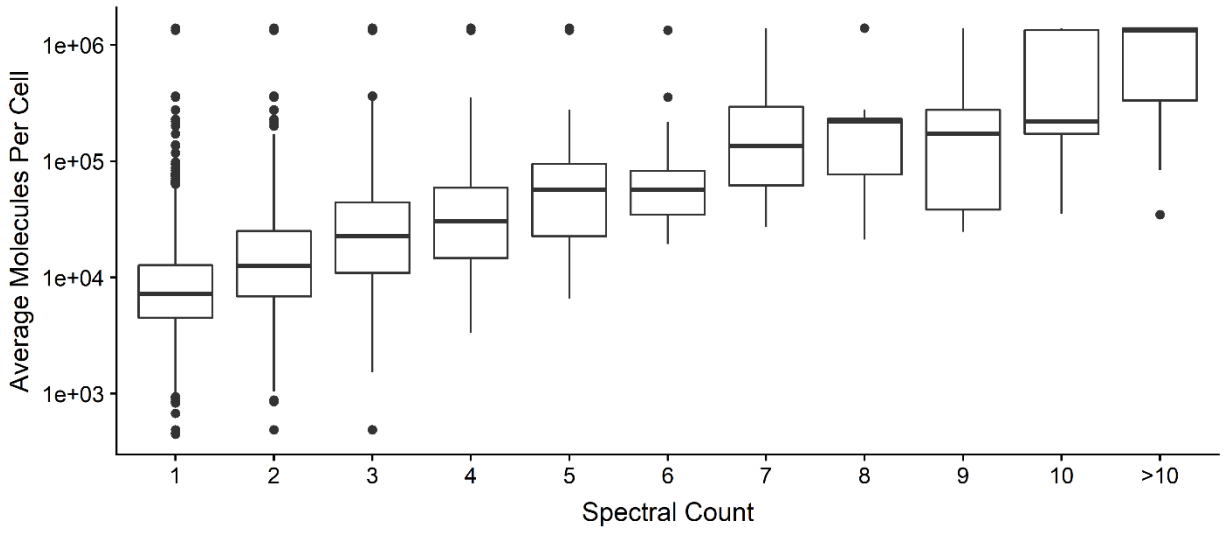


Figure S3: Spectral Counts Correlate with Estimated Protein Abundance. Boxplots show the distribution of estimated protein abundance from Ho et al.¹⁹ on corresponding proteins binned by peptide spectral counts.

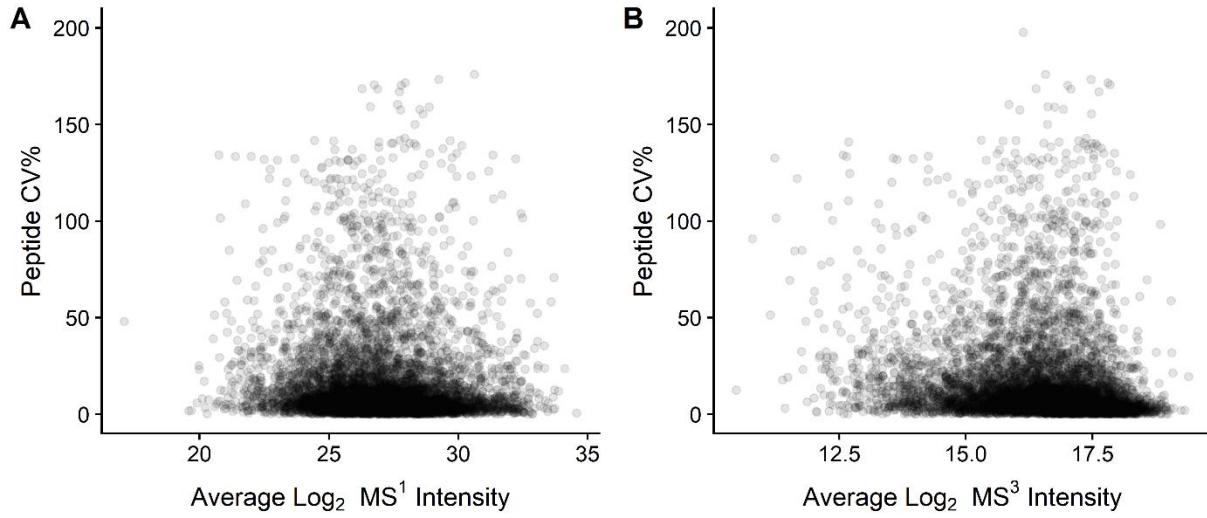


Figure S4: Peptide CV is Weakly Correlated with MS¹ and MS² Intensity. The scatterplots depict Peptide CV versus MS¹ intensity **A**) or MS³ intensity **B**). The correlation (r) for CV% versus MS¹ is -0.064, and r for CV% versus MS³ is -0.151.

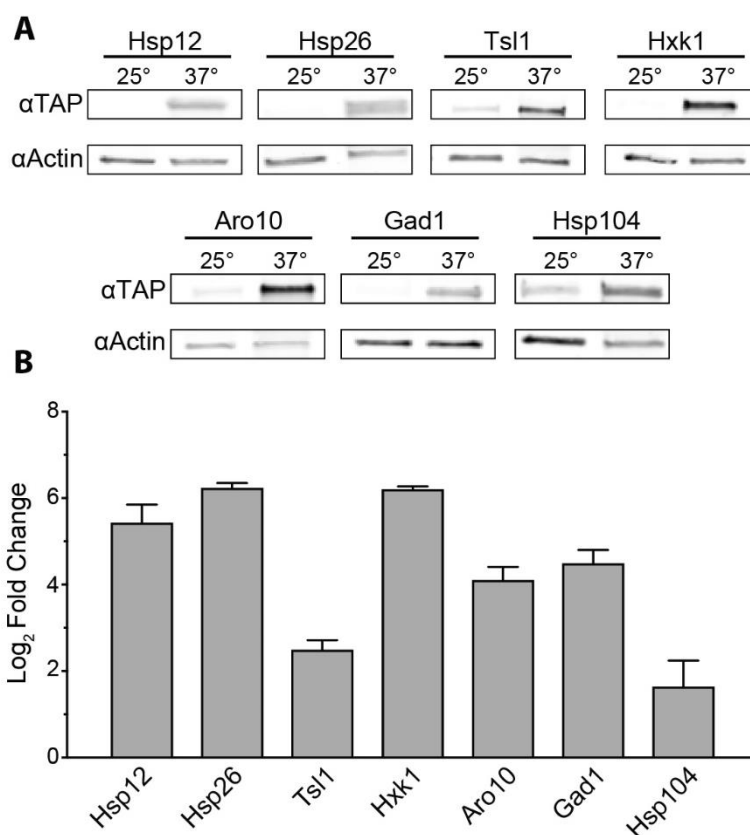


Figure S5: TMT-MS³ is an accurate detection method for changes in protein abundance. The relative abundance for seven significantly-induced proteins at 60 minutes post heat-shock was validated via quantitative western blotting. Anti-actin and anti-TAP antibodies were used to detect, simultaneously in the same blot, the Act1p loading control and the TAP-tagged proteins of interest. **A)** Representative western blots. **B)** Quantitation of relative log₂ fold changes before and after heat shock for each TAP-tagged protein following normalization to actin. Data represent the mean and standard deviation of three biological replicates. Raw images can be found in File S5, and densitometric data can be found in File S6.

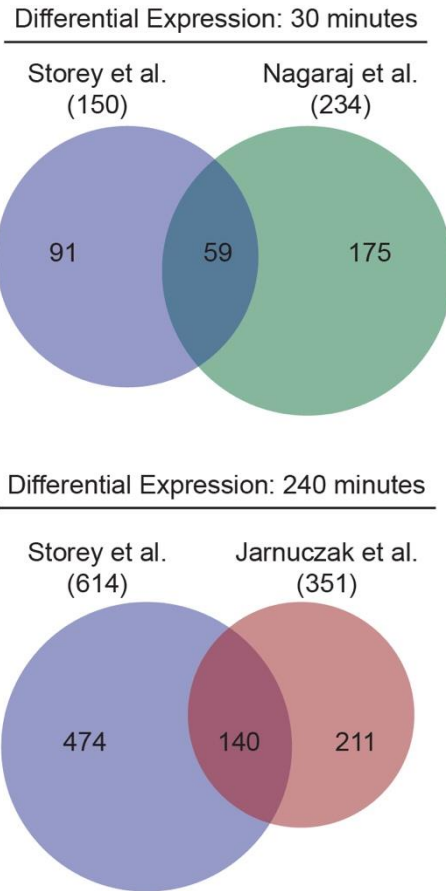


Figure S6: Comparison of differentially abundant proteins from this TMT-MS³ study to those reported by studies that used SILAC and label-free approaches. We compared significantly differentially expressed proteins from this TMT-MS³ experiment (Story et al.) to a set of SILAC (Nagaraj et al.⁴⁷) and label-free (Jarnuczak et al.⁴⁸) experiments. Because Nagaraj et al. used an FDR < 0.02, we maintained that threshold for each of these comparisons.

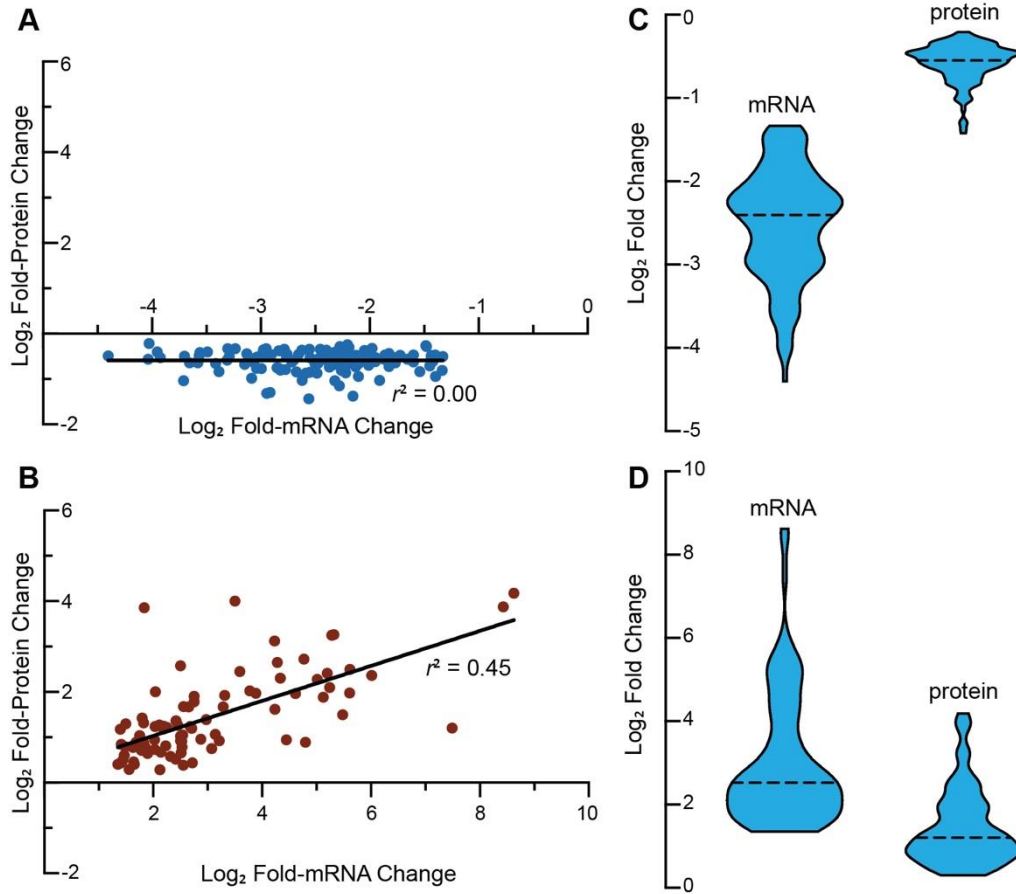


Figure S7: Evidence for buffering of protein repression. Correlation between pairs of proteins and mRNAs from Eng et al.⁴³ that were both significantly (FDR < 0.05) **A)** repressed **B)** or induced following heat shock (at 60 minutes for proteins and 15 minutes for mRNAs). The violin plots depict the density of expression values for the **C)** repressed **D)** or induced protein-mRNA pairs.

Appendix

A.1 IBC Protocol Approval



UNIVERSITY OF
ARKANSAS

Office of Research Compliance

July 24, 2019

MEMORANDUM

TO: Dr. Jeffrey Lewis
FROM: Ines Pinto, Biosafety Committee Chair
RE: Protocol Renewal
PROTOCOL #: 14007
PROTOCOL TITLE: Genomics and Physiology of Microbial Stress Responses
APPROVED PROJECT PERIOD: **Start Date** July 11, 2013 **Expiration Date** July 10, 2022

The Institutional Biosafety Committee (IBC) has approved your request, dated July 8, 2019, to renew IBC # 14007, "Genomics and Physiology of Microbial Stress Responses".

The IBC appreciates your assistance and cooperation in complying with University and Federal guidelines for research involving hazardous biological materials.

1424 W. Martin Luther King, Jr. • Fayetteville, AR 72701
Voice (479) 575-4572 • Fax (479) 575-6527


The University of Arkansas is an equal opportunity/affirmative action institution.



J. William Fulbright College of Arts and Sciences
Department of Biological Sciences

Date: December 5, 2019
To: Whom it may concern
From: Dr. Jeffrey A. Lewis
Research Advisor
Subject: Rebecca Hardman Dissertation

The majority of the work presented in this dissertation was performed by Rebecca Hardman as described in chapter author contributions. All biosafety training was completed and maintained in accordance with University of Arkansas and IBC policies regarding IBC protocol #14007.



Jeffrey A. Lewis, Ph.D.
Assistant Professor of Biological Sciences

University of Arkansas
Department of Biological Sciences
Science and Engineering 526
Fayetteville, AR 72701
479-575-7740